2014

Synaptic Organization of Noradrenergic and Opioid Circuitry in the Basolateral Amygdala: Anatomical Correlates of Memory Consolidation

Jingyi Zhang
University of South Carolina - Columbia

SYNAPTIC ORGANIZATION OF NORADRENERGIC AND OPIOID CIRCUITRY IN THE BASOLATERAL AMYGDALA: ANATOMICAL CORRELATES OF MEMORY CONSOLIDATION

by

Jingyi Zhang

Bachelor in Clinical Medicine
Wuhan University of Science and Technology, 2002

Submitted in Partial Fulfillment of the Requirements

For the Degree of Doctor of Philosophy in

Biomedical Science

School of Medicine

University of South Carolina

2014

Accepted by:

Alexander McDonald, Major Professor

David Mott, Committee Member

Marlene Wilson, Committee Member

Sandra Kelly, Committee Member

Robert Price, Committee Member

Lacy Ford, Vice Provost and Dean of Graduate Studies

ACKNOWLEDGEMENTS

First and foremost, I offer my sincerest gratitude to my mentor, Dr. Alexander McDonald, who has supported me throughout my Ph.D. study and dissertation research with his patience, enthusiasm and immense knowledge. One simply could not wish for a better or friendlier supervisor.

Besides my mentor, I would like to thank the rest of my committee members: Dr. David Mott, Dr. Marlene Wilson, Dr. Bob Price and Dr. Sandra Kelly for their encouragement and insightful comments.

I thank Dr. Jay Muller for sharing his knowledge, time and expertise.

I thank Jeffrey Davis, for his warm friendship and much needed support in my experiments.

I thank Dr. Franco Mascagni for providing such a wonderful positive environment in which to work.

I thank Dr. Violeta Zaric for her kindness, friendship and support.

I thank my friends Dr. Binyue Chang, Jing Li, Hima Vangapandu, Feng Gao, Ti Yan, Lu Yu, Siming Guo for all the fun we have had in the past several years.

I would like to thank Department of Pharmacology, Physiology and Neuroscience, and Instrumentation Resource Facility at School of Medicine University of

South Carolina which provided the support and equipments I have needed to produce and complete my dissertation.

Last, but by no means least, I thank my parents Xuwen Zhang and Peiying Sun, and my younger brother Yang Zhang who have given me their unequivocal support throughout, as always, for which my mere expression of thanks likewise does not suffice.

ABSTRACT

The studies comprising this dissertation were designed to investigate the synaptic organization of norepinephrine and opioid system in the anterior subdivision of the basolateral nucleus of amygdala (BLa) in rats. Light and electron microscopy were combined with immunohistochemistry to determine the synaptic incidence and postsynaptic targets of noradrenergic axon terminals, to localize mu opioid receptors at the ultrastructural level, and to determine whether there is convergence of norepinephrine inputs and enkephalin inputs in the BLa. It was determined that about half of the norepinephrine inputs formed synapses in the BLa and the main postsynaptic targets were small caliber CAMK+ dendritic shafts and spines of pyramidal cells in the BLa. It was determined that MOR+ profiles were found in both pre and postsynaptic profiles. The most frequent labeled structures were small caliber dendrites and terminals. Both symmetrical and asymmetrical synapses were formed by MOR+ terminals, but the asymmetrical ones were more commonly observed in the BLa. MOR+ terminals were mainly targeted spines and small distal dendrites. It was determined that there was very limited (11%) convergence between ENK+ and norepinephrine terminals. These studies will contribute to a better understanding of how the noradrenergic and opioid systems affect BLa neural activity, which is essential to unravel the underlying mechanisms of memory modulation.

TABLE OF CONTENTS

LIST OF TABLES

LIST OF FIGURES

List of Abbreviations

BLA.....Basolateral Amygdala Nucleus

BLa..... Anterior Subdivision of Basolateral Nucleus of Amygdala

BLC..... Basolateral Nuclear Complex of the Amygdala

BNST .....Bed Nucleus of the Stria Terminalis

CAMK.....Calcium/Calmodulin Kinase

CB .....Calbindin

CCK ..... Cholecystokinin

CeA .....Central Nuclear of Amygdala

CR .....Calretinin

DA.....Dopamine

DAB .....3, 3 ´-diaminobenzidine 4HCl

DBH .....Dopamine-β-Hydroxylase

Dopa.....Dihydroxyphenylalanine

DOR ..... Delta Opioid Receptor

E .....Epinephrine

ENK ..... Enkephalin

fMRI.....Functional Magnetic Resonance Imaging

GABA ..... Gamma-Aminobutyric Acid

GPCR .....G-Protein Coupled Receptor

ITC .....Intercalated Cell Mass

KOR .....Kappa Opioid Receptor

LA .....Lateral Nuclear of Amygdala

LC .....Locus Ceruleus

MOR ..... Mu Opioid Receptor

NE ..... Norepinephrine

NET.....Norepinephrine Transporter

NLOT.....Nucleus of the Lateral Olfactory Tract

NPY.....Neuropeptide Y

PAG.....Periaqueductal Gray

PTSD.....Post Traumatic Stress Disorder

PV ..... Parvalbumin

SOM.....Somatostatin

TH .....Tyrosine Hydroxylase

VIP .....Vasoactive Intestinal Peptide

V-VIP/VIP ..... Vector-Very Intense Purple

CHAPTER 1

INTRODUCTION

It is well known that emotionally arousing experiences tend to be well remembered. Emotional memory consolidation is a well-organized, highly adaptive phenomenon that helps us to remember important information and thus is critical for our survival (Roozendaal et al., 2009). Intense or chronic exposure to the stressful events can create traumatic memories which lead to mood and anxiety disorders such as post-traumatic stress disorder (PTSD) (Roozendaal et al., 2009, Goodman et al., 2012).

Considerable evidence from animal and human studies has found that the memory consolidation effects of the amygdala are selectively mediated by the basolateral amygdala (BLA), especially the anterior basolateral nucleus (BLa) (McGaugh, 2004). The BLA exerts its memory modulation function via regulating complex interactions among several neuromodulatory systems (McGaugh, 2004). A large amount of evidence supports that norepinephrine (NE) serves as a key player, and that the opioid system could affect memory consolidation by influencing NE release in the BLA (Quirarte et al., 1998, Ferry and McGaugh, 1999, McGaugh, 2004) . However, the exact circuits of the NE and opioid system are not clear.

Knowledge of the exact synapses and circuits of NE and opioids is critical for understanding how they affect each other and thus affect BLA neural activity which is essential to unraveling the underlying mechanism of memory modulation and identifying the novel drug targets for related diseases such as PTSD.

1.1 SIGNIFICANCE OF THE BLA IN MEMORY CONSOLIDATION

The BLA has reciprocal connections with the medial temporal lobe memory system which consists of the hippocampus and adjacent cortex (Pitkanen et al., 2000) . The BLA is also the major nucleus in the amygdala projecting to the striatum (McDonald, 1991, 2003). Through these connections, it modulates memory consolidation by enhancing striatal-dependent habit memory and modulating hippocampal-dependent cognitive memory during stress or anxiety situations, which may underlie some aspects of PTSD symptoms (Goodman et al., 2012). In fact, results from previous studies suggested that among the numerous nuclei in the amygdala, the BLa is the one selectively involved in memory consolidation (Tomaz et al., 1992, Parent and McGaugh, 1994, Da Cunha et al., 1999, McGaugh and Izquierdo, 2000). The exact circuit for memory consolidation is not clear, but extensive evidence has shown that the influence of the BLa in the memory consolidation involves interactions of several neuromodulatory systems including neurotransmitters and stress hormones (McGaugh, 2004). Specifically, noradrenergic, cholinergic, glucocorticoid and dopaminergic systems have been found to enhance memory consolidation (Lupien and McEwen, 1997, Hatfield et al., 1999, Power and McGaugh, 2002, McGaugh, 2004), while GABA and opioid peptides appear to block the consolidation by inhibiting the effects of the positive modulators (Quirarte et al., 1998, Hatfield et al., 1999). Taken together, the effects from these different neuromodulatory systems converge in affecting noradrenergic and muscarinic cholinergic activation (McGaugh, 2004). Knowledge of the synaptic organization of these neuromodulatory systems in the amygdala will be critical for understanding the underlying mechanisms of memory consolidation, and how these circuits may be disrupted in the disorders of emotional memory, such as PTSD.

1.2 NOREPINEPHRINE SYSTEM

The Norepinephrine (NE) system is a widespread system innervating virtually the entire central nervous system (Berridge and Waterhouse, 2003). Because of its extensive distribution, the NE system is involved in multiple brain functions, such as attention, arousal, vigilance, memory, and pain (Berridge and Waterhouse, 2003). Most of the noradrenergic neurons in the brain are concentrated in the locus ceruleus (LC), which provides the primary source of the noradrenergic innervation for hippocampus, neocortex and amygdala (Berridge and Waterhouse, 2003). As a catecholamine, NE along with dopamine (DA) and epinephrine (E) are sequential products from the same biosynthetic pathway beginning with dietary tyrosine (Nestler EJ, 2001). Tyrosine is hydroxylated by the enzyme tyrosine hydroxylase (TH) to form dihydroxyphenylalanine (Dopa). TH is the rate–limiting enzyme in the catecholamine synthesis. Then Dopa is converted into DA by an enzyme which also exists in dopamine neurons. DA is converted into NE by the dopamine-β-hydroxylase (DBH), which is only expressed in NE and E neurons. The major way of terminating NE function is by reuptake into the neuronal terminal via NE transporters (NET) (Nestler EJ, 2001). NE is catabolized by monoamine oxidase and catechol-O-methyltransferase (Nestler EJ, 2001).

NE receptors belong to the G-protein-coupled receptor (GPCR) family and they can be divided into two types, α and β adrenoceptors, both of which can be further divided into numerous subtypes with different affinity and response for NE and E (Nestler EJ, 2001). Among them, all β receptors are Gs-coupled, leading to the activation of cyclic adenosine monophosphate (cAMP) synthesis and thus triggering the protein kinase A pathway (Nestler EJ, 2001). Most α1 receptors are Gq-coupled, which trigger

the phosphatidylinositol cascade and have various effects on neuronal excitability (Nestler EJ, 2001). α2 receptors are generally coupling with Gi, causing inhibition effects in most neurons, thus they mainly serve as autoreceptors (Nestler EJ, 2001).

1.3 OPIOID SYSTEM

Endogenous opioid peptides including endorphin, enkephalin (ENK) and dynorphin are derived from three peptide precursors, proopiomelanocortin, proenkephalin and prodynorphin, respectively (Stefano et al., 2000, Drolet et al., 2001). As neuropeptides, endogenous opioids are synthesized in the cell body and then transported to axon terminals where they are released. Opioids are synthesized as large precursors (see above) and then undergo complex posttranslational processes (Nestler EJ, 2001). Unlike small-molecule neurotransmitters such as glutamate and catecholamines, which are packaged in small synaptic vesicles, opioids are packed in large dense core vesicles. Similar to other neuropeptides, opioids tend to be released by sustained neuronal activity and can diffuse a long distance after release.

Endogenous opioid peptides exert their effects via three major types of G-protein coupled receptors: mu (MOR), delta (DOR) and kappa (KOR), which are coupled to the Gi/Go family of G proteins (Drolet et al., 2001). Activation of these receptors inhibits adenylyl cyclase and modulates membrane conductance of calcium and potassium, leading to inhibitory influences upon neuronal activity (Nestler EJ, 2001). MOR is the most abundant opioid receptor in the BLA (Mansour et al., 1987, Ding et al., 1996). Opioid peptides do not bind exclusively to the receptor for which they have highest affinity. For example, enkephalin has the greatest affinity for DOR, but it also binds to MOR with high affinity.

1.4 CLINICAL SIGNIFICANCE OF THE AMYGDALA IN PTSD

Post Traumatic Stress Disorder (PTSD) is an anxiety disorder triggered by exposure to traumatic experiences such as war, disaster, terrorism, motor vehicle accidents and violence (Parsons and Ressler, 2013). Although the prevalence of the PTSD is only 6.8% in the general population, it is much higher (20-40%) for people with unexpected trauma experience such as crime victims and disaster survivals, or people with rescue or war-related occupations, for example firefighter, policemen and soldiers (Javidi and Yadollahie, 2012).Thus, PTSD is the fourth most common psychiatric diagnosis (Parsons and Ressler, 2013). Around 84% of PTSD patients have comorbid situations like alcohol and/or drug abuse, major depressive disorder and other anxiety disorders (Javidi and Yadollahie, 2012).

The amygdala is the major brain area involved in fear-related anxiety disorders including PTSD (LeDoux, 2000, Goodman et al., 2012, Pitman et al., 2012) . The findings from neuroimaging studies have shown increased activity of the amygdala in PTSD patients. (Liberzon et al., 1999, Vermetten et al., 2007, Hughes and Shin, 2011) Moreover, amygdala activation has been found to positively correlate with PTSD symptom severity (Rauch et al., 2000, Pissiota et al., 2002, Bryant et al., 2005, Protopopescu et al., 2005, Dickie et al., 2008, Brunetti et al., 2010) and decreased amygdala activity is probably related to the resilience to PTSD development after trauma exposure (Britton et al., 2005, Osuch et al., 2008). The pathological mechanism of PTSD is not very clear. It is believed that the over-consolidation of traumatic memory due to dysfunction of amygdala might contribute to its development and persistence (McGaugh, 2004, Goodman et al., 2012, Pitman et al., 2012, Parsons and Ressler, 2013). Better

understanding of the neuronal circuitry of the amygdala involved in memory consolidation may help us to further understand PTSD pathology and provide valuable information for exploring novel treatment or intervention approaches.

CHAPTER 2

FUNCTIONAL NEUROANATOMY OF AMYGDALA

The amygdala is an almond-shaped brain nuclear group located in the anteromedial part of temporal lobe (LeDoux, 2000). It is a heterogeneous structure consisting of several nuclei, each of which has distinctive neuron types, neurochemical features and connections (McDonald, 2003). Although the amygdala is a small nuclear complex, it has extensive connections between its own different nuclei and also with numerous brain areas (McDonald, 2003). Through these connections, the amygdala produces appropriate behavioral responses to salient sensory stimuli and emotion arousing events in the external world and it is a key center for emotional memory (LeDoux, 2000, Millan, 2003, Sah et al., 2003, McGaugh, 2004). Studies in rats, cats and primates are in close agreement about the connections of nuclei which are most relevant to fear learning including the lateral, basolateral and accessory basal nuclei (LeDoux, 2000, McDonald, 2003).

Most of the amygdala nuclei do not have clear borders and the nomenclature for these nuclei is not consistent among different groups (McDonald, 1998). However, it is customary to divide the amygdala nuclei into three major groups based on their anatomical and functional characteristics: the basolateral nuclear group, the cortical nuclear group and the centromedial nuclear group (McDonald, 2003). Besides, there are three additional nuclei composing the remaining parts of the amygdala, including, the

amygdalohippocampal area, the anterior amygdala area, and the intercalated cell nuclei (ITC) (McDonald, 1998).

2.1 NUCLEI AND CONNECTIONS

2.1.1 BASOLATERAL NUCLEAR GROUP

The basolateral nuclear complex of the amygdala contains three main nuclei: lateral, basolateral and basomedial nucleus (which are often referred to together as the basolateral complex (BLC)) (Sah et al., 2003). The BLC receives robust sensory inputs from the cerebral cortex and thalamus (LeDoux et al., 1984, McDonald, 1998) and it has reciprocal connections with temporal lobe memory system (Pitkanen et al., 2000). The BLC also have connections with the basal ganglia and basal forebrain.

The lateral nucleus (LA) is the principle recipient of afferents from sensory neocortex in the BLC (Pitkanen and Amaral, 1991). It receives dense fibers from unimodal sensory association area and polysensory processing areas (Romanski et al., 1993, Romanski and LeDoux, 1993, McDonald and Mascagni, 1997, McDonald, 1998). Another brain area that projects to the LA is thalamus (LeDoux et al., 1984). In turn, the LA sends inputs to other amygdalar nuclei including the central, basal and basomedial nuclei, as well as the hippocampus and parahippocampal cortex (Ottersen, 1982, Pikkarainen and Pitkanen, 2001). Functionally, the LA is the amygdala region where conditioned stimuli and unconditioned stimuli are paired during fear conditioning (Romanski et al., 1993, LeDoux, 2000, Sigurdsson et al., 2007). Therefore it is critical for fear learning.

Similar to the LA, the basolateral nucleus of the amygdala (BLA) receives projections from sensory association cortical regions and also projects back to some

cortical areas (McDonald, 1998). In addition, BLA has reciprocal connections with insular, cingulated, and prefrontal, and frontal cortex (Beckstead, 1978, Krettek and Price, 1978, Ottersen, 1982, Saper, 1984, McDonald et al., 1996). Other regions giving rise to afferents to the BLA are the thalamus and hypothalamus. In turn, the BLA sends projections to the cholinergic basal forebrain and striatum. Moreover, studies suggest that there are reciprocal connections between the BLA, hippocampus and nearby cerebral cortex, which provides an anatomical basis for the role of the BLA in emotional memory consolidation. Hippocampal projections to the BLA and basomedial amygdala appear to be involved in contextual conditioning (Maren and Fanselow, 1995), whereas cue conditioning relies more on the lateral nucleus to central nucleus pathway (LeDoux, 2000). The BLA seems to be the major source of intra-amygdaloid innervations, projecting to central, medial and lateral nuclei (Nitecka et al., 1981, Cassell et al., 1999), thus it is important for information integration inside the amygdala.

The basomedial nucleus is the major target of the outputs from the lateral nucleus (Pitkanen and Amaral, 1991, Savander et al., 1997). In addition, it also receives projections from hypothalamus and brainstem (McDonald, 1998). Through these connections, the basomedial nucleus plays a role in many autonomic and endocrine responses related to emotional behaviors (McDonald, 1998). In turn, it sends projections to the cortical sensory association areas, frontal cortex, and cingulated cortex and striatum. As mentioned earlier, the basomedial nucleus is involved in contextual conditioning via its connection with the hippocampus (Maren and Fanselow, 1995).

2.1.2 CENTRAL MEIDIAL NUCLEAR GROUP

Several nuclei make up the centromedial nuclear group, including the central nucleus, medial nucleus and intra-amygdaloid proportion of the bed nucleus stria terminalis (McDonald, 1998). The central and medial nuclei extend forward to become continuous with the bed nucleus of the stria terminalis. These three structures exhibit anatomically and functionally similarities and are often collectively referred to as "extended amygdala" (McDonald, 2003). Nuclei in this group heavily connect with olfactory, hypothalamus and brain stem, but connect with the cortex and thalamus to a less extent.

The central nucleus (CeA) is a complex structure and contains four subdivisions (McDonald, 1982a). The CeA receives extrinsic projections from the insular cortex, entorhinal cortex, hypothalamus, parabrachial nuclei, nucleus of the solitary tract and locus ceruleus (Fallon et al., 1978, Ricardo and Koh, 1978, Mason and Fibiger, 1979, Saper and Loewy, 1980, Ottersen, 1981, Russchen, 1982, Fulwiler and Saper, 1984, Augustine, 1996, McDonald and Mascagni, 1997). The CeA is also innervated by intra-amygdala afferents from other amygdala nuclei including the BLC, intercalated cell nuclei, cortical and medial nuclei (Cassell et al., 1999, Zimmerman et al., 2007). In turn, the CeA indirectly projects to the hypothalamus and brainstem via the bed nucleus of the stria terminalis as a relay site. The CeA also sends substantial inputs to the hypothalamus directly (LeDoux et al., 1988). In addition, the CeA heavily projects to the brainstem (Veening et al., 1984). Functionally, CeA serves as an output center important for mediating fear responses (Samson and Pare, 2005). CeA may also be involved in the

acquisition and consolidation of fear memory as well (Wilensky et al., 2006, Zimmerman et al., 2007).

The medial nucleus receives inputs from multiple extrinsic sources including the piriform cortex, agranular insular cortex, entorhinal cortex, ventral subiculum, and locus coeruleus (McDonald, 1998, McDonald et al., 1999, Ma and Morilak, 2005). Additionally, it is also targeted by the BLC (Walker et al., 2005). In turn, the medial nucleus sends projections to the thalamus, hypothalamus, bed nucleus of the stria terminalis and brainstem (Canteras et al., 1995). Functionally, the medial nucleus is crucial for freezing behavior induced by predator odor stimuli (Muller and Fendt, 2006).

The intra-amygdaloid proportion of the bed nucleus stria terminalis (BNST) is closely related to the stria terminalis (McDonald, 1998). Previous studies have shown that the BNST is implicated in anxiety behaviors and responses to contextual stimuli (Pego et al., 2008) (Meloni et al., 2006). Moreover, the BNST is directly involved in the regulation of the hypothalamus-pituitary-adrenal (HPA) via its projections to the hypothalamus (Pego et al., 2008). In addition, evidence shows that the BNST may be activated by less explicit information and thus mediate anxiety, whereas the CeA is activated by highly processed explicit cue information and therefore involved in stimulus-specific fear modulation (Davis and Shi, 1999).

2.1.3 CORTICAL NUCLEAR GROUP

The cortical nuclear group includes the cortical nucleus, the nucleus of the lateral olfactory tract and the periamygdaloid cortex (McDonald, 1998). Nuclei in this group lie superficially in the amygdala and they extensively connect with the olfactory bulb, hypothalamus and brain stem, but connect with the cortex and thalamus to a less extent

(McDonald, 1998). This amygdala nuclear group is heavily involved in olfactory information processing.

The cortical nucleus has reciprocal connections with the olfactory bulb and it also receives direct projections from the accessory olfactory bulb and piriform cortex (McDonald, 1998) (Turner et al 1978, Price 1990, De Olmos et al 1978, Luskin and Price 1983, Post and Mai 1980, Haberly and Price 1978b, Scalia and Winans 1975). In turn, it sends projections to several cortical areas (Kemppainen et al., 2002, Ubeda-Banon et al., 2007) (Beckstead 1978, Mufson et al 1981, Saper 1982, McDonald and Jackson 1987) including the agranular insular cortex, entorhinal cortex and infralimbic prefrontal cortex, as well as to several subcortical areas such as the hypothalamus and nucleus accumbens, hippocampus and other amygdala nuclei (Wang and Swann, 2006) (Price et al 1991, Krettek and Price 1977a,c, Wiegand 1984, Zaborszky 1982, Old and Silv 1985, Ottersen 1980, Berk and Finkelstein 1982, Conrad and Pfaff 1976a and b, Krieger et al 1979, Swanson 1976, Saunders 1988). Functionally, previous study suggests that the cortical nucleus is important for odor learning and olfactory fear conditioning (Sevelinges et al., 2004).

The nucleus of the lateral olfactory tract (NLOT) consists of three layers (McDonald, 1983). The NLOT has reciprocal connections with the olfactory bulb and piriform cortex (Schwob and Price, 1984, McDonald, 1998). The NLOT also send projections to the anterior olfactory nucleus, the olfactory tubercle, BLC, nuclear accumbens, caudate putamen and agranular insular cortex (Santiago and Shammah-Lagnado, 2004). Functionally, this amygdalar nucleus may influence nonpheromonal olfactory guided behaviors such as feeding (Santiago and Shammah-Lagnado, 2004).

The periamygdaloid cortex extensively interconnected with the olfactory bulb and piriform cortex (McDonald, 1998). This structure also projects to the hippocampus and parahippocampal regions, as well as other amygdalar nuclei including the BLC, cortical, and medial nuclei (Majak and Pitkanen, 2003). Functionally, it is an amygdaloid region processing olfactory information. Moreover, its connections with hippocampus may allow emotional significant olfactory stimuli to enter the medial temporal lobe memory system (Majak and Pitkanen, 2003).

2.1.4 OTHER NUCLEI

The remaining amygdala contains three additional nuclei. They are the amygdalohippocampal area, the anterior amygdaloid area, and the intercalated cell nuclei (ITC).

The amygdalohippocampal area receives projections from the hippocampus (Kishi et al., 2006). It provides the most substantial amygdala inputs to the endopiriform nucleus and sends a light projection to the claustrum (Majak et al., 2002).

The anterior amygdaloid area lies at the rostral pole of the amygdala and is diffusely organized (McDonald, 1998). This area is possibly involved in modulation of attention (Gastard et al., 2002).

The ITC is made up of a group of cells which are predominantly inhibitory (McDonald and Augustine, 1993). The ITC receives intrinsic projections from the BLC and extrinsic projections from the infralimbic PFC and hippocampus (McDonald et al., 1996, Royer et al., 1999, Kishi et al., 2006). In turn, it sends projections to the central and medial nuclei, and basal forebrain (Pare and Smith, 1993, Smith and Pare, 1994). Functionally, the ITC serves as a critical modulator for the communication among

amygdala nuclei, as well as between amygdala and subcortical regions (Royer et al., 1999). Evidence also indicates that ITC may be important for the extinction of fear-related memory (Royer et al., 1999).

2.2 NEURONAL MORPHOLOGY AND PHENOTYPE OF THE BLA

There are two major cell types in the BLA, pyramidal and nonpyramidal neurons (also referred to as class I and II neurons, respectively) (McDonald, 1982b). Pyramidal neurons represent the predominant cell type in the BLC and constitute about 85% of the total neuronal population in this region. These neurons contain glutamate and/or aspartate, the principle excitatory neurotransmitters in the mammalian brain. Golgi stains show that pyramidal neurons are large, spiny neurons that vary in size in different subdivisions of the BLC (McDonald, 1982b). These neurons often have a large pyramidal shaped cell bodies and dendrites with dense spines (McDonald, 1982b). Pyramidal neurons are projection neurons and their axons usually give rise to several collaterals which arborize modestly in the vicinity of the cell body (McDonald, 1982b, 1992).

Golgi stains reveal that nonpyramidal neurons are smaller neurons compared with pyramidal neurons and they are morphologically heterogeneous (McDonald, 1982b, 1985a). Nonpyramidal neurons are interneurons and characterized by spine-sparse dendrites and axons with fairly dense local arborizations. Immunohistochemistry study reveals that the majority of nonpyramidal neurons contain gamma aminobutyric acid (GABA) (McDonald, 1985a), a major inhibitory neurotransmitter in the mammalian central nervous system. They can be distinguished based upon their content of various neuropeptides (McDonald, 1985b, McDonald and Pearson, 1989), including somatostatin (SOM), vasoactive intestinal peptide (VIP), cholecystokinin (CCK), neuropeptide Y

(NPY), as well as their content of calcium binding proteins (McDonald, 1994a, 1997, McDonald and Betette, 2001, McDonald and Mascagni, 2001, Mascagni and McDonald, 2003), including parvalbumin (PV), calbindin (CB) and calritinin (CR). Because there are significant overlaps among these different types of nonpyramidal neurons in the BLC, they can be further grouped into four distinct subpopulations (Mascagni and McDonald, 2003) 1) PV+ neurons (most of them contain CB); 2) SOM+ neurons (many of them are CB+ and NPY+); 3) large CCK+ neurons (some of them are CB+) and 4) small bipolar neurons that exhibit various amount of colocalization of VIP, CR and CCK.

CHAPTER 3

NORADRENERGIC INNERVATION OF PYRAMIDAL CELLS IN THE RAT BASOLATERAL AMYGDALA

3.1 INTRODUCTION

The basolateral amygdalar nuclear complex (BLC) receives a dense noradrenergic input primarily originating from the locus coeruleus (LC) (Asan, 1998), which is heavily involved in stress and stress-related pathologies (Sved et al., 2002). Studies have shown that stressful stimuli such as foot shock induce norepinephrine (NE) release in the rat amygdala (Galvez et al., 1996, Quirarte et al., 1998). Also, human functional magnetic resonance imaging (fMRI) studies show that elevated NE neurotransmission enhances BLC responses to fear signals (Onur et al., 2009). Moreover, a large amount of evidence (Cahill et al., 1995, Ferry and McGaugh, 1999, McGaugh, 2004, Ferry and McGaugh, 2008, Roozendaal et al., 2009) indicates that the NE system in the BLC is involved in memory modulation by stress (Cahill et al., 1995, Ferry and McGaugh, 1999, McIntyre et al., 2002, McGaugh, 2004, Ferry and McGaugh, 2008, Roozendaal et al., 2009). Therefore, the LC is important for providing information about aversive stimuli to the BLC and generating appropriate responses to stressors, which suggests that the LC-NE circuit in the BLC could be a potential drug target for anxiety disorders.

Although there is abundant behavioral and clinical evidence for the role of the NE system of the BLC in stress and anxiety, there is still no clear picture about how NE affects the activity of BLC neurons. Recent studies reveal that BLC neurons can be

inhibited or excited by NE afferents from the LC (Buffalari and Grace, 2007, Chen and Sara, 2007), but in many cases it was difficult to determine whether the recorded neurons were pyramidal cells or interneurons based on their electrophysiological properties (Buffalari and Grace, 2007, Chen and Sara, 2007, Buffalari and Grace, 2009). Therefore, there is still considerable confusion regarding the differential modulation of distinct neuronal subpopulations in the BLC by the NE.

Anatomical knowledge of NE circuits in the BLC should help to clarify the uncertainties of the physiological studies. A previous study using dopamine-β-hydroxylase (DBH) as a marker for NE axons suggested that only 11% of DBH+ terminals in the BLC form synapses (Asan, 1998). This suggests that the NE innervation of the BLC is mainly mediated by non-junctional, diffuse release of NE into the extracellular space. However, a later study indicated that approximately 31% of DBH+ terminals in the lateral amygdala (LA) form synaptic junctions (Farb et al., 2010). This discrepancy may be the result of different criteria for synapse identification or the nucleus studied. Because these studies analyzed single thin sections, rather than doing serial section analysis of synapses, it seems likely that the synaptic incidence may be higher than 31%.

Previous electron microscopy studies have shown that the major postsynaptic targets of DBH+ terminals were dendritic shafts and spines, but the cell types of origin of these structures were not identified (Asan, 1998, Farb et al., 2010). Although it has been reported that 4% of DBH + terminals formed synapses with GABA+ neuronal structures, presumably interneurons, another study from the same group also indicate that 30% of DBH+ terminals contacted interneurons which exhibit choline acetyltransferase

immunoreactivity (Li et al., 2001). These inconsistent results suggest that it is still not clear about the extent that NE terminals synapse with pyramidal neurons and interneurons in the BLC.

The purpose of the study in this chapter was to determine the synaptic incidence and postsynaptic targets of NE axon terminals in the anterior subdivision of the basolateral nucleus of the amygdala (BLa), the main nucleus responsible for NE-mediated memory consolidation (McGaugh, 2004). An antibody to the norepinephrine transporter (NET) protein was used to label NE axons since a previous study of this nucleus found that visualization of DBH immunoreactivity at the ultrastructural level required immunohistochemistry procedure that hindered morphological preservation of neuronal processes and synapses (Asan, 1998). This is the first EM study of the amygdala to use NET as a marker for noradrenergic axons. An antibody to the alpha subunit of calcium/calmodulin kinase Ⅱ (CaMK Ⅱ) was used to selectively label pyramidal cells (McDonald et al., 2002) in these dual-labeling studies. To obtain a more precise estimation of the synaptic incidence of the NE innervations of the BLa, a serial section analysis of NET+ terminals and their contacts was performed.

3.2 HYPOTHESIS

Most NE axon terminals will not form synapses in the BLa and if the NE axon terminals form synapses then their major postsynaptic targets in the BLa will be distal dendritic shafts and spines.

3.3 METHODS

3.3.1 TISSUE PREPARATION

Male Sprague-Dawley rats weighing 250-350g were used in these experiments. Rats were handled in accordance with the principles of laboratory animal care and protocols approved by the University of South Carolina Institutional Animal Care and Use Committee. Brain tissue was prepared as described in previous studies of our lab (Muller et al., 2011). For light microscopy, rats were anesthetized with chloral hydrate (350 mg/kg) and perfused intracardially with phosphate buffered saline (PBS; pH 7.4) containing 0.5% sodium nitrite (50ml) followed by 4% paraformaldehyde in phosphate buffer (PB; pH 7.4) for 20 mins. Then brains were removed and post-fixed in the perfusate for three hours. For electron microscopy, rats were anesthetized and perfused intracardially with PBS containing 0.5% sodium nitrite (50ml) followed by 2% paraformaldehyde-3.75% acrolein in PB for 1min, followed by 2% paraformaldehyde in PB for 3 mins. Brains were removed and post-fixed in 2% paraformaldehyde for 1 hr. Brains were sectioned on a vibratome in the coronal plane at 50μm.

3.3.2 LIGHT MICROSCOPY IMMUNOHISTOCHEMISTRY

Single-label localization of NET+ fibers was performed in two rats using a rabbit antibody to NET (1:2000, antibody 43411, obtained from Dr. Randy D. Blakely, Vanderbilt University Medical Center). All antibodies were diluted in PBS containing 0.4% Triton X-100 and 1% normal goat serum. Sections were incubated in the primary antibody overnight at 4℃ and then processed for the avidin-biotin immunoperoxidase technique using a biotinylated goat anti-rabbit secondary antibody (1: 500, Jackson Immunoresearch Laboratories, West Grove, PA) and a Vectastain standard ABC kit

(Vector laboratories, Burlingame, CA) with nickel-intensified 3,3 ´-diaminobenzidine 4HCl (DAB, Sigma Chemical Co., St. Louis, MO, USA) as a chromogen to generate a black reaction product (Hancock, 1986). After the reactions, sections were mounted on gelatinized slides, dried overnight, dehydrated in ethanol, cleared in xylene, and coverslipped in Permount (Fisher Scientific, Pittsburgh, PA, USA). Sections were analyzed with a Nikon E600 microscopy system and digital light micrographs were taken with a Micropublisher digital camera.

3.3.3 DUAL IMMUNOFLUORESCENCE IMMUNOHISTOCHEMISTRY

Dual localization studies were performed in two rats using the rabbit NET antibody (1:1000; see above) and a mouse monoclonal antibody to dopamine-beta-hydroxylase (DBH, 1:600; clone 4F10.2, catalog #MAB308, Chemicon International Inc.), the synthetic enzyme for norepinephrine, to determine the overlapping extent of NET immunoreactivity and DBH immunoreactivity in the BLa. Sections were incubated in PBS containing 0.4% Triton X-100 and 1% normal goat serum at room temperature for two hours, and incubated overnight at room temperature in a cocktail of the rabbit NET antibody and the mouse monoclonal DBH antibody. After incubation in the primary antibody cocktail, sections were rinsed in PBS and incubated in a cocktail of goat anti-rabbit Alexa-488 and goat anti-mouse Alexa-543 labeled secondary antibodies (1:400; Invitrogen, Grand Island, NY, USA) for 3h at room temperature. All secondary antibodies were highly cross-adsorbed by the manufacturer to ensure specificity for primary antibodies raised in the particular species. Sections were then rinsed in PBS and mounted on glass slides using Vectashield mounting medium (Vector Laboratories).

Sections were examined with a Zeiss LSM 510 Meta microscope. Fluoresence of Alexa 488 (green) and Alexa 543 (red) dyes was analyzed using filter configurations for sequential excitation via 488nm and 543nm channels. Digital images were adjusted for brightness and contrast using Photoshop 6.0 software. Control sections were processed with one of the two primary antibodies omitted and only the color of the corresponding secondary fluorescent antibody was observed on the appropriate channel in these sections. These results indicated that the secondary antibodies were specific for rabbit or mouse IgG and that there was no "crosstalk" between the red and green channels (Wouterlood et al., 1998).

3.3.4 ELECTRON MICROSCOPY DOUBLE LABELING IMMUNOHISTOCHEMISTRY

For electron microscopy studies, a sequential dual-labeling immunoperoxidase method was used in three rats to observe the NE innervation of pyramidal cells in the anterior subdivision of the basolateral nucleus of the amygdala (BLa) (bregma level -2.1 through -3.0) (Paxinos and Watson, 1986). To enhance penetration of antibodies, sections were either subjected to a freeze-thaw procedure or were incubated with low levels of Triton-X-100 (0.02-0.04%) in the antibody solutions. For freeze-thaw, sections were crypoprotected in 30% sucrose in PB for 3 hours, followed by three cycles of freezing-thawing over liquid nitrogen to facilitate antibody penetration. Sections were then rinsed in PB and incubated in a blocking solution (PBS containing 3% normal goat serum and 1% BSA) for 30 mins at room temperature. All antibodies were diluted in the blocking solution. Sections were incubated in the rabbit antibody to NET (1:2000) overnight at 4℃ and then processed using a biotinylated goat anti-rabbit second antibody for one hour

(Jackson Immunoresearch Laboratories, West Grove, PA) and a Vectastain standard ABC kit (Vector laboratories, Burlingame, CA) with DAB as the chromogen. After rinsing, sections were incubated in an avidin/biotin blocking solution (Vector Laboratories, Burlingame, CA). Sections were then incubated overnight at 4℃ in mouse anti-CaMK antibody (1:500; Sigma) to label pyramidal cells. For CaMK immunoreactivity, sections were processed using a biotinylated goat anti-mouse secondary antibody (1:200, Jackson Immunoresearch Laboratories) and an Elite ABC kit (Vector Laboratories). CaMK immunoreactivity was then visualized by using a Vector-VIP (Very Intense Purple) peroxidase substrate kit (V-VIP, Vector laboratories). This step produces a reaction product that appears purple in the light microscope and granular in the electron microscope, which was easily distinguishable from the diffuse DAB immunoperoxidase reaction product.

3.3.5 PROCEDURE FOR ELECTRON MICROSCOPY

After the immunocytochemical reactions, sections were post-fixed in 2% osmium tetroxide in 0.16 M sodium cacodylate buffer (pH=7.4) for 1 hour, dehydrated in ethanol and acetone, and then flat embedded in Polybed 812 (Polysciences, Warrington, PA) in slide molds between sheets of Aclar (Ted Pella, Redding, CA). Selected areas of the BLa were remounted onto resin blanks. Silver thin sections were collected on formvar-coated slot grids, stained with uranyl acetate and lead citrate, and examined with a JEOL-200CX electron microscope. Micrographs were taken with an AMT XR40 digital camera system (Advanced Microscopy Techniques, Danvers, MA)

3.3.6 ANALYSIS

Two 50μm vibratome sections from each animal were analyzed. From these sections, areas with robust presence of both labels were chosen for quantitative analysis. NET+ terminals

were followed and fully or partially reconstructed in 3 to 13 serial thin sections. Serial sections were helpful for verifying labels in small and/or lightly immunoreactive structures, and for determining synaptic contacts. NET+ varicosities were considered to form synapses if they showed the following characteristics: 1) parallel presynaptic and postsynaptic membranes exhibiting membrane thickening, 2) clustered vesicles associated with the presynaptic membrane, and 3) a synaptic cleft containing dense material. Postsynaptic neuronal profiles receiving synapses from NET+ varicosities were identified as somata, large caliber dendritic shafts (diameter >1 μm), small caliber dendritic shafts (diameter <1 μm), and spines according to established morphological criteria (Peters A, 1991). Although CaMK is a reliable marker for pyramidal cells and their processes in the BLa, many spines of the pyramidal cells do not exhibit CaMK immunoreactivity (McDonald et al., 2002). However, since the results of previous studies suggest that the great majority of spines observed in electron microscopy studies belong to pyramidal cells (Muller et al., 2006), all spines, whether CaMK + or not, were considered to be of pyramidal cell origin. Some NET+ terminals contacted glial cell processes. These glia cell processes were identified by their irregular shape and their tendency to fill the space between neuronal structures.

3.3.7 ANTIBODY SPECIFICITY

The NET antibody we used was obtained from the cytoplasmic NET epitope (amino acids 585-602). Previous study (Schroeter et al., 2000) has shown that this NET antibody labeling confined to NE neuronal somata, axons and dendrites, but absent from adrenergic and dopaminergic neurons. It recognizes a single 80-kDa band corresponding to the mature N-glycosylated NET protein in western blot of brain samples. Pre-adsorption with the peptide eliminates immunoblots and immunostaining of tissue sections. Additionally, its specificity was validated by the toxin treatment which destroys most of NE neurons. Meanwhile, CaMK antibody has been reported to be a reliable

marker for pyramidal cell perikarya and dendrites (McDonald and Mascagni, 2002). The specificity of CaMK antibody has been well documented in previous studies and it recognizes both phosphorylated and nonphosphorylated forms of the kinase (McDonald et al., 2002). Therefore, we use this NET and CaMK antibodies to find out how noradrenergic inputs synapse with pyramidal cells.

3.4 RESULTS

3.4.1 LIGHT MICROSCOPY OBSERVATIONS

NET+ axons were distributed across the basolateral nuclear complex of the amygdala (BLC). NET+ axons were denser in the BLa than in the lateral and central nuclei (Figure 3.1.A). NET+ axons had small or large varicosities with relatively short inter-varicose segments and ran in all directions (Figure 3.1.B). Dual localization experiments of NET and DBH revealed that almost all axons were dual-labeled (Figure 3.2). However, there were few varicosities that were DBH positive but NET negative, and some inter-varicose segments were NET positive but DBH negative (Figure 3.2.C).

3.4.2 ELECTRON MICROSCOPY OBERSERVATIONS

At the electron microscopy level, NET+ profiles consisted of thin unmyelinated axons and varicosities containing synaptic vesicles (Figures 3.3-3.5, 3.7-3.9). The peroxidase reaction product was distributed throughout these NET + profiles, with accumulations near the plasma membrane and the outer membrane of vesicles and mitochondria. NET+ terminals were round or ovoid, with closely packed small, round clear synaptic vesicles, sometimes associated with large clear vesicles (Figures 3.3-3.5, 3.7-3.9). Occasional medium size, dense-core vesicles were also seen (Figures 3.3.B and 3.7). These terminals ranged in size from 0.16 to 1.3 μm in diameter and some of them contained one or more mitochondria. The morphology of NET+ profiles was consistent

with descriptions of DBH+ profiles reported in previous studies of the basolateral amygdala. (Asan, 1998, Li et al., 2001, Li et al., 2002, Farb et al., 2010).

NET+ terminals formed synapses with both CaMK+ and unlabeled profiles in our dual-labeling preparations, and their postsynaptic targets include somata, large and small caliber dendrites, and spines (Figures 3.3-3.6) (Table 3.1). No direct contact with endothelial cells was observed, but in one case, a small NET terminal apposed a glial process which surrounded a blood vessel. The synaptic incidence of NET+ terminals was determined by examining each terminal in 3 to 13 serial thin sections, averaging 6.5 ± 2.3 (Mean ± SD). The average number of serial sections used to reconstruct terminals forming synapses (6.6 ± 2.4) was virtually identical to the non-synaptic terminals (6.5 ± 2.3). Terminals which lacked distinct contours or occurred in too few available sections to identify synapse formation were excluded from the analysis. About half (45/98 or 46%) of NET+ terminals formed synapses. The size of terminals forming synapses ranged from 0.2 - 0.96 µm in diameter, averaging 0.45 ± 0.19 µm (Mean ± SD). Terminals which did not form synapses ranged in size from 0.16 to 1.28 µm in diameter, averaging 0.61 ± 0.25 µm. Both symmetrical and asymmetrical synapses were observed, but symmetrical synapses were more common (38/45 or 84%) (Table 3.1).

Most (38/45 or 84%) of the synapses were formed with pyramidal cells (CaMK+ structures and spines) (Figures 3.3-3.5) (Table 3.1). The main postsynaptic target were small dendritic shafts (15/38 or 39%) (Figures 3.3.A, 3.3.B and 3.5.C) and spines (14/38 or 37%) (Figures 3.4 and 3.5.D). However, some also occurred on large dendritic shafts (8/38 or 21%) (Figures 3.3.C and 3.3.D), and one symmetrical synapse was found on a CaMK+ soma (Figures 3.5.A and 3.5.B). Synapses formed with unlabeled neuronal

processes, presumably interneurons, mainly targeted small dendritic shafts (Figure 3.7). In two instances, NET+ axons appeared to encapsulate an unlabeled axon terminal and its postsynaptic spine (Figures 3.8 and 3.9). In additional to the neuronal profiles, some NET+ terminals (7/98 or 7.1%) formed apposition with astrocytic processes that sometimes had characteristics of synapses (Figure 3.10).

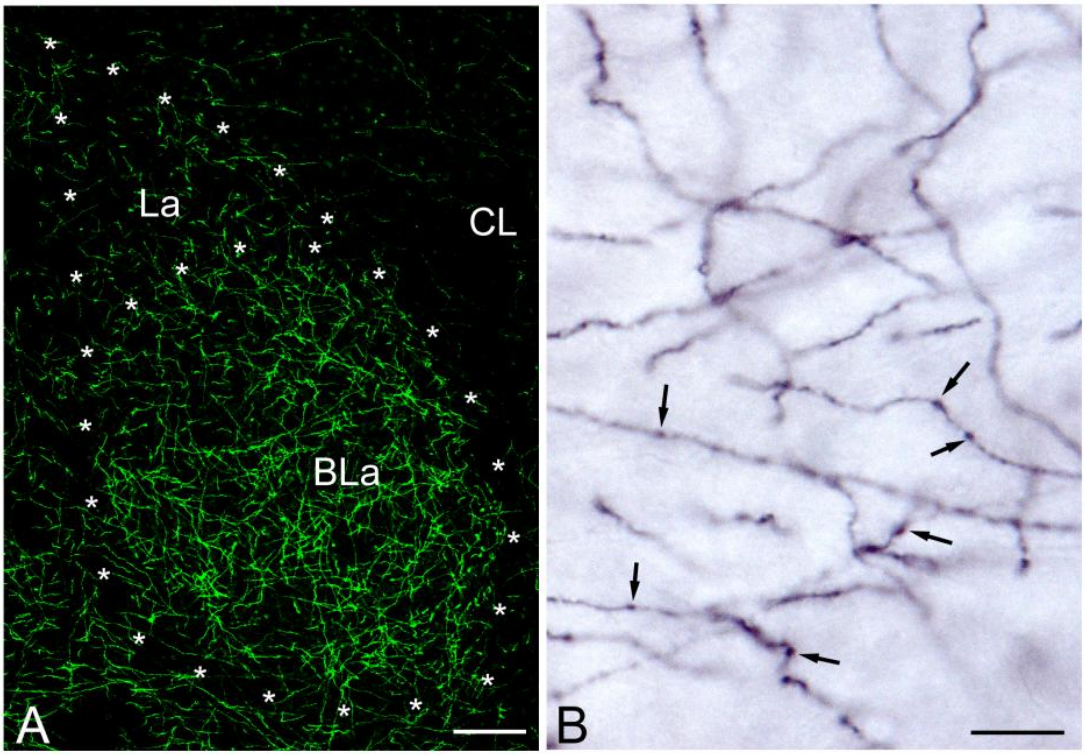

Figure 3.1 NET immunoreactivity in the BLa. **A,** Lower power immunofluorescence micrograph illustrating NET+ fibers (green) in the BLa, La (lateral nucleus) and CL (later subdivision of central nucleus) at bregma level -2.1. **B,** High power micrograph illustrating NET+ fiber morphology in the BLa using nickel-enhanced DAB as a chromogen in an immunoperoxidase preparation. Arrows point to the NET+ varicosities. Scale bar=100μm in A, 10μm in B

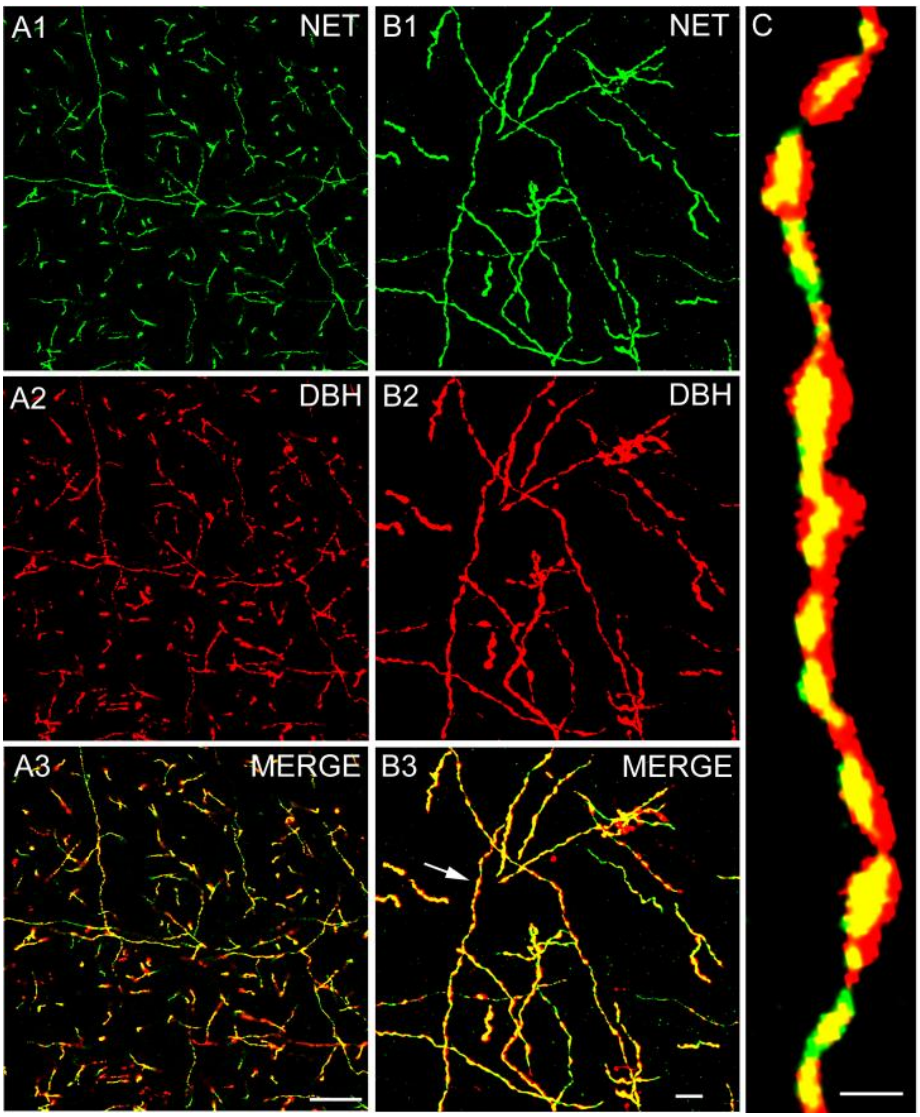

Figure 3.2 NET and DBH immunoreactivity in the BLa. **A1-A3:** Lower power immunofluorescence micrographs. (A1) Green channel micrograph showing NET antibody labeled axons in the BLa. (A2) Red channel micrograph showing DBH antibody labeled axons in the same field as A1. (A3) Merged image showing dual localization of NET and DBH in yellow. Virtually all axons are double-labeled. **B1-B3:** Higher magnification Z series reconstruction (1μm between optical sections for 12 sections) NET and DBH immunoreactivity in the BLa. (B1) NET (green) in the BLa. (B2) DBH (red) in the same field as B1. (B3) Merged image showing co-localization of NET and DBH in yellow. Virtually all axons are double-labeled (yellow). Arrows point to an axon segment which is enlarged in C. **C:** High power Z series reconstruction of an axon segment shown in B3. Double-labeled structure showing yellow. Scale bar=50μm in A1-3, 10μm in B1-3, 1μm in C

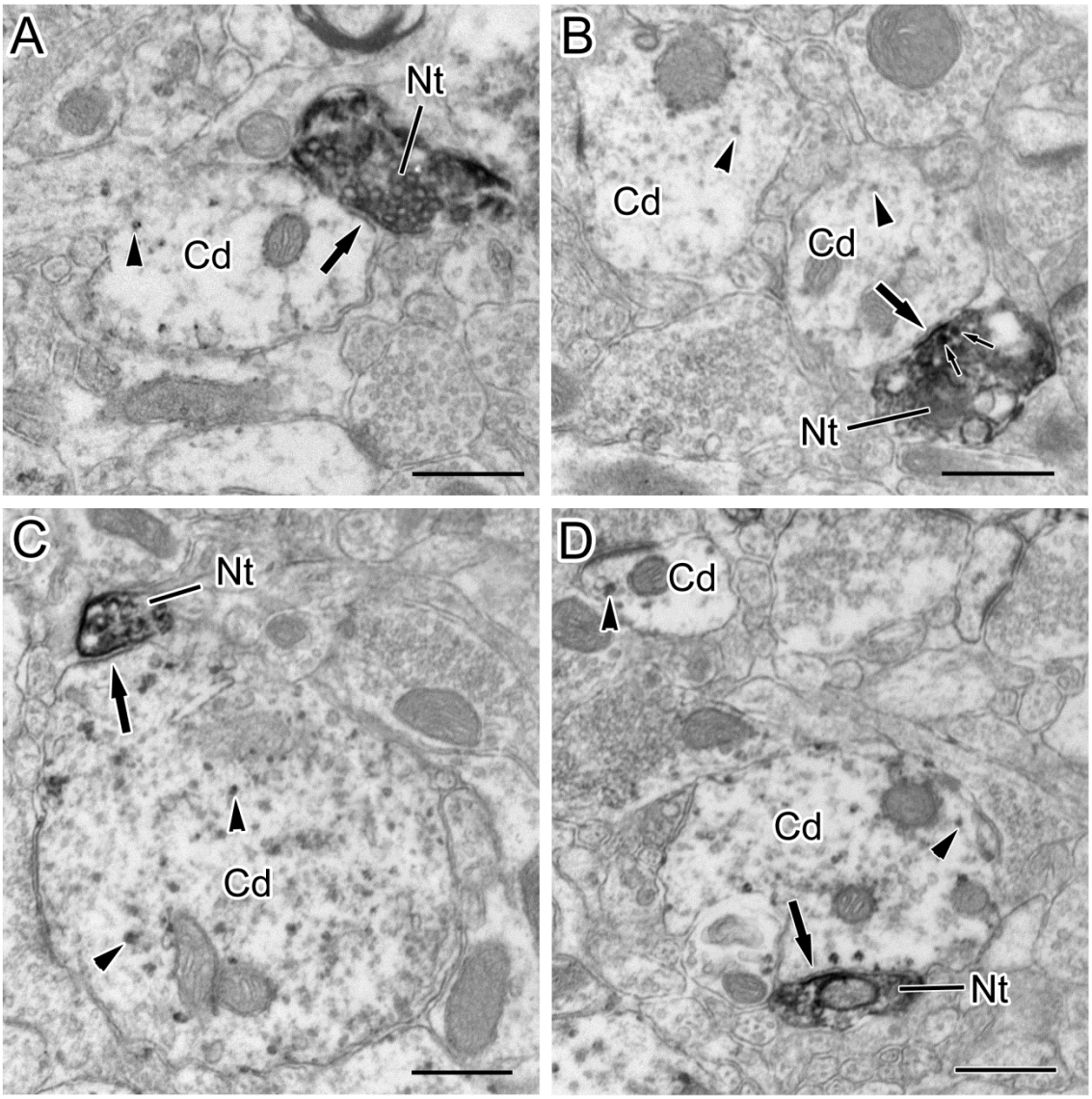

Figure 3.3 NET+ terminals innervate CaMK+ dendrites. **A and B:** NET terminals (Nt) form symmetrical synapses (arrows) with small caliber (<1 μm) CaMK+ pyramidal cell dendrites (Cd). The NET+ terminal in B contains two small dense core vesicles (small arrows). **C and D:** NET terminals (Nt) form symmetrical synapses (arrow) with large caliber (≥1 μm) CaMK+ pyramidal cell dendrites (Cd). Arrowheads indicate the particulate V-VIP label for CaMK. Scale bar=0.5μm.

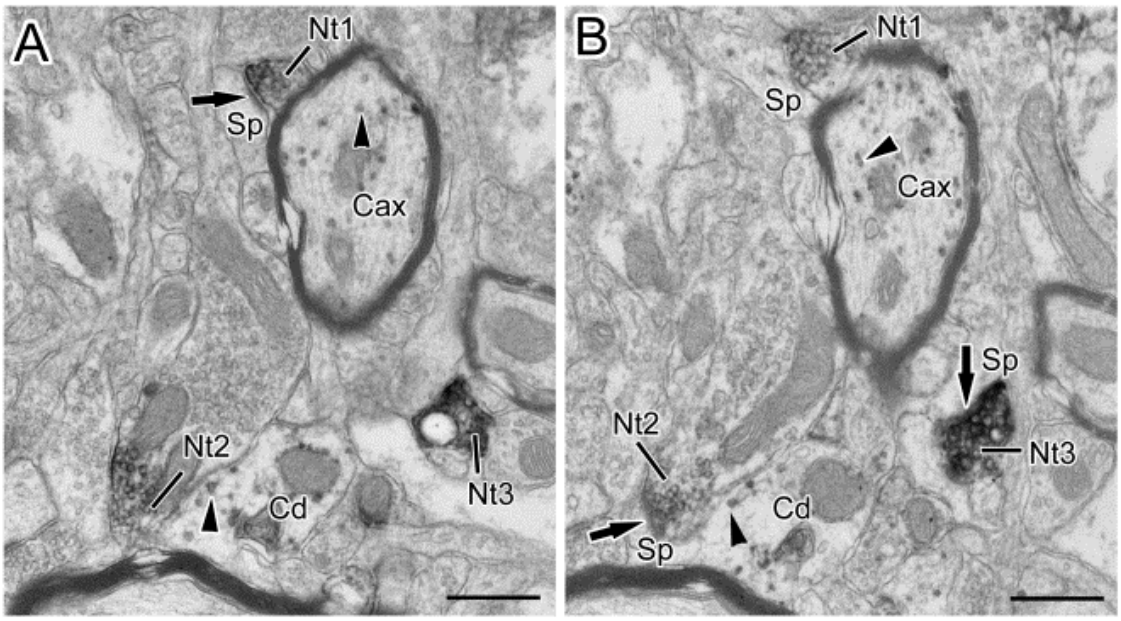

Figure 3.4 NET+ terminals innervate CaMK+ spines. **A and B:** Two adjacent thin sections through three NET+ terminals (Nt1-3) which form symmetrical (Nt2 in A and Nt3 in B) and asymmetrical (Nt 1 in A) synapses (arrow) with spines (sp). Arrowheads indicate the particulate V-VIP labels for CaMK. A and B are the 2nd and 3rd sections, respectively, from a 6-section series. Scale bar=0.5µm.

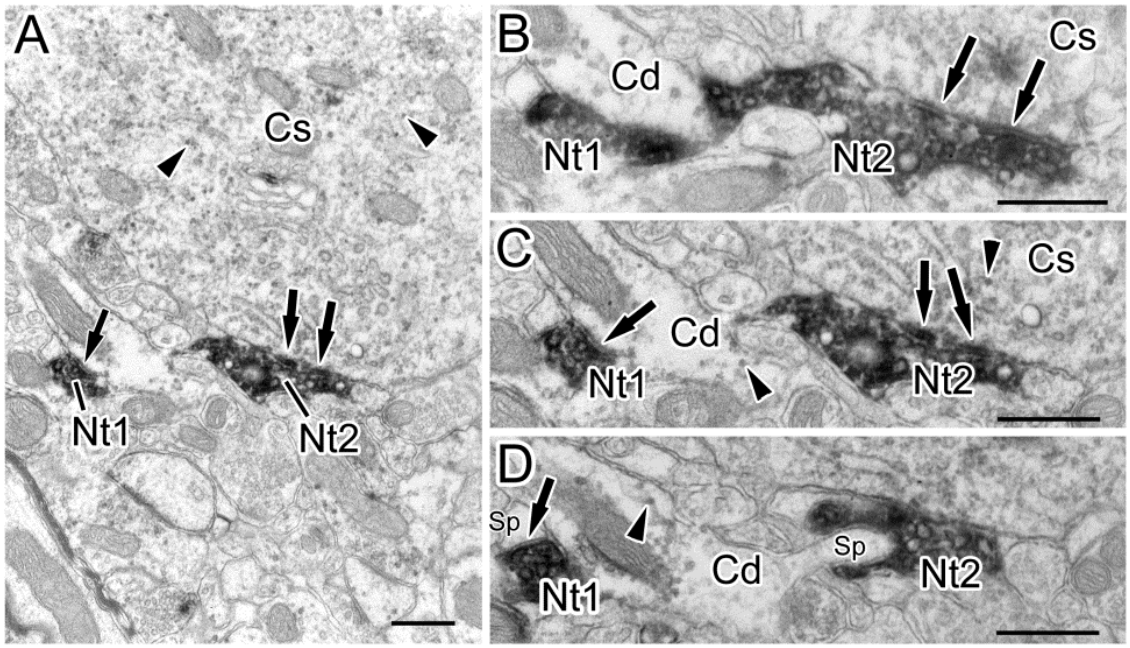

Figure 3.5 An NET+ axon forms multiple contacts with a CaMK+ pyramidal cell soma and adjacent CaMK+ dendritic processes. **A:** Low power micrograph showing two terminals (Nt1 and Nt2) of a single NET+ axon form symmetrical synapses (arrows) with a CaMK + dendrite (left) and a CaMK+ soma (right, Cs) **B-D:** High power micrograph showing three sections in a serial passing through the axon shown in A (C corresponds to the section shown in A). (B) Nt2 forms a symmetrical synapse (arrows) with a CaMK+ soma (Cs, also seen in C). (C) Nt1 forms a synapse (arrows) with a CaMK+ dendrite. This synapse appears symmetrical in this section, but appears to be associated with postsynaptic density in B. (D) Nt2 surrounds and forms a symmetrical synapse (arrow) with a spine (Sp, right) which is extending from a CaMK+ dendrite (Cd). Nt1 form a symmetrical synapse with another spine (Sp, left). Arrowheads indicate the particulate V-VIP labels for CaMK. B-D are the 12^{th}, 10^{th} and 8^{th} sections, respectively, from a 12-section series. Scale bar=0.5µm.

Table 3.1 Postsynaptic Targets of NET + terminals in the BLa in preparations dual labeled for NET and CaMK.

Postsynaptic Targets	+S	+LD	+SD	Sp	-S	-LD	-SD	Total Number
Symmetrical NET synapses	1 3%	7 18%	13 34%	12 32%	1 3%	0 0	4 10%	38 100%
Asymmetrical NET synapses	0 0	1 14%	2 29%	2 29%	0 0	1 14%	1 14%	7 100%
Total Number of NET synapses	1 2%	8 18%	15 34%	14 31%	1 2%	1 2%	5 11%	45 100%

Note: +: CaMK labeled; **-:** unlabeled; **S,** soma; **LD**, large dendrite (diameter ≥1 µm); **SD**, small dendrite (diameter <1 µm); **Sp**, spine. n=98.

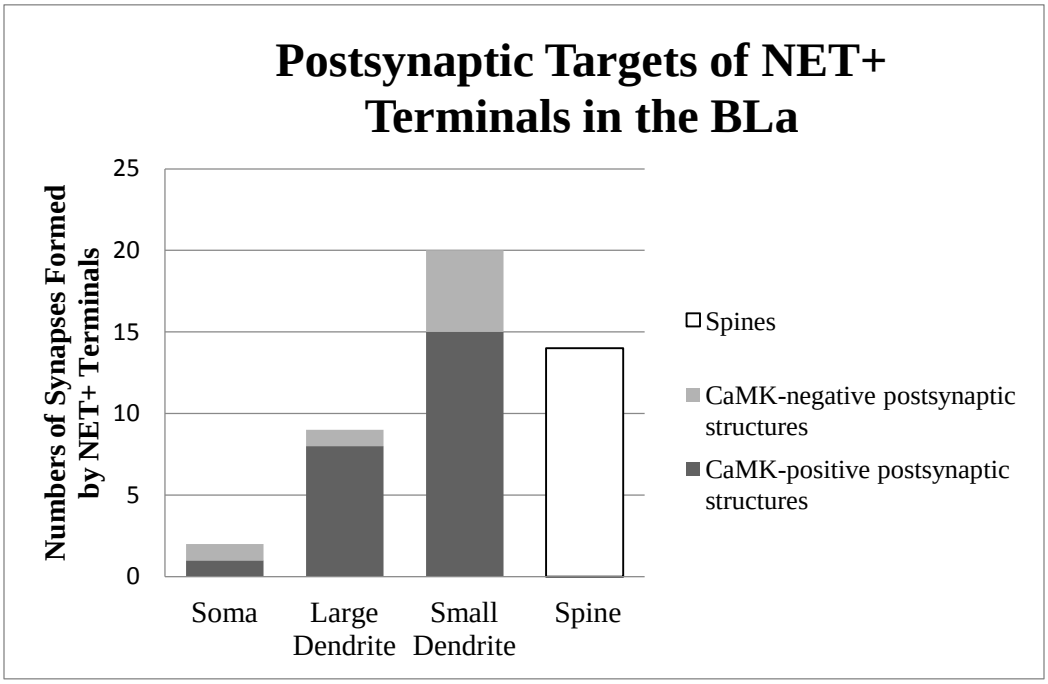

Figure 3.6 Histogram showing the number of synapses of NET+ terminals with CaMK positive (dark gray) or negative (light gray) and spines (white)

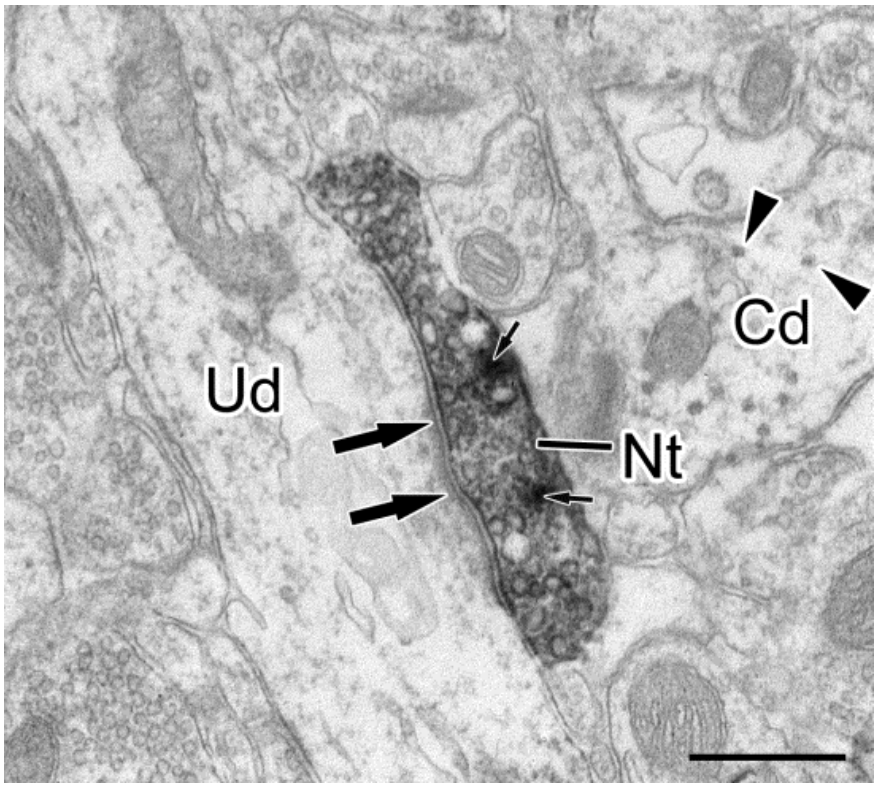

Figure 3.7 A NET+ terminal innervates an unlabeled dendrite. A NET+ terminal (Nt) forms an asymmetrical synapse (arrows) with an unlabeled dendrite (Ud). Arrowheads indicate the particulate V-VIP label for CaMK. Small arrows show the dense core vesicles. Scale bar=0.5μm.

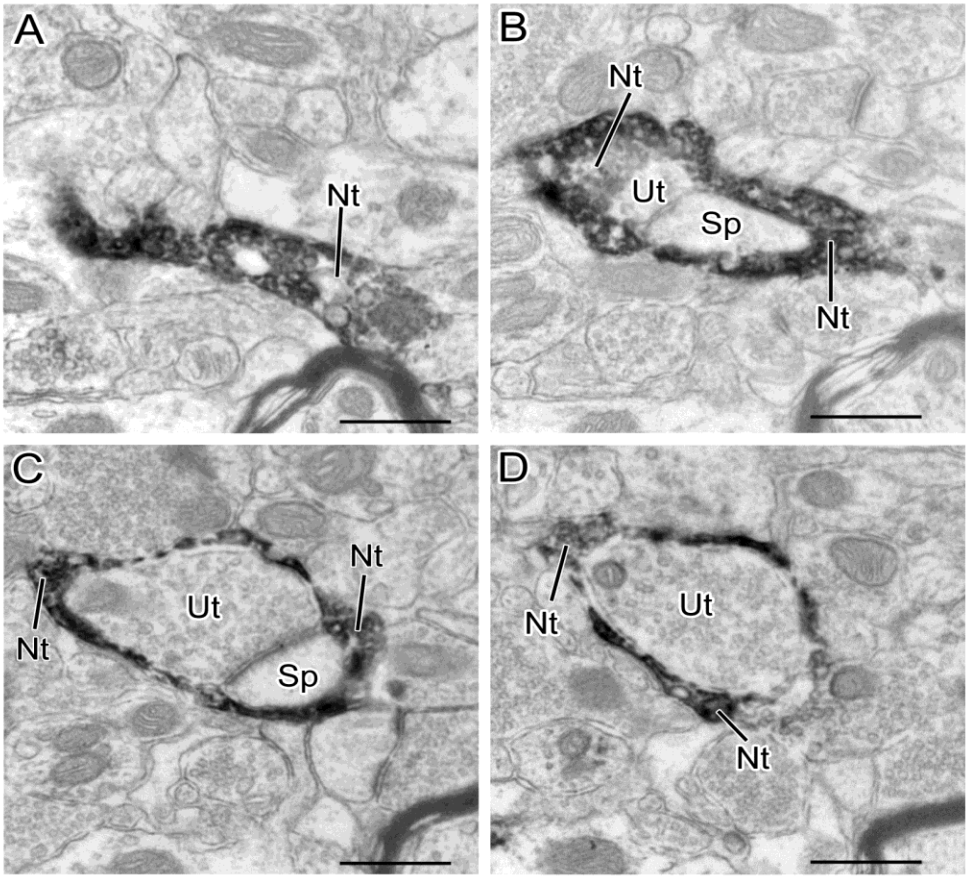

Figure 3.8 A NET+ terminal surrounds a synaptic structure. **A-D:** Four sections in sequential order from serial thin sections through an NET+ terminal (Nt) that envelopes a synapse formed by an unlabeled terminal (Ut) and its postsynaptic spine (Sp). The NET terminal (Nt) appears to form a synapse with the spine (Sp) in B. A-D are the 1st, 4th,8th, and 12th sections, respectively, from a 13-section series. Scale bar=0.5µm.

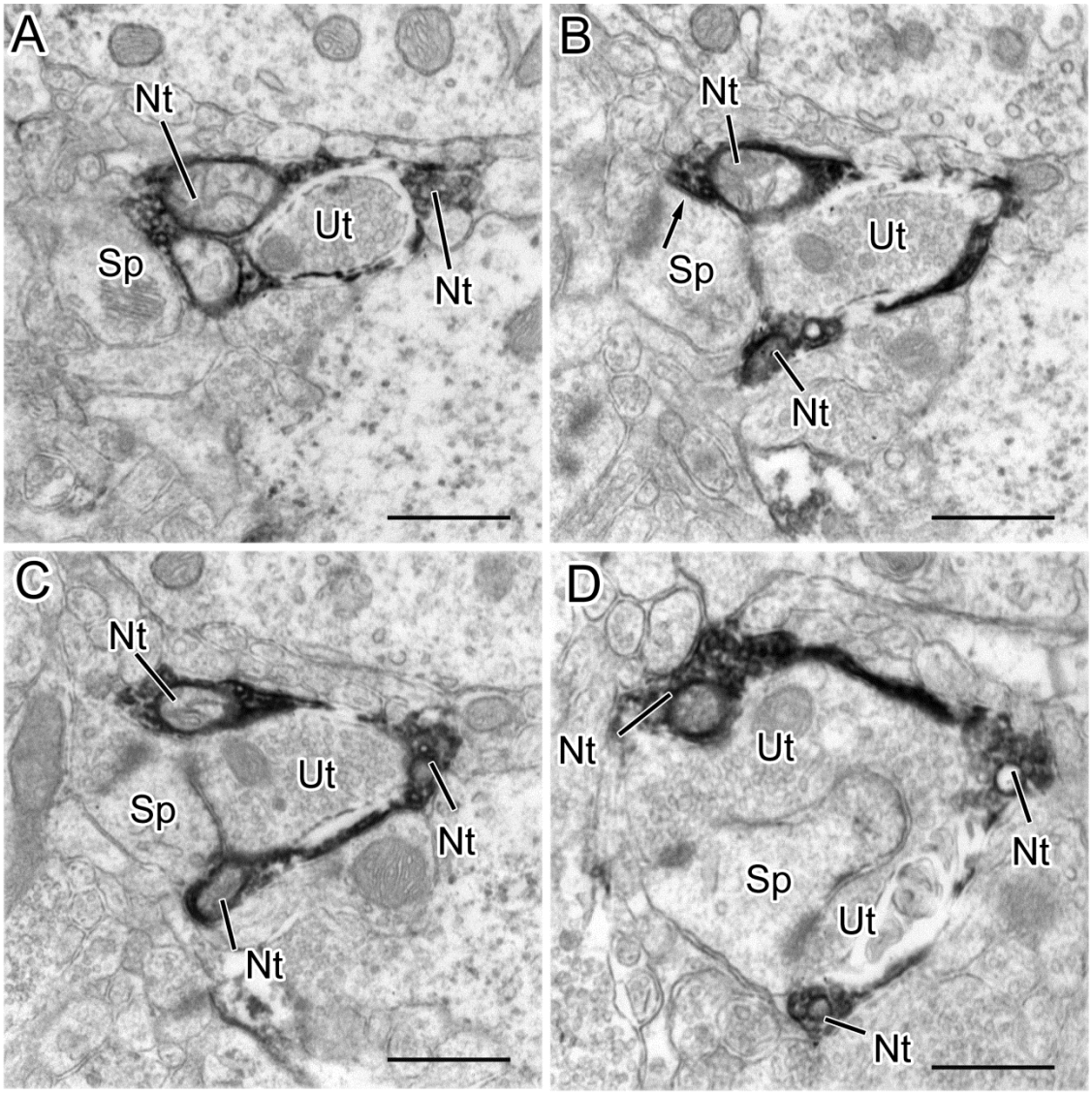

Figure 3.9 A NET terminal surrounds a synaptic structure. **A-D:** Four sections in sequential order from a series of sections through an NET+ axon terminal (Nt) that envelops a synapse formed by an unlabeled axon terminal (Ut) and its postsynaptic spine (Sp). The NET terminal appears to form a synapse with the spine in B (arrow). A-D are the 2nd, 6th, 8th and 12th sections, respectively, from a 12 section series. Scale bar=0.5µm.

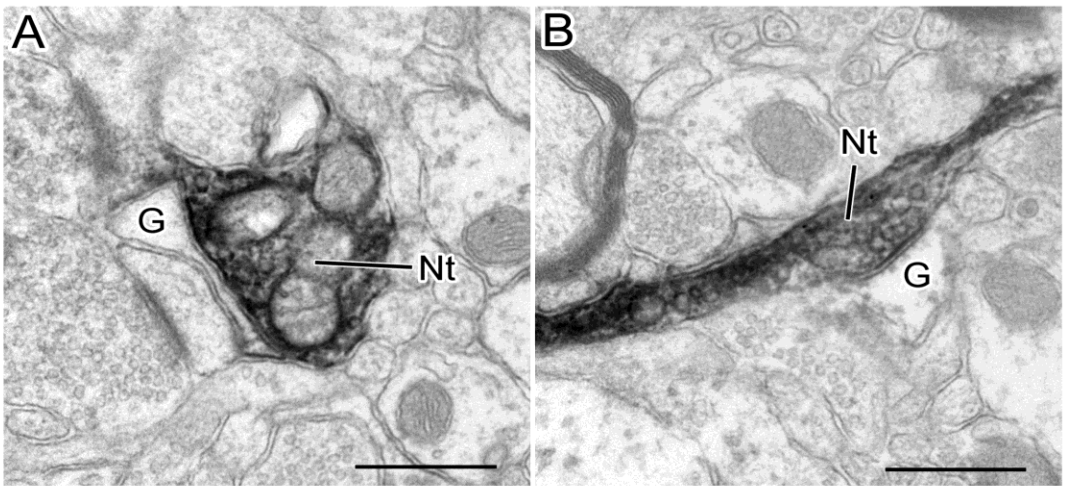

Figure 3.10 NET+ terminals contact with astrocytic processes. **A and B:** NET+ terminals (Nt) form synapse like contacts with astrocytic processes (G); Scale bar=0.5µm.

3.5 DISCUSSION

This is the first study to use NET as a marker for NE fibers in the amygdala. The distribution of NET immunoreactivity is consistent with observations of nisoxetine autoradiographic labeling of NET in the amygdala (Hipolide et al., 2005, Smith and Porrino, 2008). At both light and electron microscopy levels, the morphology of NET+ fibers in our investigation seems to be identical to that described in previous studies of cortex using the same antibody as a NE axon marker (Miner et al., 2003). Our dual labeling light microscopy results revealed that DBH was more concentrated in terminals, and NET tends to localize in the axons and terminals, but their staining mostly overlapped in the BLa. This is the first NE study in the BLa using CaMK immunohistochemistry to identify pyramidal cells. In addition, it is also the first NE study conducting serial section analysis, which should provide a relatively precise estimate of synaptic incidence. According to our observations, only half of the NET+ terminals form synapses in the BLa and the most frequent targets of these terminals are smaller dendritic shafts and spines of pyramidal cells.

3.5.1 ANATOMICAL CONSIDERATIONS

A previous study using DBH as a marker for NE axons suggested that 11% of DBH+ terminals in the basolateral complex of the amygdala formed synapses (Asan, 1998). However, a later study suggested that approximately 31% of DBH terminals in the LA formed synaptic junctions (Farb et al., 2010). The discrepancy may represent differences in synapse identification criteria, experimental methods, or the nucleus studied. A stronger fixation (acrolein) may have contributed to the higher synapse incidence in Farb's results. We used acrolein in our study, but the higher (46%) synaptic incidence is most likely due to the analysis of serial sections. However, only some of the

NET+ terminals were completely followed during our observation since the average analyzed distance (average section numbers for analysis × section thickness =0.42 μm) is less than the average size of NET+ axon terminal (0.52 μm). It is possible that we missed some of the synaptic formations. Moreover, if the plane of section is not favor for the synapses, we might also miss them. It seems that the actual synaptic incidence of NE in the BLa may be higher than 46%.

However, this number (46% or even higher) is still much lower than the synaptic incidence of other neurotransmitters in previous BLa studies of our lab, such as serotonin (76%), dopamine (77%) and acetylcholine (76%), which used the same technique and analysis strategy (Muller et al., 2007, 2009, Muller et al., 2013). This indicates that the NE system is unique in the BLa. This suggests that NE axons in the BLa function partly by non-junctional, diffuse release of NE in the extracellular space.

There are similar disagreements about noradrenergic synaptic incidence in the rat cortex. An early study using DBH immunohistochemistry revealed that more than half of the DBH-positive varicosities form synapses in the central nervous system (Olschowka et al., 1981) and the vast majority of noradrenergic projections form synapses in the visual and frontoparietal cortex (Papadopoulos et al., 1989). Later studies suggested that only 15-20% of NE terminals form synapses in neocortex and hippocampus (Seguela et al., 1990, Umbriaco et al., 1995). However, a recent study reported a higher percentage (24%) of synapse formation in the prefrontal cortex using NET as a marker for NE axons. (Miner et al., 2003). These differences in synaptic incidence appear to be due to differences in criteria for synapse identification, fixation, cortical area studied, and the extent of serial section analysis.

Consistent with previous investigations in the amygdala, NET+ terminals mainly synapsed with dendrites and spines; very few were seen with somata. Our double labeling preparations revealed that CaMK+ smaller dendrites and spines were the most frequent postsynaptic targets of noradrenergic system in BLa. Thus, the synaptic modulation of the BLA by NE afferents from LC would appear to be mediated primarily by inputs to the distal dendrites of pyramidal cells.

It has been reported that 4.4% of DBH+ terminals form synapses with dendrites of GABA+ interneurons in BLa (Li et al., 2002). We observed a higher rate of synapse formation (16%) with unlabeled neuronal structures, (i.e., presumptive interneurons), but it is possible that some of these unlabeled structures were false negatives. Li and colleagues only observed asymmetrical synapses with interneurons, but we found that NET+ terminals also formed symmetrical synapses with unlabeled dendrites.

Although both symmetrical and asymmetrical synapses were found in our preparations, NET+ terminals predominantly formed symmetrical synapses with both labeled and unlabeled structures, which is consistent with previous reports (Asan, 1998, Farb et al., 2010). Since symmetrical synapses are typically inhibitory and the asymmetrical ones are excitatory, the general effect of NE inputs on the BLa neurons possibly is inhibitory. But, this assumption is based on the glutamate and GABA systems; it may not be true if applying to other neurotransmitter systems, like NE. For example, almost all cholinergic synapses in the BLa are symmetrical, but acetylcholine mainly has excitatory effects on BLa neurons (Muller et al., 2011). The presence of symmetrical or asymmetrical synapses may represent different types of receptors. Previous studies have found that there are several different subtypes of alpha and beta adrenergic receptors

expressed in BLa neurons. For example, Farb reported that β-adrenergic receptors are present in pyramidal and interneuron cell bodies, dendritic shafts and spines in the LA (Farb et al., 2010). An earlier study revealed that NE directly excited interneurons via the α1 adrenergic receptor in BLa (Kaneko et al., 2008).

Interestingly, we observed that two NET+ terminals send out sheet-like extensions that envelope an unlabeled terminal and its postsynaptic spine. Both of these NET+ terminals appeared to form symmetrical synapse with the spine. This unique structure has also been seen in the frontal cortex ((Seguela et al., 1990). However, it is not clear about the functional significance of this kind of configuration. This NET+ enclosure may isolate the unlabeled synapses from surrounding structures and thus make it only under NE control.

We observed some synapse-like appositions of NET+ terminals with astrocytic processes suggesting neuronal-glial interactions. This finding is consistent with previous observations of the astrocytic localization of β-adrenergic receptors in rat brain (Aoki, 1992, Farb et al., 2010).

3.5.2 FUNCTIONAL IMPLICATIONS

Considering that only about half of NET+ terminals form synapses in the BLa, non-junctional, diffuse release of NE into the extracellular space could be involved in NE modulation of BLa functions. This intercellular communication mode, called volume transmission (VT), was first introduced by Agnati and Fuxe (Agnati et al., 1986). Unlike traditional junctional or wired transmission (WT), VT lacks any wire-like channel connecting signal sources and targets. VT utilizes the same set of neurotransmitters and receptors as WT, but VT signals can be released from axons without synaptic membrane specialization, and they could diffuse in the extracellular space for a long distance

(Agnati et al., 2010). VT is principally responsible for the tonic control of brain function through extrasynaptic receptors, and most CNS drugs primarily affect VT instead of WT (Vizi et al., 2010).

Moreover, unlabeled terminals were found in the vicinity of some NET+ terminals including the sheet-like structures mentioned earlier, but they don't have synaptic contact with NET+ terminals. This finding suggests that presynaptic effects of NE on BLa neuronal circuit may come from NE released from non-synaptic junctions by VT or spillover from synaptic terminals (Huang et al., 1996, Ferry et al., 1997, Braga et al., 2004).

LC neurons fire in two distinct activity modes: tonic and phasic (Berridge and Waterhouse, 2003). The synaptic formations we observed in the present study seem to contribute to the NE release in the BLa during the phasic mode activity of the LC in response to salient sensory stimuli like footshock as well as direct electrical stimulation of the LC in vivo since the response of the BLa neuron has a relative short latency and a temporal relationship with the excitation of LC neurons (Chen and Sara, 2007). Nonsynaptic transmission may contribute to tonic NE release in the BLa which is essential for arousal and attention (Berridge and Waterhouse, 2003).

BLa neurons exhibit heterogeneous, but prominently, inhibiting responses to phasic LC activation (Chen and Sara, 2007). Studies using iontophoresis of NE into the BLa found similar results (Buffalari and Grace, 2007). Responses were observed in putative pyramidal neurons and interneurons identified based on firing rate and antidromic activation by cortical stimulation (Buffalari and Grace, 2007, Chen and Sara,

2007). Therefore our finding that NET+ terminals primarily synapse with CaMK+ pyramidal projection neurons is consistent with these electrophysiological results.

Previous studies revealed that increasing the activity of NE system has multiple actions on different types of neurons in the BLC (Chen and Sara, 2007, Buffalari and Grace, 2009), which is mediated by different types of adrenoceptors. It has been shown that NE inputs to BLC exert potent α2 adrenergic receptor mediated inhibition of spontaneous activity and attenuation of evoked activity for most pyramidal cells, but NE also has excitatory effects mediated by β adrenergic receptors for a small portion of pyramidal cells in BLC (Buffalari and Grace, 2007). Together with our findings, these observations suggest that the effect of NE inputs on neuronal activity was determined by localization of the adrenergic receptors expressed on BLa neurons. Further investigations on the distribution and expression of different types of adrenergic receptors in BLa neurons and glia will help to unravel how NE circuits modulate amygdalar activity.

Studies in humans and animals have shown that noradrenergic activation in the amygdala is essential for the formation and recall of memories involving emotional events (Berridge and Waterhouse, 2003, McGaugh, 2004). The N-methyl-D-aspartate (NMDA) receptor is known to play a key role in synaptic plasticity underlying learning and memory (Sigurdsson et al., 2007). Previous studies in rat BLa have shown that both pyramidal cells and non-pyramidal cells exhibit NMDA receptor subunit 1 (NMDAR1) immunoreactivity, and NMDAR1 is located in the dendrites and spines (McDonald, 1994b, Farb et al., 1995, Radley et al., 2007) . According to our observations, distal dendritic shaft and spines are the major postsynaptic targets of NE inputs in the BLa,

which suggests that NE inputs could affect synaptic plasticity by modulating NMDA receptor activities.

CHAPTER 4

MU OPIOID RECEPTOR LOCALIZATION IN THE RAT BASOLATERAL AMYGDALA

4.1 INTRODUCTION

The endogenous opioid system plays an important role in the process of stress adaptation by attenuating or terminating stress responses (Drolet et al., 2001). Endogenous opioid peptides including enkephalin, dynorphin and endorphin, produce their effects via three major types of G-protein coupled receptors: mu, delta, and kappa (Drolet et al., 2001). Preproenkephalin knock-out mice which have an endogenous deficit in enkephalin, elicit stronger anxiety and depressive PTSD-like symptoms than wild type animals (Kung et al., 2010). Overexpression of preproenkephalin in the amygdala potentiates the anxiolytic effects of benzodiazepine (Kang et al., 2000). Considerable evidence indicates that mu opioid receptors (MORs) in the BLA are also involved in stress related hypoalgesia (Helmstetter et al., 1995, Helmstetter et al., 1998, Shin and Helmstetter, 2005). Although BLA neurons do not directly project to nociceptive areas such as the periaqueductal gray (PAG), the BLA has extensive connections with the central amygdala which has dense reciprocal connections with the PAG (Hopkins and Holstege, 1978, Rizvi et al., 1991, Harris, 1996). It is believed that MORs activation reduces the GABA inhibition to pyramidal neurons in the BLA by modulating the presynaptic potassium channels and therefore affects the neurotransmission in this BLA to PAG pathway (Helmstetter et al., 1998, Finnegan et al., 2006, Sah, 2006). Additionally, the opioid system in the BLa has been reported to be involved in regulating memory storage: the opiate antagonist

naloxone has been found to enhance retention in inhibitory avoidance and this effect can be reversed by the mu opioid receptor (MOR) agonist DAMGO (Introini-Collison et al., 1995).

Naloxone mainly binds to MOR, the most widely distributed opioid receptor in rat brain (Mansour et al., 1987, Paden et al., 1987). Autoradiographic receptor binding studies found that the amygdala contains dense MORs, and the BLA has a greater abundance of MORs than the central amygdala (Mansour et al., 1987). Despite the fact that MOR activation in the BLA is highly involved in regulation of stress response and memory consolidation, little is known about how MOR affects neural activity in the BLA. Knowledge about the ultrastructural localization of MORs in the BLA may help us understand the underlying mechanism of opioid action. Electron microscopy combined with immunocytochemistry was used in the present investigation to study the ultrastructural localization of MORs in the BLa.

Early electrophysiological studies have shown that MOR activation can hyperpolarize a subpopulation of interneurons and also disinhibit pyramidal cell by inhibiting GABA release in the BLA, indicating that MORs may present in the cell bodies, dendrites and axon terminals of some interneurons (Sugita and North, 1993). One later study found that MOR activation also inhibits pyramidal cells via activating a potassium current in their dendrites in the BLA, suggesting that MORs may be expressed in the dendrites of pyramidal cells as well (Faber and Sah, 2004).

4.2 HYPOTHESIS

MORs are located in somata, dendrites and axon terminals of neurons in the BLa.

4.3 METHODS

4.3.1 TISSUE PREPARATION

A total of five male Sprague-Dawley rats weighing 250-350g were used in this study. Rats were handled in accordance with the principles of laboratory animal care and protocols approved by the University of South Carolina Institutional Animal Care and Use Committee. Rats were anesthetized with a ketamine mixture (ketamine: 85mg/kg; xylazine: 8mg/kg; acepromazine: 4mg/kg) and perfused intracardially with PBS containing 1% sodium nitrite, followed by 2% paraformaldehyde-3.75% acrolein in phosphate buffer(PB) for 1 minute, followed by 2% paraformaldehyde in PB for 20 minutes. Brains were removed and post-fixed in 2% paraformaldehyde for one hour. Brains were sectioned on a vibratome in the coronal plane at 60 μm.

4.3.2 LIGHT MICROSCOPY IMMUNOHISTOCHEMISTRY

Light microscopy MOR localization was performed in rats using a rabbit antibody to MOR antibody (1:1000, ImmunoStar, Hudson, WI). All antibodies were diluted in PBS containing 0.4% Triton X-100 and 1% normal goat serum. Sections were incubated in the primary antibody overnight at 4℃ and then processed for the avidin-biotin immunoperoxidase technique using a biotinylated goat anti-rabbit secondary antibody (1: 500, Jackson Immunoresearch Laboratories, West Grove, PA) and a Vectastain standard ABC kit (Vector laboratories, Burlingame, CA) with nickel-intensified 3,3 ´- diaminobenzidine 4HCl (DAB, Sigma Chemical Co., St. Louis, MO, USA) as a chromogen to generate a black reaction product (Hancock, 1986). After the reactions, sections were mounted on gelatinized slides, dried overnight, dehydrated in ethanol, cleared in xylene, and coverslipped in Permount (Fisher Scientific, Pittsburgh, PA, USA).

Sections were analyzed with a Nikon E600 microscopy system and digital light micrographs were taken with a Micropublisher digital camera.

4.3.3 ELECTRON MICROSCOPY IMMUNOHISTOCHEMISTRY

Immunoperoxidase methods were used to observe the ultrastructural localization of MORs in the BLa. Sections were incubated in the MOR antibody (1:1000, ImmunoStar, Hudson, WI) with 0.02% Triton-X overnight in a cold room after 30 minutes in a blocking solution (PBS containing 3% normal goat serum , 1% BSA and 0.02% Triton-X). All antibodies were diluted in the blocking serum. Then sections were processed using a biotinylated goat anti-rabbit antibody (1:500, Jackson ImmunoResearch, West Grove, PA) and a Vectastain standard ABC kit (Vector Laboratories, Burlingame, CA). MOR immunoreactivity was then visualized using a Vector-VIP (Very Intense Purple) peroxidase substrate kit (Vector Laboratories, Burlingame, CA). This step produced a reaction product that appears purple in the light microscope and granular in the electron microscope.

4.3.4 PROCEDURE FOR ELECTRON MICROSCOPY

Sections were then post-fixed in 2% osmium tetroxide in 0.16 M sodium cacodylate buffer for one hour, dehydrated in ethanol and acetone, and flat embedded in Polybed 812 (Polysciences, Warrington, PA) in slide molds between sheets of Aclar (Ted Pella, Redding, CA). Selected areas of the BLa were remounted onto resin blanks. Silver thin sections were collected on formvar-coated slot grids, stained with uranyl acetate and lead citrate and examined with a JEOL-200CX electron microscope. Micrographs were taken with an AMT XR40 digital camera system (Advanced Microscopy Techniques, Danvers, MA).

4.3.5 ANALYSIS

Vibratome sections from three rats (one for each animal) with the best labeling quality were selected for thin sectioning and analysis. From these sections, areas with the best morphology and immunohistochemistry for MORs were chosen for quantitative analysis. About 3600 μm^2 area from each section was used for counting and a total of 2378 labeled profiles were counted. Numbers from three rats were pooled together for analysis. Medium or large structures (≥0.2μm) were counted as labeled only if they contained two or more labeled granules. Small structures (<0.2μm) were counted as long as they contained one labeled granule. MOR+ profiles were identified as somata, large caliber dendritic shafts (diameter ≥1μm), small caliber dendritic shafts (diameter <1μm), spines, axons, axon terminals, and glia processes according to established morphological criteria (Peters A, 1991). MOR labeled terminals were followed and fully or partially reconstructed in 3 to 13 serial thin sections. Serial sections were helpful for verifying label in small and/or lightly immunoreactive structures, and for determining synaptic contacts. MOR labeled terminals were considered to form synapses if they showed the following characteristics: 1) parallel presynaptic and postsynaptic membranes exhibiting membrane thickening, 2) clustered vesicles associated with the presynaptic membrane, and 3) a synaptic cleft containing dense material. Asymmetrical and symmetrical synapses were identified based on the presence or absence of a prominent postsynaptic density and the widths of their synaptic clefts. Asymmetrical synapses usually have wider synaptic clefts (20nm) than symmetrical ones (12nm) (Peters A, 1991). Postsynaptic neuronal profiles receiving synapses from MOR labeled terminals were identified as MOR labeled or unlabeled somata, large caliber dendritic shafts (diameter ≥1μm), small

caliber dendritic shafts (diameter <1μm), or spines according to established morphological criteria (Peters A, 1991)

4.3.6 ANTIBODY SPECIFICITY

The rabbit polyclonal MOR antiserum (ImmunoStar, Cat. 24216) used in this study was raised against a synthetic peptide corresponding to amino acids 384-398 of the carboxyl terminus of the rat MOR1 coupled to bovine thyroglobulin with glutaraldehyde. Specificity of this antibody has been well documented in previous studies (Gracy et al., 1997, Deng et al., 2007, Likhtik et al., 2008). An earlier study in our lab demonstrated that pre-absorption of the MOR antiserum with MOR eliminated all immunostaining, but cross-absorption of MOR antiserum with non-matching peptides did not affect immunostaining (Wilson et al., 2002).

4.4 RESULTS

4.4.1 LIGHT MICROSCOPY OBSERVATIONS

At the light microscopy level, MOR immunoreactivity (MOR-ir) presents a wide uneven distribution through the amygdala, consistent with the dense but differential DAMGO binding in the individual amygdala nuclei observed in the autoradiographic binding studies (Mansour et al., 1987). Strongest staining was found in the intercalated nuclei (Figure 4.1). Much lighter neuropil labeling was observed in the basolateral amygdala (Figure 4.1.A). Few interneurons were found labeled in their somata and processes in both the BLa and lateral nucleus of the amygdala (Figure 4.1.B). These findings are consistent with previous light microscopy immunohistochemistry studies (Ding et al., 1996, Wilson et al., 2002).

4.4.2 ELECTON MICROSCOPY OBSERVATION

At the electron microscopy level, MOR positive (MOR+) structures included somata, dendritic shafts, spines, axon terminals, thin unmyelinated or myelinated axons, and glia processes (Figure 4.2). Only three MOR+ somata were found in our preparations. One MOR+ soma had a round smooth nuclear membrane and a modest amount of cytoplasm, which are characteristics of pyramidal cells (Figure 4.3.A). In the other case, a soma received multiple asymmetrical synapses, typical of interneurons (Figure 4.3.B). In these MOR+ somata, the MOR-ir was seen in the cytoplasm and was found associated with the Golgi apparatus or endoplasmic reticulum (Figure 4.4).

The most frequently labeled structures in the neuropil were dendritic structures. Counts of MOR+ profiles revealed that large-caliber dendrites, small caliber dendrites and spines comprised 11.1% (265/2378), 50.5% (1200/2378) and 10.8% (258/2378) of all MOR+ profiles, respectively (Figures 4.2, 4.4-4.6). It is impossible to definitely identify the cell type of origin of these MOR+ dendrites, based only on their morphological features. Nevertheless, the presence of spines on some MOR+ dendrites suggests that they may belong to pyramidal cells (Figures 4.4.B, 4.5.B and 4.5.C) (Muller et al., 2006) . We also found several dendrites received multiple asymmetrical synapses (Figure 4.4.C), which is a characteristic of interneuronal dendrites in the BLa (Muller et al., 2011). MOR-ir in these labeled dendrites and spines was mainly cytoplasmic (Figures 4.4-4.6 and 4.8), but MOR+ labeling near the plasma membranes was observed in many cases as well (Figures 4.5and 4.8).

MOR-ir was also seen in small unmyelinated or myelinated axons, but only in a few cases. However, MOR labeling was commonly observed in axonal terminals,

constituting 20.9% (497/2378) of MOR+ profiles (Figure 4.2). V-VIP particulate reaction product in these MOR labeled terminals was often associated with synaptic vesicles, near the active zone or occurred randomly in the varicosities (Figures 4.3.A, 4.4.C, 4.5.A, 4.5.C and 4.8). About 40% (197/497) of MOR+ terminals formed synapses. MOR+ terminals formed synapses with both labeled and unlabeled profiles, and their postsynaptic targets included somata, large and small dendritic shafts, and spines (Figures 4.3.A. 4.4.C 4.7 and 4.8) (Table 4.1). Both asymmetrical (82%, 162/197) and symmetrical synapses (18%, 35/197) were observed, but asymmetrical synapses were more common (Figures 4.3.A, 4.4.C, 4.7 and 4.8) (Table 4.1). The main postsynaptic targets of MOR+ terminals were unlabeled spines (61%, 121/197, asymmetrical 97% symmetrical 3%), labeled spines (13%, 25/197, asymmetrical 80%, symmetrical 20%) and labeled small caliber dendritic shafts (13%, 25/197, asymmetrical 44%, symmetrical 56%) (Figures 4.3.A, 4.4.C, 4.7) (Table 4.1). Some MOR + terminals form large asymmetrical synapses, suggesting that they might be glutamatergic (Figures 4.8.C-E) (LeDoux et al., 1991, Stefanacci et al., 1992, Brinley-Reed et al., 1995).

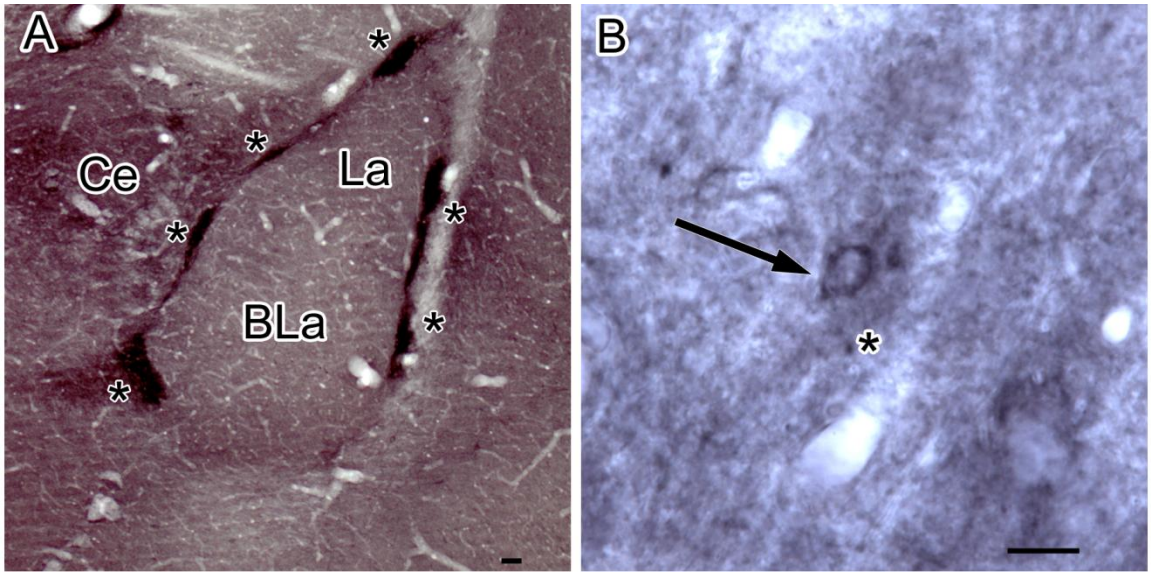

Figure 4.1 Light micrographs of MOR immunohistochemistry in the BLa using nickel-DAB as a chromogen in an immunoperoxidase preparation. **A:** Low power micrograph illustrating MOR immunohistochemistry in the BLa, lateral nucleus (La), central nucleus (Ce) and intercalated nuclei (stars) at bregma level -2.1. **B:** High power micrograph illustrating one MOR+ interneuron (arrow) and nearby MOR+ punctate structure (star), possibly a MOR+ dendritic shaft. Scale bar=50μm in A; 10μm in B.

Table 4.1 Postsynaptic targets of MOR+ terminals in the BLa**.**

	So-	**LD-**	**SD-**	**Sp-**	**So+**	**LD+**	**SD+**	**Sp+**	**Total**
Asymmetrical MOR+ Synapses	0 0	3 1.9%	8 4.9%	117 72.3%	1 0.6%	2 1.2%	11 6.8%	20 12.3%	162 100%
Symmetrical MOR+ Synapses	2 5.7%	0 0	2 5.7%	4 11.4%	1 2.9%	7 20%	14 40%	5 14.3%	35 100%
Total MOR+ Synapses	2 1%	3 1.5%	10 5.1%	121 61.4%	2 1%	9 4.6%	25 12.7%	25 12.7%	197 100%

Note: So-: Unlabeled Soma; **LD-:** unlabeled large dendrite (diameter ≥1μm); **SD-:** unlabeled small dendrite (diameter <1μm); **Sp-:** unlabeled spine; **So+:** MOR+ spines; **LD+:** MOR+ large dendrite (diameter ≥1μm); **SD+:** MOR+ small dendrite (diameter <1μm); **Sp:** MOR+ spines.

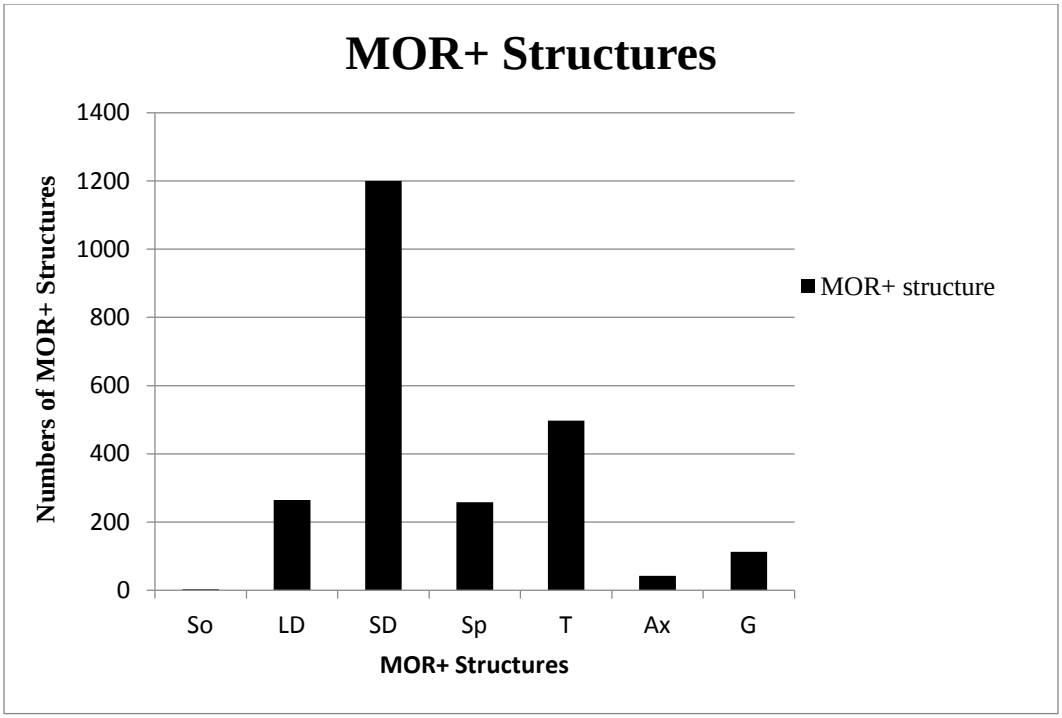

Figure 4.2 Histogram showing the number of each MOR+ structure observed in the quantitative analysis of the BLa. **So:** Soma; **LD:** large caliber dendrite (diameter ≥1μm); **SD:** small caliber dendrite (diameter <1μm); **Sp:** spine; **T:** terminal; **Ax:** axon; **G:** glial.

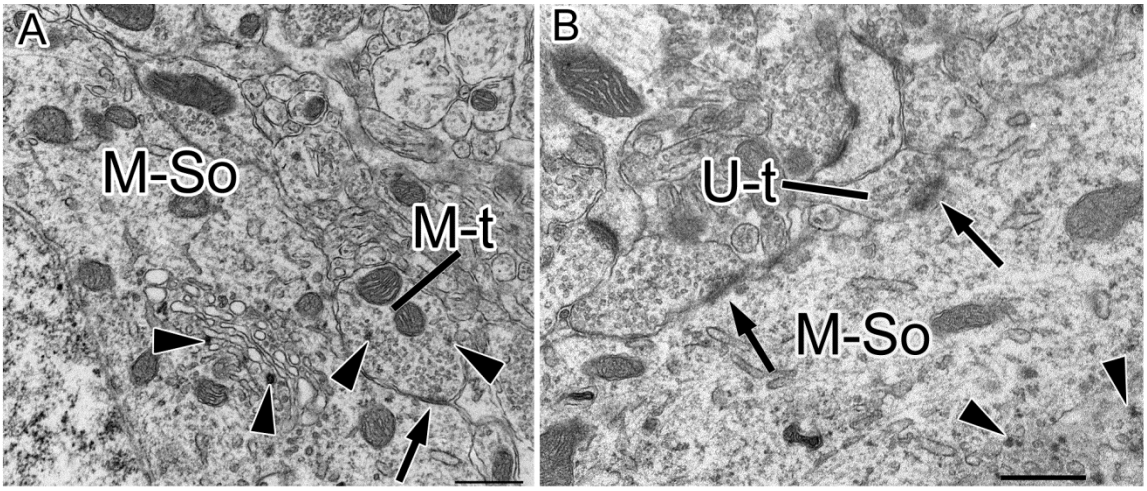

Figure 4.3 Electron micrographs of MOR+ somata in the BLa. **A:** A MOR+ soma (M-So) is contacted by a MOR+ terminal (M-t), forming a symmetrical synapse (arrow). MOR-ir is present near the Golgi apparatus. **B:** A MOR+ soma (M-So) receiving asymmetrical synaptic contacts from two unlabeled terminals (arrow). Arrowheads show granule MOR label. Arrowheads point to the MOR labeling. Scale bar=0.5µm.

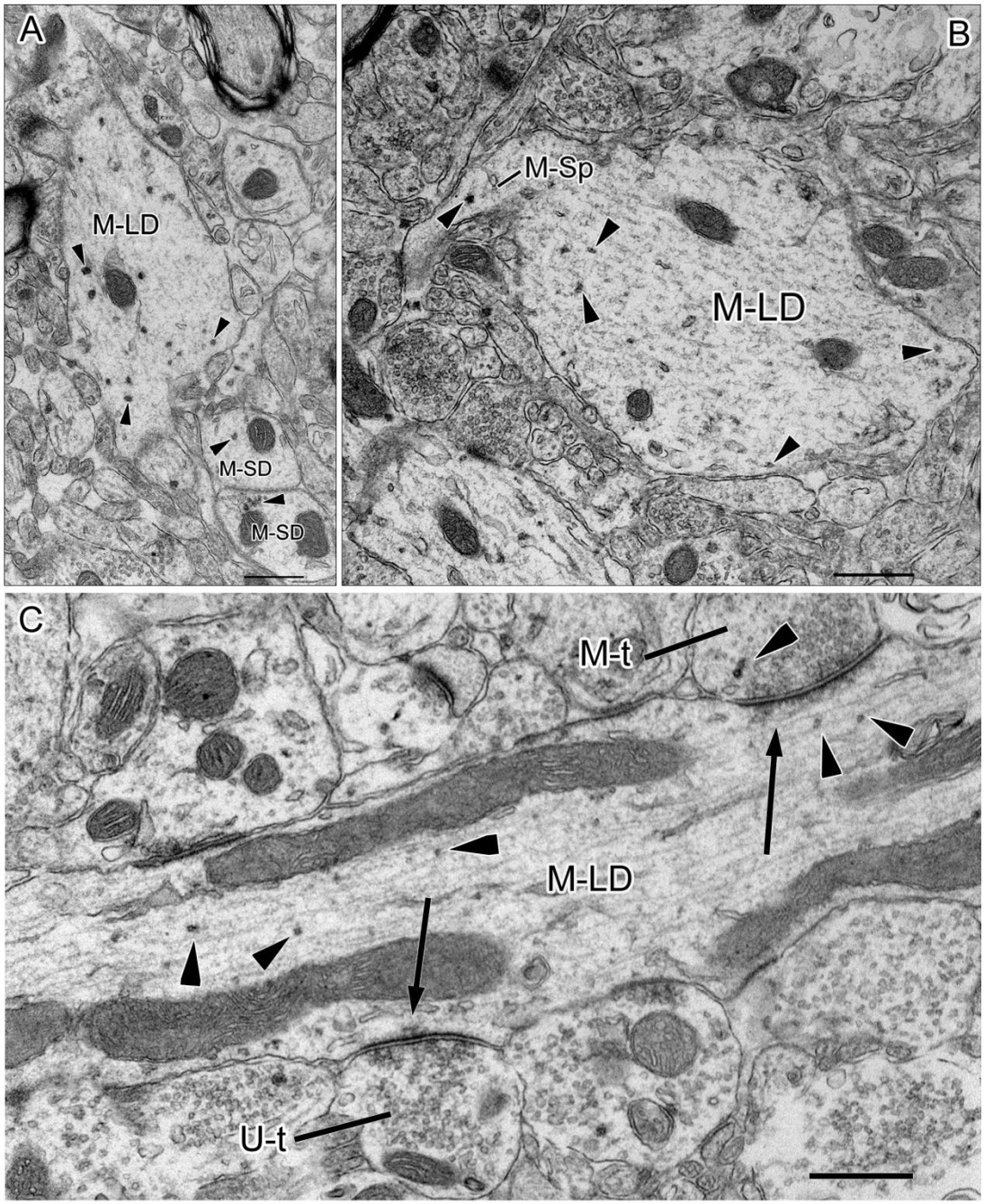

Figure 4.4 Electron micrographs of MOR+ large caliber (≥1µm) dendrites. **A:** A large caliber MOR+ dendrite (M-LD) and two nearby small caliber MOR+ dendrites (M-SD) **B:** A large caliber MOR+ dendrite (M-LD) with a MOR+ spine (M-Sp). The spine suggests that this dendrite may belong to a pyramidal cell. **C:** A longitudinally sectioned large caliber MOR+ dendrite receives multiple asymmetrical synapses (arrow) from either MOR+ (M-t) or unlabeled (U-t) terminals, suggesting that this dendrite may belong to an interneuron. Arrowheads show granules of MOR label. Arrowheads point to the MOR labeling. Scale bar=0.5µm.

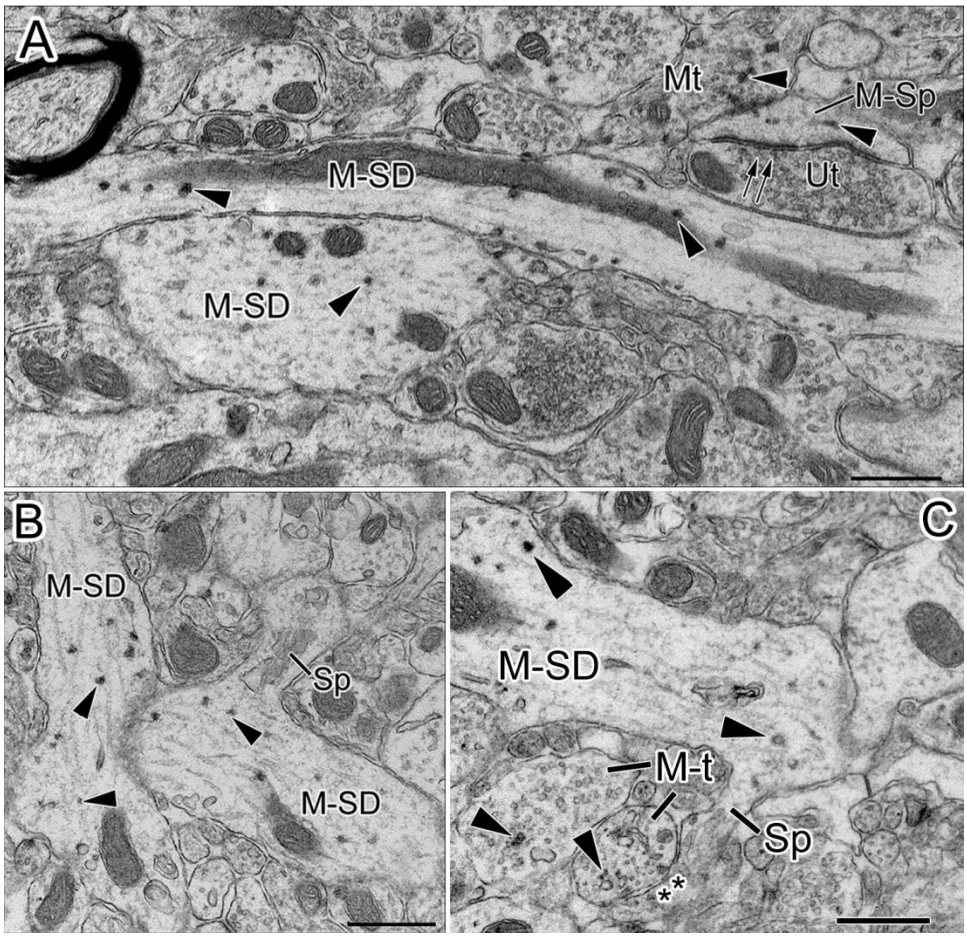

Figure 4.5 Electron micrographs of MOR+ small caliber (<1μm) dendrites. **A:** A long MOR+ small caliber dendrite (M-SD) and adjacent MOR+ (M-t) or unlabeled (U-t) axon terminals which both form asymmetrical synapses (arrows) with a MOR+ spine (M-Sp). There is another small caliber dendrite (M-SD) nearby. **B:** Two small caliber MOR+ dendrites (M-SD), one of which has a spine (Sp), suggesting that it might belong to a pyramidal cell. **C:** One small caliber MOR+ dendrites (M-SD) with a spine (Sp) contacted (stars) by a MOR+ terminal (M-t), suggesting it might belong to a pyramidal cell. There is another MOR+ terminal (M-t) nearby. Arrowheads show granules of MOR labeling. Scale bar=0.5μm.

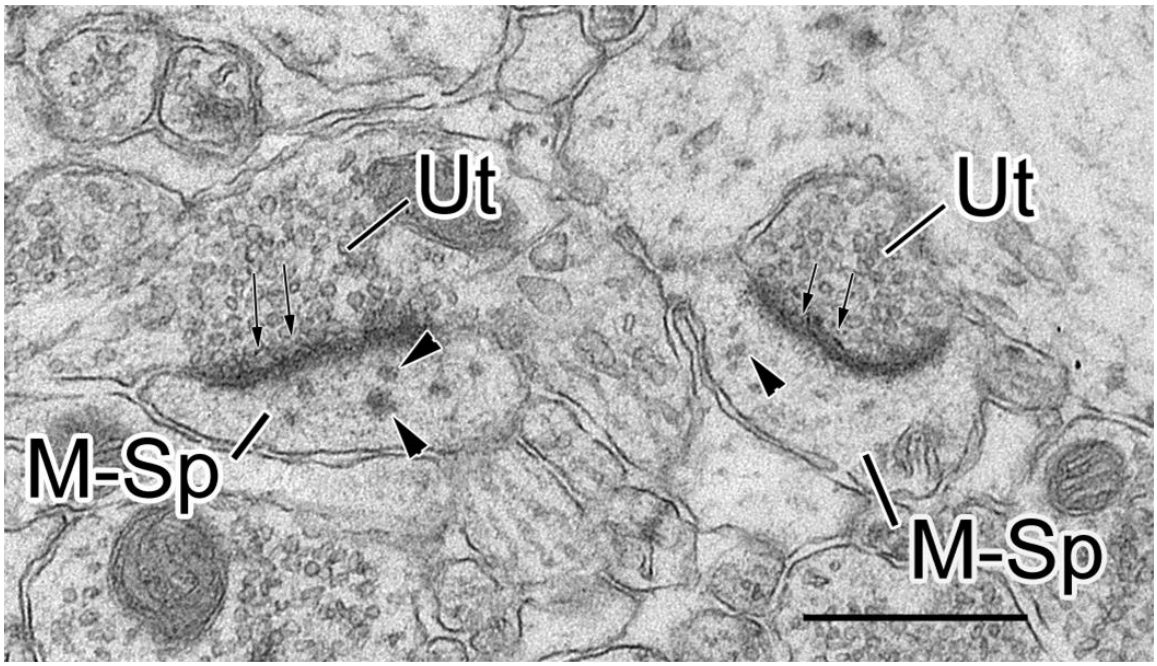

Figure 4.6 Electron micrograph of MOR+ spines. Two MOR+ spines receive asymmetrical synaptic contacts (arrows) from unlabeled terminals (Ut). Arrowheads show granules of MOR label. Arrowheads point to the MOR labeling. Scale bar=0.5 µm.

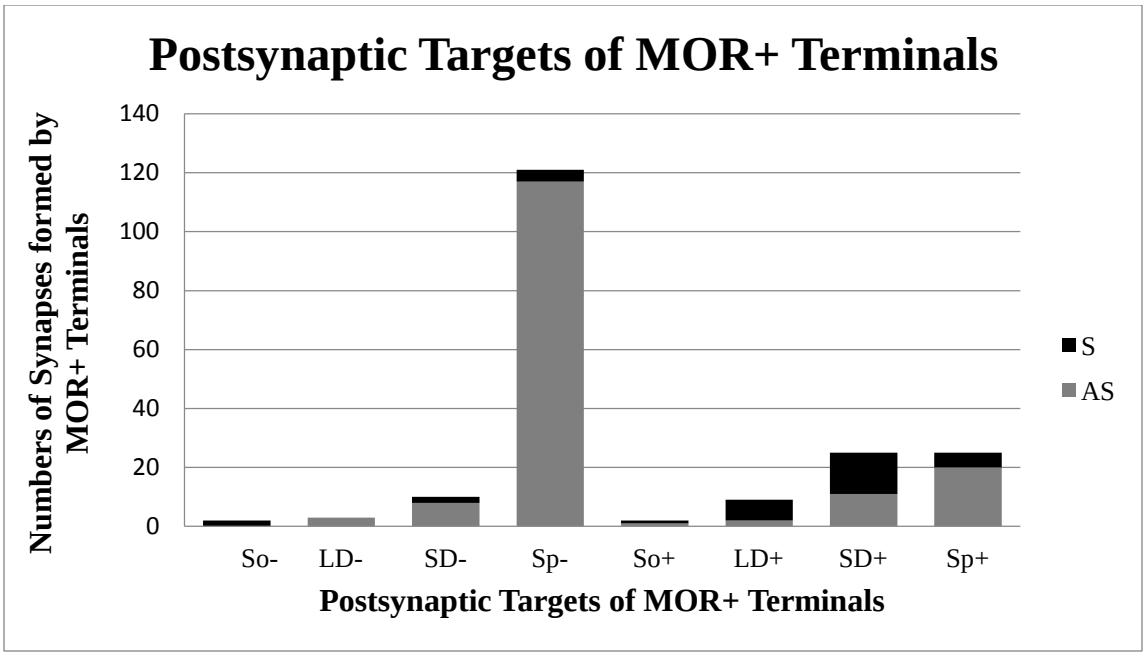

Figure 4.7 Histogram showing the number of symmetrical (S, Black) or asymmetrical (AS, dark gray) synapses of MOR+ terminals with various MOR labeled (+) or unlabeled (-) structures. **So:** soma; **LD:** large caliber dendrite (≥1μm); **SD:** small caliber dendrite (<1μm); **Sp:** spine;

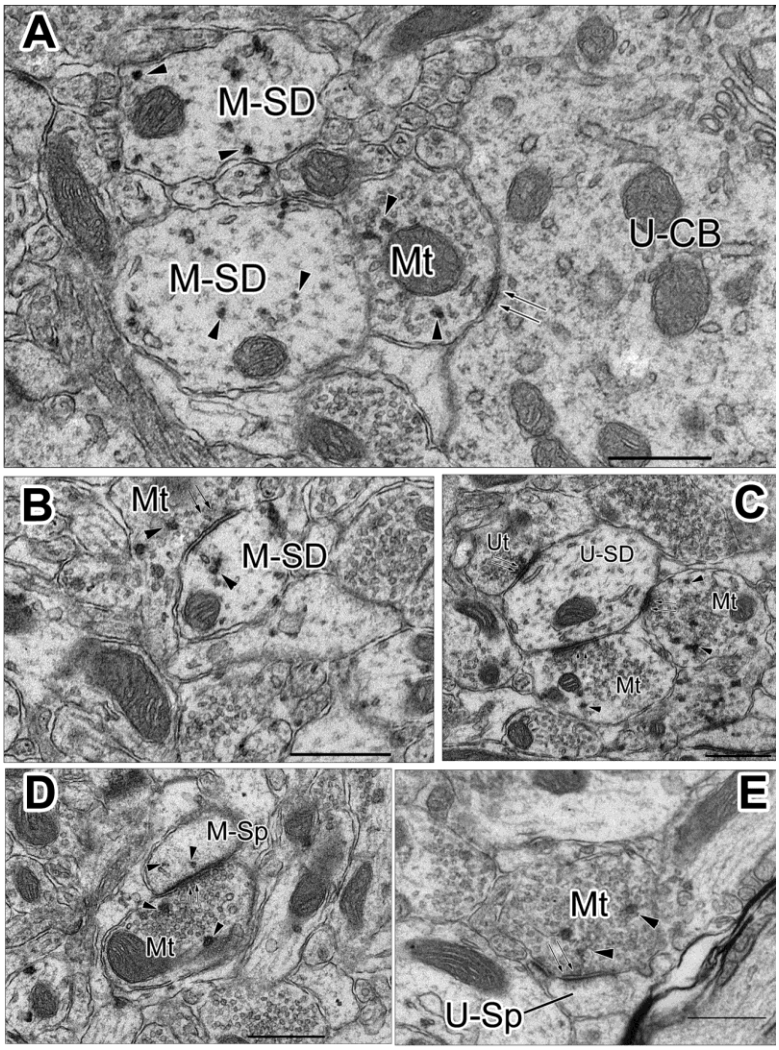

Figure 4.8 Electron micrographs of various postsynaptic targets of MOR+ terminals. **A:** A MOR+ terminal (M-t) forms a symmetrical synapse (arrows) with an unlabeled cell body (U-CB). There are two MOR+ small caliber dendrites (M-SD) nearby. **B:** A MOR+ terminal (M-t) form a symmetrical synapse (arrows) with a MOR+ small caliber dendrite (M-SD). **C:** Two MOR+ terminals (M-t) form asymmetrical synapses (arrows) with an unlabeled small caliber dendrite (U-SD) which also receives an asymmetrical synapse from an unlabeled terminal (U-t). Multiple asymmetrical synapses are indicative of interneuronal dendrite. **D:** A MOR+ terminal (M-t) form an asymmetrical synapse (arrows) with a MOR labeled spine (M-Sp). **E:** A MOR+ terminal (Mt) form an asymmetrical synapse (arrows) with a MOR labeled spine (M-Sp). Arrowheads show granules of MOR label. Arrowheads point to MOR label. Scale bar=0.5 µm.

4.5 DISCUSSION:

The electron microscopy analysis of MOR distribution in the BLa revealed that MOR-ir is present in diverse populations of neuronal profiles and glial processes as well. The most frequently labeled structures were small caliber dendrites and terminals. MOR+ terminals formed synapses with both labeled and unlabeled profiles. The main postsynaptic targets of MOR+ terminals forming asymmetrical synapses were unlabeled spines, while the main targets of MOR+ terminals forming symmetrical synapses were MOR+ small caliber dendritic shafts.

4.5.1 ANATOMICAL CONSIDERATIONS

The ultrastructural distribution of MOR in the BLa was consistent with previous MOR binding and immunohistochemistry studies in the amygdala, which revealed dense MOR binding and high level of MOR immunoreactivity in the basolateral amygdala. (Mansour et al., 1987, Ding et al., 1996). Similar to previous research in the central amygdala and a very limited analysis in the BLa (Glass et al., 2005, Glass et al., 2009), MOR immunoreactivity was found in both pre and post-synaptic neuronal profiles in the present study.

Counts of MOR+ structures showed that small distal dendrites are most commonly labeled. Although we could not determine their cell type of origin based only on their anatomical features, some of these dendrites exhibited spines, a characteristic of pyramidal cell dendrites. In addition, the large numbers of spines and dendrites in the labeled profiles suggests that they are coming from pyramidal cells since 85% of BLa neurons are pyramidal cells (McDonald, 1992). Very few dendrites received multiple asymmetrical synaptic contacts, which is typical of interneurons. Together, these findings

indicate that most of the MOR+ dendrites appear to belong to pyramidal projection neurons, but some are interneurons.

MOR+ terminals formed synapses with both labeled and unlabeled profiles, and their postsynaptic targets included somata, large and small caliber dendritic shafts, and spines. Both symmetrical and asymmetrical synapses were observed, but asymmetrical synapses were more common. Since most asymmetrical synapses are glutamatergic in the BLa (Pare et al., 1995), the majority of MOR+ terminals might be glutamatergic. Moreover the major postsynaptic targets of MOR+ terminals were spines, which is also the main target of glutamatergic projections to the BLa from cortical, thalamus and other nuclei of amygdala (LeDoux et al., 1991, Stefanacci et al., 1992, Brinley-Reed et al., 1995), which further confirms this possibility. Additionally, it has been reported that opioids inhibit NE release in the amygdala during stress (Quirarte et al., 1998), thus some of MOR+ terminals might be noradrenergic, in particular those forming symmetrical synapses, which is the major synapse type formed by noradrenergic inputs in the BLa (Zhang et al., 2013).

MOR labeling in our preparation was found to be more commonly associated with cytoplasmic organelles, but the MOR-ir was also found near the plasma membrane in many cases as well. MOR has to be inserted into membrane to be functional. Although the V-VIP particles do not represent the precise location of the antigen due to diffusion of the peroxidase reaction product, it is highly possible that the MOR-ir near the plasma membrane may reflect membrane-associated receptors and the ones associated with cytoplasmic organelles may serve as a reserve pool of MORs or be in the process of being transported to other parts of neurons. Actually, ultrastructural studies using

immunogold techniques, which provide more accurate antigen localization, have found that MOR-ir was located both in the cytoplasm and plasmalemma in the central lateral amygdala (Glass et al., 2009, Beckerman and Glass, 2011). Conversely, earlier immunogold studies reported that the MORs are almost exclusively located in plasmalemma in the striatal patch compartment (Wang et al., 1996, Wang and Pickel, 2001) and the shell of nucleus accumbens (Gracy et al., 1997). Future studies using immunogold techniques are required to provide a more precise subcellular distribution of MORs in the BLa.

4.5.2 FUNCTIONAL IMPLICATIONS

The fact that MOR-ir was observed in both pre and post synaptic profiles suggests that MOR can modulate BLa neurons both pre and postsynaptically, which agrees with electrophysiological results indicating that MOR activation leads to membrane hyperpolarization and inhibits neurotransmitter release in the BLC (Sugita and North, 1993, Faber and Sah, 2004, Finnegan et al., 2006).

Although MOR activation is associated with inhibition of amygdala function (Liberzon et al., 2002) in general, the effects of MOR activation on the individual neurons is complicated. A previous study reported that MOR activation hyperpolarizes a subpopulation of neurons and inhibits GABA release in the lateral amygdala (LA) (Sugita and North, 1993), indicating that MOR may be located in the terminals of interneurons in the LA. Another study in the BLA found that activation of presynaptic MOR receptors primarily attenuates GABAergic inputs to the central amygdala projecting pyramidal cells in the BLA though Kv1.1/1.2 channels (Finnegan et al., 2006), which also suggest that the MOR activation probably occurs in interneuronal terminals. This is consistent with our observations that some of the MOR+ axon terminals in the BLa form

symmetrical synapses, typical of GABAergic inhibitory interneuron (McDonald and Mascagni, 2002). This MOR induced GABA release inhibition, and hence pyramidal cell disinhibition, may also contribute to stress associated hypoalgesia through the BLA-central amygdala- PAG pathway (Hopkins and Holstege, 1978, Rizvi et al., 1991, Harris, 1996). Moreover, we also observed a few MOR+ interneurons, which may be part of the hyperpolarized subpopulation during MOR activation in the earlier study (Sugita and North, 1993). Additionally, many MOR+ dendrites in present preparation have been found to give rise to spines, which is characteristic of pyramidal cells. These MORs in dendrites may modulate pyramidal cell excitability via affecting potassium channels, which have been shown in the LA (Faber and Sah, 2004).

Considering that dendritic spines of pyramidal cells in the BLa are also the major target of excitatory inputs from the cortex, thalamus and pyramidal neurons of the LA and BLA (LeDoux et al., 1991, Stefanacci et al., 1992, Brinley-Reed et al., 1995), MOR might be involved in modulating the effects of these inputs to BLa pyramidal cells. In fact, MORs have been found to be closely colocalized with glutamatergic receptors in the BLa (Glass et al., 2005), which may contribute to the neuronal plasticity in the amygdala related to opioid addiction (Scavone et al., 2011). Spines in the BLa are also major neural compartments receiving modulatory inputs such as cholinergic, norepinephrine, dopamine and serotonin (Muller et al., 2011, Zhang et al., 2013) (Muller et al., 2007, 2009) indicating that MOR could postsynaptically influence their effects on the BLa as well.

The majority of the asymmetrical synapses formed by MOR+ terminals may be glutamatergic since most asymmetrical synapses are glutamatergic in the BLa (Pare et al.,

1995). It is highly possible that MORs may be involved in modulation of glutamate release in the BLa. Some of the symmetrical synapses formed by MOR+ terminals might be noradrenergic. A recent ultrastructural study demonstrated that noradrenergic inputs mainly form symmetrical synapses in the BLa (Zhang et al., 2013). MORs in noradrenergic terminals might explain the effects of opioid peptidergic drug administration on norepinephrine release in the amygdala (Quirarte et al., 1998), which is thought to be the major way that opioids are involve in memory modulation during stress (Introini-Collison et al., 1995, McGaugh, 2004).

CHAPTER 5

LIMITED CONVERGENCE OF ENKEPHALIN AND NOREPINEPHRINE INPUTS IN THE RAT BASOLATERAL AMYGDALA

5.1 INTRODUCTION

Accumulating evidence indicates that norepinephrine (NE) and opioid systems in the amygdala are heavily involved in stress adaptation and memory consolidation of emotionally arousing experiences (Introini-Collison et al., 1995, Drolet et al., 2001, McGaugh, 2004, Roozendaal et al., 2009). Studies have shown that stressful stimuli such as footshock induce norepinephrine release in the rat amygdala (Galvez et al., 1996, Quirarte et al., 1998). Moreover, post-training drug treatment studies using adrenergic agonists and antagonists indicate that activating the NE system in the basolateral amygdala enhances memory retention of inhibitory avoidance (Ferry and McGaugh, 1999, McGaugh, 2004, Ferry and McGaugh, 2008).

Endogenous opioid peptides include endorphin, enkephalin (ENK) and dynorphin derived from three peptide precursors, proopiomelanocortin (POMC), proenkephalin (ProEnK) and prodynorphin (ProDyn), respectively (Stefano et al., 2000, Drolet et al., 2001). These opioid peptides produce their effects via three types of G-protein coupled receptors: mu, delta and kappa. Preproenkephalin knockout mice elicit stronger anxiety and depressive PTSD-like symptoms than wild type animals (Kung et al., 2010). In addition, the opiate antagonist naloxone has been found to enhance memory retention in inhibitory avoidance and this effect could be reversed by mu opiate receptor (MOR)

agonists (Izquierdo and Graudenz, 1980, Introini-Collison et al., 1989, Introini-Collison et al., 1995). The memory regulating effects of opioids are believed to be mediated through the modulation of the NE system, since intra-amygdala activation of MORs impairs memory by inhibiting NE release, and facilitating NE function compensates this memory impairment effects (Introini-Collison et al., 1995). Considering the sparse projection to the BLa from beta-endorphin expressing neurons in hypothalamus (Gray et al., 1984), ENK may be the major endogenous opioid peptide which is involved in the memory modulation function of MORs in the amygdala.

The major postsynaptic targets of NE inputs in the BLa are distal dendrites and spines (Zhang et al., 2013), which are also the main MOR+ profiles (results from chapter 4). Thus it is possible that NE inputs and ENK inputs may both synapse with these postsynaptic structures, similar to the locus ceruleus where ENK and epinephrine terminals converge on the same structures (Van Bockstaele et al., 1996). However, there have been no ultrastructural studies examining the convergence of NE and ENK terminals in the BLa. Also, there have been no previous electron microscopy investigations of ENK in the BLa. All the previous studies have concentrated on examining the presynaptic interaction of ENK and NE system (Izquierdo and Graudenz, 1980, McGaugh et al., 1988, Introini-Collison et al., 1989, Introini-Collison et al., 1995, Quirarte et al., 1998). The present study utilized dual-immunocytochemistry staining combined with electron microscopy to investigate the extent of the convergence of NE and ENK terminals onto common structures in the BLa, which will provide information about whether there may also be postsynaptic interactions of NE and ENK in the BLa.

5.2 HYPOTHESIS

There may be convergence of NE and ENK inputs on distal dendritic shafts and spines of BLa neurons.

5.3 METHODS

5.3.1 TISSUE PREPARATION

Five male Sprague-Dawley rats weighing 250-350g were used in this study. Rats were handled in accordance with the principle of laboratory animal care and protocols approved by the University of South Carolina Institutional Animal Care and Use Committee. Brain tissue was prepared as described in previous studies of our lab (Muller et al., 2011) . Rats were anesthetized with a ketamine mixture (ketamine: 85mg/kg; xylazine: 8mg/kg; acepromazine: 4mg/kg) and perfused intracardially with PBS containing 1% sodium nitrite, followed by 2% paraformaldehyde-3.75% acrolein in phosphate buffer (PB) for 1 minute, followed by 2% paraformaldehyde in PB for 20 minutes. Brains were removed and post-fixed in 2% paraformaldehyde for one hour. Brains were sectioned on a vibratome in the coronal plane at 60μm.

5.3.2 LIGHT MICROSCOPY IMMUNOHISTOCHEMISTRY

Single-label localization of ENK was performed in two rats using a rabbit antibody to methionine-enkephalin (met-ENK) (1:1000, ImmunoStar, Hudson, WI). All antibodies were diluted in PBS containing 0.4% Triton X-100 and 1% normal goat serum. Sections were incubated in the primary antibody overnight at 4℃ and then processed for the avidin-biotin immunoperoxidase technique using a biotinylated goat anti-rabbit secondary antibody (1: 500, Jackson Immunoresearch Laboratories, West Grove, PA) and a Vectastain standard ABC kit (Vector laboratories, Burlingame, CA)

with nickel-intensified 3,3 ´-diaminobenzidine 4HCl (DAB, Sigma Chemical Co., St. Louis, MO, USA) as a chromogen to generate a black reaction product (Hancock, 1986). After the reactions, sections were mounted on gelatinized slides, dried overnight, dehydrated in ethanol, cleared in xylene, and coverslipped in Permount (Fisher Scientific, Pittsburgh, PA, USA). Sections were analyzed with a Nikon E600 microscopy system and digital light micrographs were taken with a Micropublisher digital camera.

5.3.3 DOUBLE LABELING ELECTRON MICROSCOPY IMMUNOHISTOCHEMISTRY

Double labeling immunohistochemistry was performed to detect the convergence extent of NE and ENK terminals in the BLa at the electron microscopy level. To enhance penetration of antibodies, sections were incubated with low level of Triton-X-100 (0.02%) in the antibody dilutions. Section were incubated in a mouse monoclonal NET antibody (1:2000 NET-05, obtained from Dr. Randy D. Blakely, Vanderbilt University Medical Center) overnight at 4℃ after 30 minutes in a blocking solution (PBS containing 3% normal goat serum , 1% BSA and 0.02% Triton-X), and then processed using a biotinylated goat anti-mouse antibody (Jackson ImmunoResearch, West Grove, PA) and a Vectastain standard ABC kit (Vector Laboratories, Burlingame, CA) with 3,3 ´-diaminobenzidine 4HCl (DAB, Sigma Chemical Co., St. Louis, MO, USA) as the chromogen. After rinsing, sections were incubated in an avidin/biotin blocking solution (Vector Laboratories, Burlingame, CA). Sections were then incubated overnight at 4℃ in rabbit anti-met-enkephalin antibody (1:1000, ImmunoStar) to label ENK structures. For ENK immunohistochemistry, sections were processed using a biotinylated goat anti-rabbit secondary antibody (1: 500, Jackson Immunoresearch Laboratories, West Grove,

PA) and an Elite ABC kit (Vector Laboratories, Burlingame, CA), with Vector-VIP as a chromogen. This process produces a reaction product that appears purple at the light microscopy level and granular at the electron microscopy level. It was easily distinguished from the diffuse DAB immunoperoxidase reaction product at the ultrastructural level.

5.3.4 PROCEDURE FOR ELECTRON MICROSCOPY

After the immunohistochemical reactions, sections were then post-fixed in 2% osmium tetroxide in 0.16 M sodium cacodylate buffer for one hour, dehydrated in ethanol and acetone, and flat embedded in Polybed 812 (Polysciences, Warrington, PA) in slide molds between sheets of Aclar (Ted Pella, Redding, CA). Selected areas of the BLa were remounted onto resin blanks. Silver thin sections were collected on formvar-coated slot grids, stained with uranyl acetate and lead citrate and examined with a JEOL-200CX electron microscope. Micrographs were taken with an AMT XR40 digital camera system (Advanced Microscopy Techniques, Danvers, MA).

5.3.5 ANALYSIS

Vibratome sections from three rats (one for each animal) with the best labeling quality were selected for thin sectioning and analysis. From these thin sections, areas with the best morphology and robust presence of both NET and ENK labels were chosen for quantitative analysis. During data collection, each NET + terminal was centered in the field and then MOR+ terminals in the same field as the NET+ terminal were counted and used for analysis. All the pictures were taken at the 36,000 magnification in which the area of each field is around $4.4 \times 5.5\ \mu m^2$. Labeled terminals were followed for 3 to 11 serial thin sections. Contacts of NET+ and ENK+ terminals with ENK labeled or

unlabeled neuronal structures in the BLa were classified as either synapses or apposition. Synapses were identified using standard criteria: 1) parallel presynaptic and postsynaptic membranes exhibiting membrane thickening, 2) clustered vesicles associated with the presynaptic membrane, and 3) a synaptic cleft containing dense material. Contacts which did not meet these criteria were identified as appositions. Asymmetrical and symmetrical synapses were identified based on the presence or absence of a prominent postsynaptic density and the widths of their synaptic clefts. Asymmetrical synapses usually have wider synaptic clefts (20nm) than symmetrical ones (12nm) (Peters A, 1991). Postsynaptic neuronal profiles receiving synapses from ENK-labeled terminals were identified as ENK- labeled or unlabeled somata, large caliber dendritic shafts (diameter ≥1μm), small caliber dendritic shafts (diameter <1μm), or spines according to established morphological criteria (Peters A, 1991). The percentage of labeled terminals (NE or ENK) contacting a common structure was determined. In addition, the percentage of terminals contacting each other was determined as well.

5.3.6 ANTIBODY SPECIFICITY

The mouse monoclonal anti-NET primary antibody (1:2000 NET-05, obtained from Dr. Randy D. Blakely, Vanderbilt University Medical Center) used in this study was raised against amino acids 5-17 of the amino-terminus of mouse NET. Specificity of this antibody has been demonstrated by absence of immunolabeling in NET knock out tissue or following pre-adsorption in previous studies (Matthies et al., 2009, Erickson et al., 2011).

The met-enkephalin antibody used in present study has been well documented in the previous studies (Wilson et al., 2002). It has very limited recognition of leucine-ENK

and has no cross reaction with endorphin or dynorphin (Cheng et al., 1995, Wilson et al., 2002).

Two control groups were used in the experiment. First group omitted ENK primary antibody but was performed all the same procedure as double labeling group, second group omitted NET primary antibody but was performed all the same procedures as the double labeling group. No purple labels were observed in the first group. No DAB labels were observed in the second group. Therefore the secondary antibodies were specific for mouse or rabbit IgG.

5.4 RESULTS

5.4.1 LIGHT MICROSCOPY OBSERVATIONS

At the light microscopy level, ENK immunoreactivity (ENK-ir) presents a distribution pattern which is similar to the observation in a previous study (Wilson et al., 2002). Dense neuropil staining was found in the neuropil of the intercalated nuclei (Figure 5.1.A). ENK+ somata were observed mainly in the central nucleus and only a few ENK+ nonpyramidal interneurons were found in the lateral and basolateral amygdala (Figure 5.1), which is consistent with results of a preproenkephalin mRNA binding study (Harlan et al., 1987). Moderate neuropil labeling was found in the central amygdala but there was only very light neuropil labeling in lateral and basolateral amygdala (Figure5.1.A).

5.4.2 ELECTRON MICROSCOPY OBSERVATIONS

Dual labeling using ENK and NET antibodies show that both labels are concentrated in terminals (Figures 5.2-5.4). ENK immunoreactivity (ENK-ir) was also seen in somata, dendrites, spines and axons (Figures 5.2 and 5.3.A). ENK terminals were

round to ovoid with small vesicles that were round and clear (Figures 5.2.A, 5.3 and 5.4). About 70% (110/157) of ENK+ terminals formed synapses with either ENK+ or unlabeled structures (Figures 5.2.A, 5.3 and 5.4.A). Postsynaptic targets of these ENK+ terminals included ENK+ and unlabeled dendritic shafts and spines (Figures 5.2A, 5.3 and 5.4.A). ENK+ terminals mainly formed asymmetrical synapses and their most frequent targets were the ENK+ or unlabeled spines (Figures 5.2.A). In a few cases symmetrical synapses formed by ENK+ terminals were observed and most of them were with small distal dendritic shafts (Figures 5.3.A).

NET+ profiles consisted of thin unmyelinated axons and varicosities containing synaptic vesicles (Figures 5.2-5.4). The peroxidase reaction product was distributed throughout these NET + profiles, with accumulations near the plasma membrane and the outer membrane of vesicles and mitochondria. This diffuse DAB reaction product was easily distinguished from the particulate Vector-VIP reaction product of ENK labeling. NET+ terminals were round or ovoid in shape with closely packed small, round clear synaptic vesicles, sometimes associated with large clear vesicles, similar to the descriptions of DBH+ profiles and NET+ profiles reported in previous studies of the basolateral amygdala (Asan, 1998, Li et al., 2001, Li et al., 2002, Farb et al., 2010, Zhang et al., 2013). NET terminals mainly formed symmetrical synapses and they targeted both ENK+ and unlabeled structures, including, dendritic shafts, spines and somata, consistent with previous studies (Li et al., 2001, Li et al., 2002, Zhang et al., 2013).

There was a very limited convergence of NET and ENK inputs in the BLa. 11% of ENK terminals (17/157) contacted a common neuronal structure with an NET terminal in the same field (Figures 5.3-5.5). The targets and types of contacts formed by

converging terminals were described in Table 5.1. In general, the most frequent common targets were small caliber dendritic shafts and spines (Figures 5.3 and 5.4) (Table 5.1). For one case, NET+ and ENT+ terminals contacted the same ENK+ cell body. Similarly, a large caliber dendritic shaft was observed only once to be a common target of NET and NET terminals. In most instances of convergence, ENK+ terminals formed asymmetrical synapses or appositions whereas NET+ terminals formed symmetrical synapses or appositions (Figures 5.3 and 5.4) (Table 5.1). In addition, NET+ and ENK+ terminals contacted each other in five cases (Figures 5.3.B and 5.4.B)

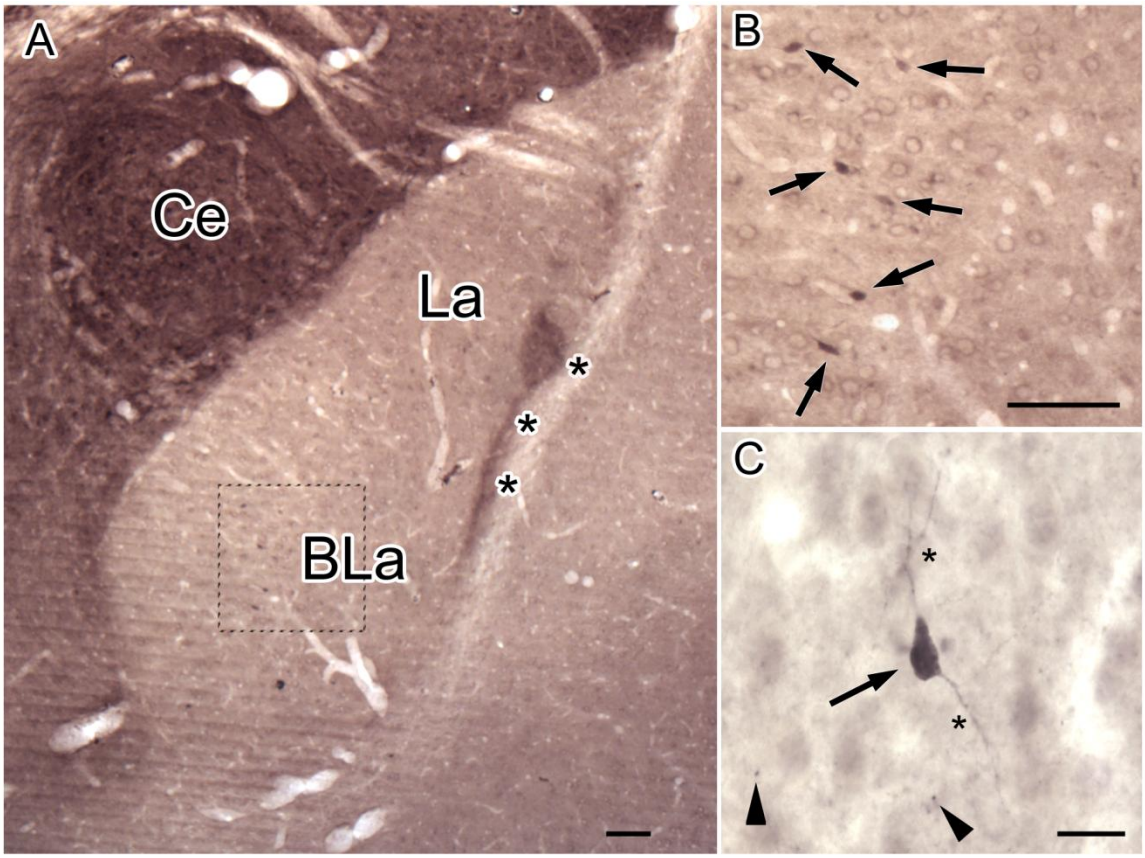

Figure 5.1 Light micrographs of ENK immunohistochemistry in the BLa using nickel DAB as a chromogen in an immunoperoxidase preparation. **A:** Low power micrograph illustrating ENK immunohistochemistry in the BLa, lateral nucleus (La), central nucleus (Ce) and intercalated nuclei (stars) at bregma level-2.1.**B:** Higher power micrograph of the boxed area in A, illustrating several ENK+ interneurons (arrows). **C:** High power micrograph illustrating an ENK+ interneuron (arrow) and its processes (stars). Punctate ENK+ structures (arrow head) maybe ENK+ axon terminals. Scale bar=100µm in A, 50µm in B, 10µm in C.

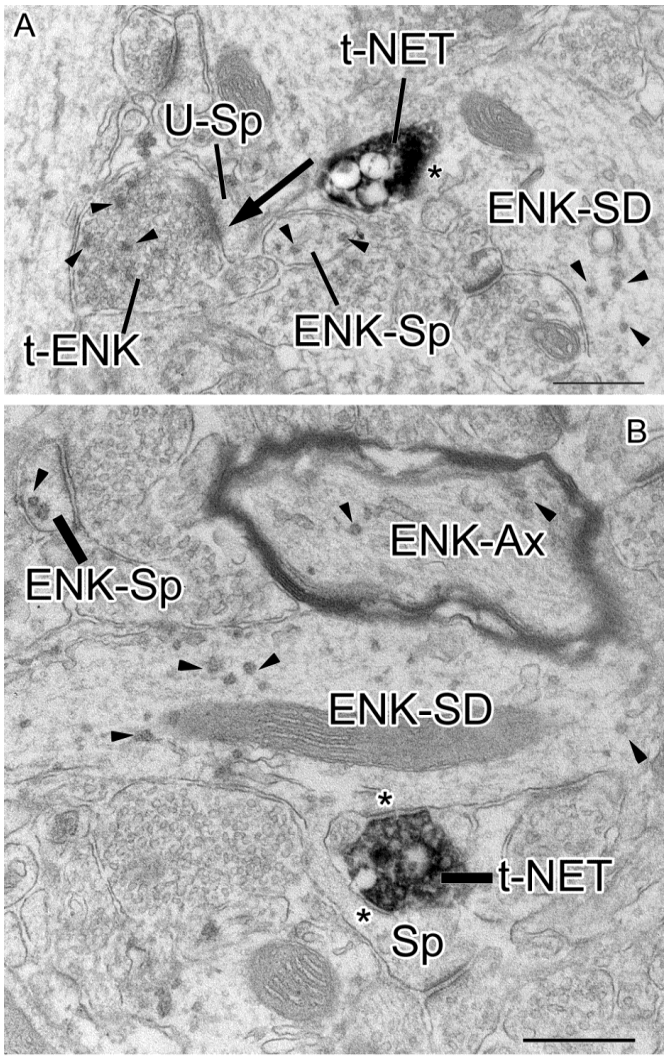

Figure 5.2 Electron micrographs of the BLa immunostained for NET and ENK. **A:** A NET+ terminal (t-NET) and an ENK+ terminal (t-ENK) are found in the same field, but they do not target the same structure. The ENK+ terminal forms an asymmetrical synapse (arrow) with an unlabeled spine (U-sp). The NET terminal contacts (asterisk) an ENK+ small caliber dendrite (ENK-SD). There are also an ENK+ spine (ENK-Sp) and ENK+ small caliber dendrite (ENK-SD) in this field. **B:** A NET+ terminal forms an apposition (asterisk) with an ENK+ small caliber dendrite (ENK-SD) and a spine (Sp) arising from it. There is an ENK+ spine (ENK-Sp) and an ENK+ myelinated axon (ENK-Ax) nearby as well. Arrowhead indicates Vector VIP granule labeling. Scale bar=0.5μm.

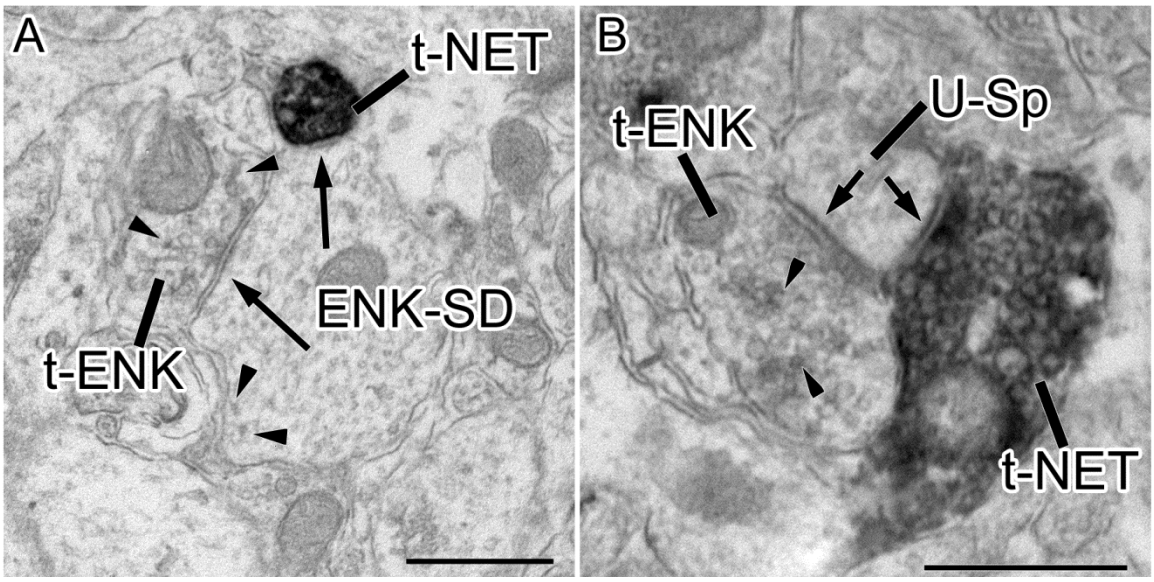

Figure 5.3 Electron micrographs showing synaptic convergence of NET+ and ENK+ terminals in the BLa. **A:** A NET+ terminal (t-NET) and an ENK+ terminal (t-ENK) target (arrow) the same ENK+ small caliber dendrite (ENK-SD), both forming symmetrical synapses (arrows). ENK labeling in this small dendrite is much more obvious in the adjacent sections. **B:** An unlabeled spine (U-Sp) receives symmetrical synapses (arrows) from NET+ and ENK + terminals. Arrowheads indicate V-VIP granule labeling. Scale bar=0.5µm.

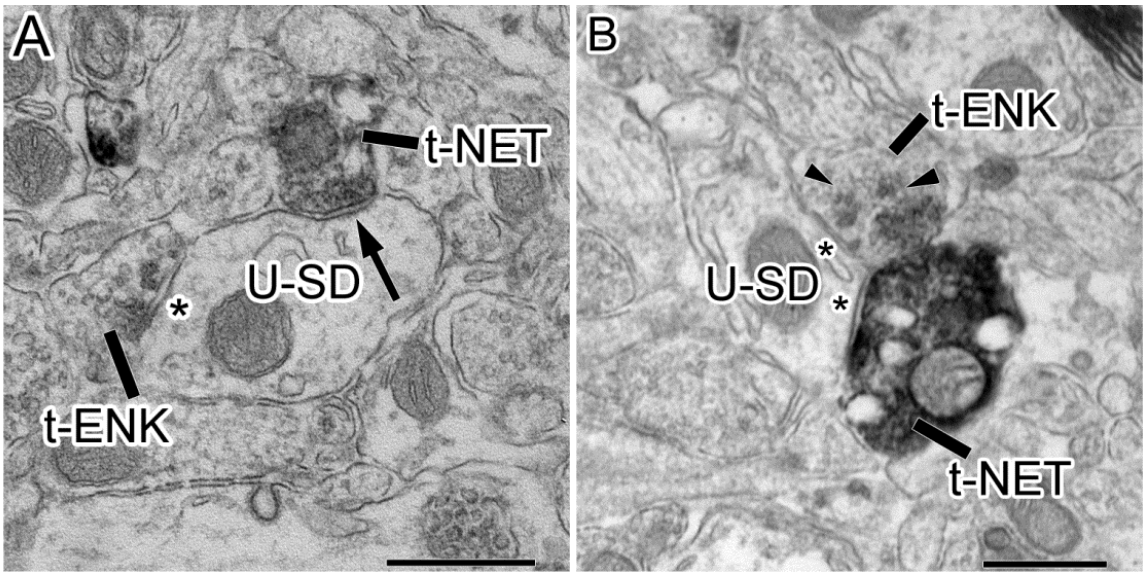

Figure 5.4 Electron micrographs showing convergence of NET+ and ENK+ terminals in the BLa. **A:** A NET+ terminal (t-NET) forms a symmetrical synapse (arrow) with an unlabeled small caliber dendrite (U-SD). An ENK+ terminal (t-ENK) form an apposition (asterisk) with the same dendrite. **B:** A NET+ terminal and an ENK+ terminal form appositions with an unlabeled SD (U-SD) and with each other. Arrowheads indicate V-VIP granule labeling. Scale bar=0.5µm.

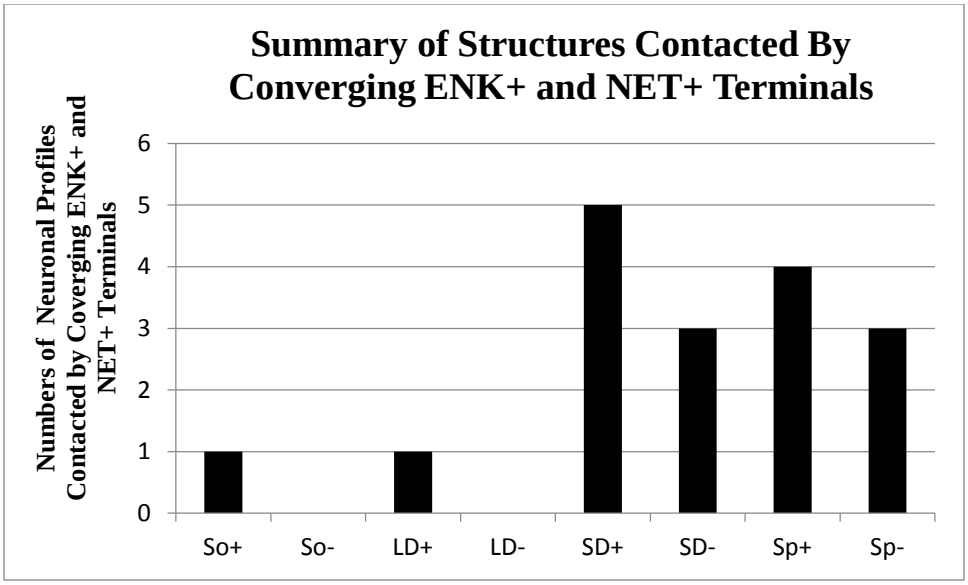

Figure 5.5 Histogram showing numbers of each type of neuronal profiles in the BLa contacted by converging ENK+ and ENT+ terminals. **+:** ENK labeled; **-:** unlabeled; **So:** soma; **LD:** large caliber dendrite (diameter ≥1μm); **SD:** small caliber dendrite (diameter <1μm); **Sp:** spine;

Table 5.1 Targets and types of contacts of converging ENK+ terminals and NET+ terminals in the BLa.

ENK+ Terminals	Target	ENK Contact	NET Contact
EM08-T1	Sp+	AS	S
EM08-T2	Sp+	AS	S
EM08-T16	Sp-	AS	Apposition
EM08-T19	Sp-	AS	S
EM08-T21	SD+	AS	S
EM08-T22	SD+	S	S
EM08-T24	Sp+	AS	Apposition
EM08-29b	SD-	Apposition	S
EM08-T31	SD+	Apposition	Apposition
EM10-T07	LD+	Apposition	Apposition
EM10-T13	SD-	AS	Apposition
EM10-T25	So+	Apposition	S
EM11-T04-a	SD+	S	Apposition
EM11-T04-b	SD+	Apposition	S
EM11-T07	SD-	Apposition	S
EM11-T42	Sp-	S	S
EM11-T50	Sp+	AS	Apposition

Note: +: ENK labeled; **-:** unlabeled; **So:** soma; **LD:** large caliber dendrite (diameter ≥1μm); **SD:** small caliber dendrite (diameter <1μm); **Sp:** spine; **S:** symmetrical synapse; **AS:** asymmetrical synapse.

5.5 DISCUSSION

This is the first investigation to study the ultrastructural localization of ENK in the BLa and also the first investigation to study the possible convergence of NET and ENK axon terminals onto common structures in the BLa. Our results show a limited convergence.

5.5.1 ANATOMICAL CONSIDERATIONS

ENK axon terminals mainly formed asymmetrical synapses indicating that they most likely derived from glutamatergic axons, which is consistent with the previous study showing that more than 95% of ENK+ cells in the BLa expressed vGLUT1 (Poulin et al., 2008). Since glutamatergic pyramidal cells are the major neuron type in the BLa (McDonald, 1992), it is possible that some of ENK+ terminals forming asymmetrical synapses are coming from local collateral axons of pyramidal cells. Additionally, the BLa is one of the amygdaloid divisions that send ENK projections to the central amygdala, indicating that at least some of the projection neurons in the BLa express ENK (Poulin et al., 2006). Another possible origin of these ENK+ terminals are extra glutamate inputs from thalamus and cortex. Very few ENK+ axon terminals formed symmetrical synapses, characteristic of GABAergic synapses. These terminals may belong to BLa interneurons or neurons of the intercalated nucleus, since BLa neurons are under the inhibitory control of the intercalated neurons and there are extensive colocalization of preproenkephalin mRNA and GAD mRNA in the intercalated nuclei (Royer et al., 1999, Poulin et al., 2008) .

ENK+ terminals predominantly formed asymmetrical synapses with ENK+ spines and distal dendrites, but formed symmetrical synapses with dendritic spines as well. This synaptic organization is similar to the inputs to pyramidal cell observed before in the BLa

(Brinley-Reed et al., 1995), indicating that ENK terminals mainly synapse on pyramidal cells, which give rise to most of the spines in the BLa (McDonald, 1992).

ENK-ir was also found in various postsynaptic neuronal structures, including somata, axons, dendritic shafts and spines. ENK-ir was also seen in spiny dendrites in the striatum, which is thought probably to be related to spine plasticity (McCollum et al., 2012). The function of ENK located in postsynaptic compartment of BLa neurons and striatal neurons is not clear.

We found very limited convergence of ENK and NET terminals in the BLa. The extent of convergence may be underestimated due to incomplete terminal analysis. The convergence will be missed if the observing plane is not favor for analyzing convergence.

5.5.2 FUNCTIONAL IMPLICATIONS

Our observations reveal that ENK terminals predominantly form synapses with distal dendrites and spines, which probably originate from pyramidal cell in the BLa. Interestingly, MOR activation has been reported to participate in determining the normal morphology and function of spines in the hippocampus, which could also occur in the amygdala as well through the abundant synaptic contacts of ENK terminals with spines (Liao et al., 2005). Moreover, distal dendrites and spines of pyramidal cells are also the major neuronal compartment of BLa neurons receiving glutamatergic inputs from cortex, thalamus and other nuclei of amygdala and are also targeted by neuromodulatory systems (LeDoux et al., 1991, Stefanacci et al., 1992, Brinley-Reed et al., 1995, Muller et al., 2011, Zhang et al., 2013), indicating that the ENK could involve in the modulation of these inputs.

Although we observed very limited convergence between ENK and NET terminals, if these converging ENK and NET terminals are activated simultaneously, they

could act concomitantly on the neuronal activity of targeted BLa neurons. Nevertheless, the low rate of convergence suggests that postsynaptic interaction may not the major way that these two systems affect each other, at least not by point to point interaction. Moreover, considering that ENK as a peptide neurotransmitter could diffuse in the extracellular space and act on distant targets by volume transmission, it is also possible that ENK could possibly affect NE terminals in this way.

Opioid receptors and adrenoceptors are both G protein coupled receptor; their activation triggers a cascade of cell signaling response. If they are closely colocalized in neuronal profiles, they may affect each other via the interactions of the cell signaling pathways. Earlier studies suggested that MOR and DOR may colocalize with α2 adrenoceptor in a subpopulation of neurons in central and posterior portion of the medial amygdala, which may relate to the alleviation of opiate withdrawal symptoms by α2 adrenergic agonist (Freedman and Aghajanian, 1985). Farb reported that β adrenoceptors are present in the somata, dendritic shafts and spines in the lateral amygdala neurons (Farb et al., 2010). Our findings in chapter 4 indicate that MORs also exist in various postsynaptic compartment in the BLa. Because of the similarity of cell type and synaptology between lateral and basolateral amygdala, it is possible that MOR and β adrenoceptors might colocalize in the BLa as well, which provide an opportunity of two receptors affecting each other through cell signaling pathway.

There were five cases of ENK+ terminals directly contacting NET+ terminals. Although previous investigations revealed that MOR activation inhibits NE release in the BLa (Introini-Collison et al., 1995), this very low rate of direct contact indicates that there are few, if any ENK+ axon terminals affecting NET release. However, ENK maybe

released into extra-synaptic space and then diffuse to the NET terminals. Thus it will be interesting to see whether there is expressing of MOR or DOR on the NET terminals.

CHAPTER 6

GENERAL DISCUSSION

6.1 SUMMARY

In general, we have the following major findings in these studies. First, about half of NET+ axon terminals form synapses in the BLa and the major targets of these terminals were distal dendritic shafts and spines of pyramidal cells. The low synaptic incidence indicates that non-synaptic diffusion might be involved in NE modulation of BLa functions. The fact that NE inputs target the same neuronal compartment as glutamatergic projections to the BLa indicates a possible involvement of NE in long term potentiation, which is the cellular mechanism of memory potentiation. Second, MOR-ir was found in various neuronal profiles and the most frequent labeled structures were small caliber dendrites and terminals. Both symmetrical and asymmetrical synapses were formed by MOR+ terminals, while the asymmetrical ones were more commonly observed. The postsynaptic targets of MOR+ terminals included a variety of labeled or unlabeled neuronal profiles as well, but MOR+ terminals primarily targeted spines with or without MOR-ir, as well as MOR+ small distal dendrites. These data suggest that MOR is involved in both presynaptic and postsynaptic modulation of neuronal activity in the BLa. Third, there was very limited (11%) convergence between ENK+ and NET+ terminals. In addition, our results also reveal that ENK+ axon terminals mainly form asymmetrical synapses in the BLa, indicating that most of ENK+ terminals might be glutamatergic.

6.2 FUNCTIONAL IMPLICATION RELATED TO MEMORY CONSOLIDATION DURING STRESS

Extensive evidence indicates that the amygdala is a key center mediating the modulatory effects of hormones and neurotransmitters on memory consolidation, which selectively occur in the BLa nucleus, the focus of this dissertation (Roozendaal et al., 2009). The interactions of several modulatory systems converge in influencing NE and muscarinic cholinergic activations in the BLa and therefore modulate the memory consolidation in the BLa and other brain areas that receive projections from the BLa (McGaugh, 2004).

The BLa receives a dense noradrenergic projection primarily originating from the LC (Asan, 1998). LC neurons fire in two distinct activity modes: tonic and phasic. LC neurons exhibit phasic responses to salient sensory stimuli such as foot shock, which have a relatively short latency (Berridge and Waterhouse, 2003). Most of the behavioral paradigms using acute stressful or emotional stimuli might elicit the phasic response, whereas the chronic stress model might highly relate to tonic responses. The synaptic formations we observed in the present study probably contribute to the NE release during phasic mode, whereas volume transmission might be more involved in regulating the tonic activity of LC neurons.

We found that distal dendritic shafts and spines of pyramidal cells are the major postsynaptic targets of NE inputs in the BLa, which is also the main target of excitatory inputs to CaMK+ pyramidal cells arising from cortical, thalamic and intra-amygdalar sources (LeDoux et al., 1991, Stefanacci et al., 1992, Brinley-Reed et al., 1995). In addition, previous studies in rat BLa have shown that both pyramidal cells and

nonpyramidal cells exhibit high levels of NMDA receptor subunit1 (NMDAR1) in their dendrites and spines (Farb et al., 1995, Radley et al., 2007). Thus, NE inputs are in a position to modulate synaptic plasticity in synapses forming by these various projections via modulating NMDAR currents. Moreover, we found that small distal dendrites were commonly labeled by MOR+ and many of them exhibited spines, a characteristic of pyramidal cell dendrites. Since 85% of BLa neurons are pyramidal cells (McDonald, 1992), this suggests that most of the MOR+ dendrites might belong to pyramidal cells in the BLa. Therefore, MOR is in a position to affect synaptic plasticity like NE inputs probably via eliciting membrane hyperpolarization. In addition, our ENK labeling results reveal that most of ENK axon terminals form asymmetrical synapses in the BLa indicating they most likely are derived from glutamatergic axons, which might come in part from local collateral axons of pyramidal cells, or inputs from thalamus and cortex. These extra amygdala inputs have been found to primarily target the distal dendritic part of pyramidal cells where the MOR was located according to our results. Thus, ENK released from glutamatergic inputs to pyramidal cells may activate MORs in pyramidal cells.

Large numbers of MOR+ terminals indicate that MOR is highly involved in the presynaptic regulation of the BLa as well. These MOR+ terminals commonly formed asymmetrical synapses and primarily targeted spines, which are characteristics of glutamatergic projections to the BLa from cortical, thalamus and other nuclei of amygdala (LeDoux et al., 1991, Stefanacci et al., 1992, Brinley-Reed et al., 1995) as mentioned above. Therefore, it is highly possible that MORs may be involved in modulation of glutamate release in the BLa. Some of the MOR+ terminals forming

symmetrical synapses might be NE terminals, since NE inputs mainly formed symmetrical synapses in the BLa as our results have shown (Zhang et al., 2013). This might explain the effect of opioid peptidergic drug administration on NE release in the amygdala (Quirarte et al., 1998) , which is believed to be that major way that opioids are involved in memory modulation during stress (Introini-Collison et al., 1995, McGaugh, 2004).

Previous studies have concentrated on examining the presynaptic interactions of the ENK and NE systems. Our studies of convergence were designed to investigate their postsynaptic interactions. We found a limited convergence between ENK+ and NET+ terminals and in most cases of convergence, ENK+ formed asymmetrical synapses or appositions whereas NET+ terminals formed symmetrical synapses. It appears that postsynaptic interaction may not be the major way that these two systems affect each other, at least not by point to point interactions. Because ENK as a peptide neurotransmitter that could diffuse in the extracellular space and act on distant targets by volume transmission, it is possible that ENK could affect NE terminals in this way. Especially, our results show a relatively diverse distribution of MOR in the BLa that could be activated by ENK.

Except for regulating the plasticity inside the amygdala, NE system activation in the BLa could also be involved in memory consolidation in other brain areas. For example, the caudate-putamen is related to learning specific cues while the hippocampus is associated with spatial learning and context conditioning (Packard et al., 1994, Packard and Teather, 1998). Both types of learning in both areas are modulated by the BLa (Packard et al., 1994, Packard and Teather, 1998) . The BLa is thought to influence their

functions via the extensive efferents arising from BLa pyramidal cells, which are the major projection neurons in the BLa. Thus the excitability of BLa pyramidal cells is critical for memory consolidation. β-adrenoceptors have been shown to mediate both the memory consolidation effects and the excitatory effects of NE in the BLa (Gean et al., 1992, Huang et al., 1996, Ferry et al., 1997). On the contrary, α2-adrenoceptors seems to produce inhibitory effects. The two kinds of synapses we observed in our NET labeling studies, i.e., symmetrical and asymmetrical synapses, might represent the different adrenoceptors.

Interestingly, only small populations of pyramidal cells were excited by NE in the BLa via β-adrenoceptors (Buffalari and Grace, 2007). Moreover, an earlier study suggested that memory facilitation effects of post-training systemic administration of naloxone might be mediated via release of the beta-adrenergic effects from the tonic inhibitory influence of endogenous opioids (Izquierdo and Graudenz, 1980). We observed a very limited convergence between ENK + and NET+ terminals. It is possible that the small population of the BLa neurons excited by NE are receiving the converging ENK inputs and thus under inhibitory control of enkephalin, whereas the naloxone blocks the MOR activation and thus terminate the inhibitory effects of ENK inputs, therefore BLa neurons were excited by NE via β-adrenoceptors activation.

6.3 FUNCTIONAL IMPLICATION RELATED TO HYPOALGESIA

We also found that some MOR+ axon terminals form symmetrical synapses, indicating they may come from interneurons. Previous study has shown that activation of presynaptic MOR could attenuate GABAergic inputs to the central amygdala projecting pyramidal neurons in the BLA (Finnegan et al., 2006) . This pyramidal cell disinhibition

might contribute to stress associated hypoalgesia through the BLA-central amygdala-PAG pathway.

6.4 FUNCTIONAL IMPLICATION RELATED TO PTSD

The NE system and opioid system mainly affect pyramidal cells in the BLa according to our results, which was summarized in Figure 6.1. NE, ENK and MOR labeled terminals predominantly synapse with the distal small caliber dendritic shafts and spines in the BLa, indicating that they are at the position that could regulate the effects of specific input and thus might differentially modulate memory consolidation about information from different sources in the BLa. This might explain why the PTSD patients remember certain significant cues during traumatic experiences and later on this trauma related cue becomes a trigger for maladaptive defensive behaviors in those patients. One promising direction for PTSD treatment is pharmacologically intervention initiated soon after trauma exposure, which could reduce or eliminate the development of the PTSD in some traumatized individuals (Lindgren et al., 2013) (Cukor et al., 2009). The β-adrenoceptor antagonist propranolol has been found to decrease the strength of newly acquired emotional memory both in experimental trials and clinical samples (Chamberlain et al., 2006) (Lindgren et al., 2013). Moreover, the acute administration of morphine has been found to limit fear conditioning in patients with traumatic injury (Bryant et al., 2009). Similarly, another study in combat injury also reported that morphine used during early trauma care could reduce the subsequent development of PTSD (Holbrook et al., 2010). This early stage intervention might function through blocking the facilitation of synaptic plasticity in the synapses formed by salient sensory inputs. As a result, this intervention might change the emotional valence of these salient

stimuli and therefore prevent the enhancement of the related memory. Moreover, the individual differences at this step might contribute to the individual differences in susceptibility for PTSD.

In addition, NE and ENK both target the somata and proximal large caliber dendrites of pyramidal neurons in some cases in the BLa. This suggests that they could directly control the firing of the BLa pyramidal cells and therefore affect synaptic plasticity in other brain areas receiving projections from them. Thus, the output pathway of these pyramidal cells is critical for determining what kind of memory is enhanced. It has been reported that stress and anxiety can enhance dorsal striatal-dependent habit memory but impede the hippocampal-dependent cognitive memory, which explains some aspects of PTSD (Goodman et al., 2012) . During robust emotional arousal, BLA activation leads to memory modulation which impairs the hippocampal dependent memory processes, resulting in a reliance on dorsal striatum dependent habit memory (Packard and Wingard, 2004, Wingard and Packard, 2008, Packard and Gabriele, 2009). Therefore NE and ENK could be involved in this process by affecting the excitability of certain pyramidal cell populations which connect with either hippocampal or striatal structures.

Based on our results, these two systems appear to have opposite effects on the BLa neuronal activity since NET+ terminals mainly form symmetrical synapses and ENK+ terminals mainly form asymmetrical synapses in the BLa, which has been supported by previous electrophysiological and behavioral studies (McGaugh, 2004) . But, how these two systems affect each other is very complex. There is very limited synaptic convergence of NET and ENK inputs onto the same neuronal target in the BLa.

But these two systems show potentials for volume transmission: only half of the NET terminals form synapses and extrasynaptic adrenoceptors have been found in the amygdala (Farb et al., 2010, Zhang et al., 2013) ; ENK as a neuropeptide could diffuse for a long distance and reach extra-synaptic receptors, especially considering the widely spread distribution of MOR we found in chapter 4. Therefore, it is highly possible that these two systems could interact with each other even without convergence. The opioid system might serve as a tonic inhibitory control over the NE system. The appropriate memory modulation may involve a delicate balance of these two systems as well as their interactions with other neuromodulatory systems. To figure out the exact mechanism, we need more information about precise localization of their receptors and their morphological relationship with each other and other neuromodulatory systems in the BLa.

6.5 FUTURE DIRECTIONS

Our results suggest a complicated interaction between opioid and NE system, which includes both pre- and post-synaptic effects. Since both synapses and volume transmission affect NE functions, the localization of specific adrenoceptors and their morphological relationships to opioid receptors and inputs is critical to understanding how the NE system affects BLa neuron activity. It would be interesting to explore these relationships using Immunogold silver staining. Our results also suggest that ENK and MOR might locate in glutamatergic inputs to the BLa. Therefore it would be interesting to utilize PHAL tracing technique and immunohistochemistry for ENK or MOR to see the origin of these ENK or MOR contained glutamatergic inputs.

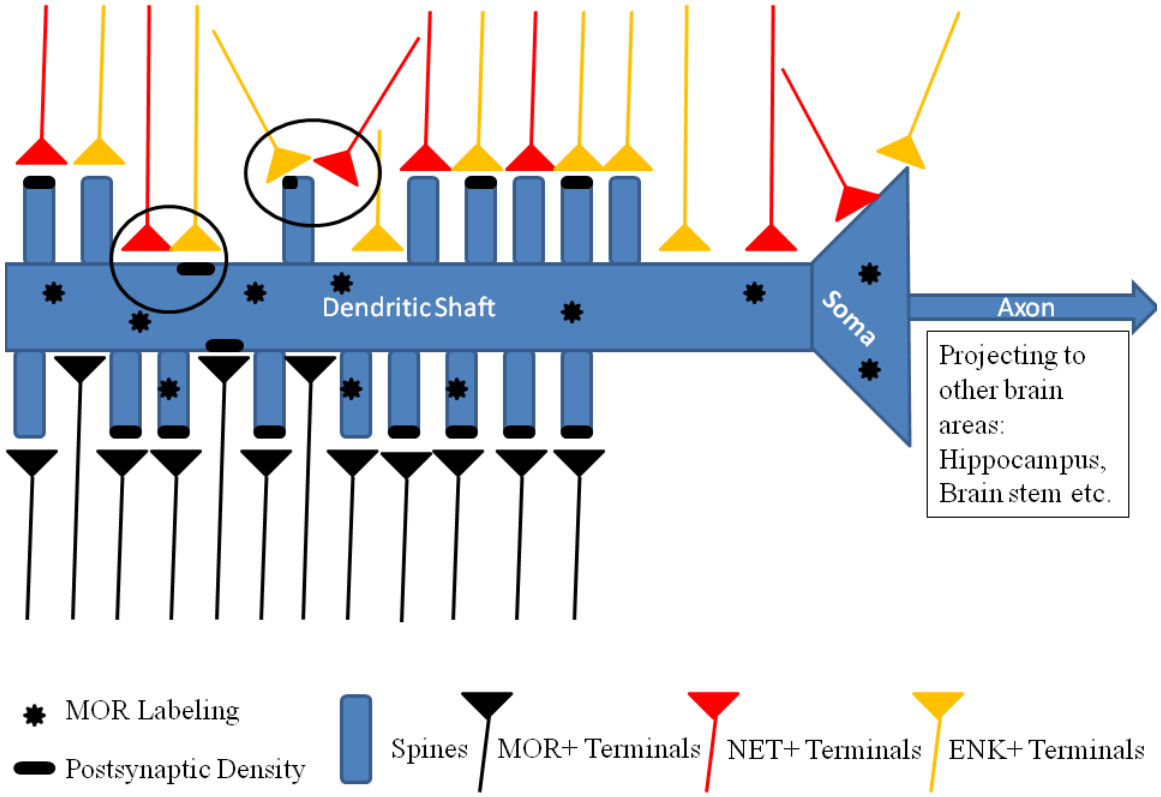

Figure 6.1 Schematic diagram of synaptology of NE and opioid system with pyramidal cells in the BLa. NET+ terminals (Red) mainly form symmetrical synapses with distal dendritic shafts and spines; ENK+ terminals (Yellow) mainly form asymmetrical synapses (containing postsynaptic density) with distal dendritic shafts and spines. Both ENK+ and ENK+ also contact with somata and proximal dendrites of BLa Neurons. There are limited convergences (black circle) of ENK+ and NET+ terminals onto either distal dendritic shafts or spines. MORs (black stars) are mainly present on terminals, distal dendritic shafts and spines. Terminals containing MOR (Black) mainly form asymmetrical synapses (containing postsynaptic density) with MOR+ (black star) or unlabeled spines as well as MOR+ (black star) distal dendritic shafts. The BLa affects synaptic plasticity in other brain areas via its projection to those areas.

REFERENCES

Agnati LF, Fuxe K, Zoli M, Ozini I, Toffano G, Ferraguti F (1986) A correlation analysis of the regional distribution of central enkephalin and beta-endorphin immunoreactive terminals and of opiate receptors in adult and old male rats. Evidence for the existence of two main types of communication in the central nervous system: the volume transmission and the wiring transmission. Acta physiologica Scandinavica 128:201-207.

Agnati LF, Guidolin D, Guescini M, Genedani S, Fuxe K (2010) Understanding wiring and volume transmission. Brain research reviews 64:137-159.

Aoki C (1992) Beta-adrenergic receptors: astrocytic localization in the adult visual cortex and their relation to catecholamine axon terminals as revealed by electron microscopic immunocytochemistry. The Journal of neuroscience : the official journal of the Society for Neuroscience 12:781-792.

Asan E (1998) The catecholaminergic innervation of the rat amygdala. Advances in anatomy, embryology, and cell biology 142:1-118.

Augustine JR (1996) Circuitry and functional aspects of the insular lobe in primates including humans. Brain research Brain research reviews 22:229-244.

Beckerman MA, Glass MJ (2011) Ultrastructural relationship between the AMPA-GluR2 receptor subunit and the mu-opioid receptor in the mouse central nucleus of the amygdala. Experimental neurology 227:149-158.

Beckstead RM (1978) Afferent connections of the entorhinal area in the rat as demonstrated by retrograde cell-labeling with horseradish peroxidase. Brain Res 152:249-264.

Berridge CW, Waterhouse BD (2003) The locus coeruleus-noradrenergic system: modulation of behavioral state and state-dependent cognitive processes. Brain research Brain research reviews 42:33-84.

Braga MF, Aroniadou-Anderjaska V, Manion ST, Hough CJ, Li H (2004) Stress impairs alpha(1A) adrenoceptor-mediated noradrenergic facilitation of GABAergic transmission in the basolateral amygdala. Neuropsychopharmacology : official publication of the American College of Neuropsychopharmacology 29:45-58.

Brinley-Reed M, Mascagni F, McDonald AJ (1995) Synaptology of prefrontal cortical projections to the basolateral amygdala: an electron microscopic study in the rat. Neuroscience letters 202:45-48.

Britton JC, Phan KL, Taylor SF, Fig LM, Liberzon I (2005) Corticolimbic blood flow in posttraumatic stress disorder during script-driven imagery. Biological psychiatry 57:832-840.

Brunetti M, Sepede G, Mingoia G, Catani C, Ferretti A, Merla A, Del Gratta C, Romani GL, Babiloni C (2010) Elevated response of human amygdala to neutral stimuli in mild post traumatic stress disorder: neural correlates of generalized emotional response. Neuroscience 168:670-679.

Bryant RA, Creamer M, O'Donnell M, Silove D, McFarlane AC (2009) A study of the protective function of acute morphine administration on subsequent posttraumatic stress disorder. Biological psychiatry 65:438-440.Bryant RA, Felmingham KL, Kemp AH, Barton M, Peduto AS, Rennie C, Gordon E, Williams LM (2005) Neural networks of information processing in posttraumatic stress disorder: a functional magnetic resonance imaging study. Biological psychiatry 58:111-118.

Buffalari DM, Grace AA (2007) Noradrenergic modulation of basolateral amygdala neuronal activity: opposing influences of alpha-2 and beta receptor activation. The Journal of neuroscience : the official journal of the Society for Neuroscience 27:12358-12366.

Buffalari DM, Grace AA (2009) Anxiogenic modulation of spontaneous and evoked neuronal activity in the basolateral amygdala. Neuroscience 163:1069-1077.

Cahill L, Babinsky R, Markowitsch HJ, McGaugh JL (1995) The amygdala and emotional memory. Nature 377:295-296.

Canteras NS, Simerly RB, Swanson LW (1995) Organization of projections from the medial nucleus of the amygdala: a PHAL study in the rat. The Journal of comparative neurology 360:213-245.

Cassell MD, Freedman LJ, Shi C (1999) The intrinsic organization of the central extended amygdala. Annals of the New York Academy of Sciences 877:217-241.

Chamberlain SR, Muller U, Blackwell AD, Robbins TW, Sahakian BJ (2006) Noradrenergic modulation of working memory and emotional memory in humans. Psychopharmacology 188:397-407.

Chen FJ, Sara SJ (2007) Locus coeruleus activation by foot shock or electrical stimulation inhibits amygdala neurons. Neuroscience 144:472-481.

Cheng PY, Svingos AL, Wang H, Clarke CL, Jenab S, Beczkowska IW, Inturrisi CE, Pickel VM (1995) Ultrastructural immunolabeling shows prominent presynaptic vesicular localization of delta-opioid receptor within both enkephalin- and nonenkephalin-containing axon terminals in the superficial layers of the rat cervical spinal cord. The Journal of neuroscience : the official journal of the Society for Neuroscience 15:5976-5988.

Cukor J, Spitalnick J, Difede J, Rizzo A, Rothbaum BO (2009) Emerging treatments for PTSD. Clinical psychology review 29:715-726.

Da Cunha C, Roozendaal B, Vazdarjanova A, McGaugh JL (1999) Microinfusions of flumazenil into the basolateral but not the central nucleus of the amygdala enhance memory consolidation in rats. Neurobiology of learning and memory 72:1-7.

Davis M, Shi C (1999) The extended amygdala: are the central nucleus of the amygdala and the bed nucleus of the stria terminalis differentially involved in fear versus anxiety? Annals of the New York Academy of Sciences 877:281-291.

Deng YP, Xie JP, Wang HB, Lei WL, Chen Q, Reiner A (2007) Differential localization of the GluR1 and GluR2 subunits of the AMPA-type glutamate receptor among striatal neuron types in rats. Journal of chemical neuroanatomy 33:167-192.

Dickie EW, Brunet A, Akerib V, Armony JL (2008) An fMRI investigation of memory encoding in PTSD: influence of symptom severity. Neuropsychologia 46:1522-1531.

Ding YQ, Kaneko T, Nomura S, Mizuno N (1996) Immunohistochemical localization of mu-opioid receptors in the central nervous system of the rat. The Journal of comparative neurology 367:375-402.
Drolet G, Dumont EC, Gosselin I, Kinkead R, Laforest S, Trottier JF (2001) Role of endogenous opioid system in the regulation of the stress response. Progress in neuro-psychopharmacology & biological psychiatry 25:729-741.
Erickson SL, Gandhi AR, Asafu-Adjei JK, Sampson AR, Miner L, Blakely RD, Sesack SR (2011) Chronic desipramine treatment alters tyrosine hydroxylase but not norepinephrine transporter immunoreactivity in norepinephrine axons in the rat prefrontal cortex. Int J Neuropsychopharmacol 14:1219-1232.
Faber ES, Sah P (2004) Opioids inhibit lateral amygdala pyramidal neurons by enhancing a dendritic potassium current. The Journal of neuroscience : the official journal of the Society for Neuroscience 24:3031-3039.
Fallon JH, Koziell DA, Moore RY (1978) Catecholamine innervation of the basal forebrain. II. Amygdala, suprarhinal cortex and entorhinal cortex. The Journal of comparative neurology 180:509-532.
Farb CR, Aoki C, Ledoux JE (1995) Differential localization of NMDA and AMPA receptor subunits in the lateral and basal nuclei of the amygdala: a light and electron microscopic study. The Journal of comparative neurology 362:86-108.
Farb CR, Chang W, Ledoux JE (2010) Ultrastructural characterization of noradrenergic axons and Beta-adrenergic receptors in the lateral nucleus of the amygdala. Frontiers in behavioral neuroscience 4:162.
Ferry B, Magistretti PJ, Pralong E (1997) Noradrenaline modulates glutamate-mediated neurotransmission in the rat basolateral amygdala in vitro. The European journal of neuroscience 9:1356-1364.
Ferry B, McGaugh JL (1999) Clenbuterol administration into the basolateral amygdala post-training enhances retention in an inhibitory avoidance task. Neurobiology of learning and memory 72:8-12.
Ferry B, McGaugh JL (2008) Involvement of basolateral amygdala alpha2-adrenoceptors in modulating consolidation of inhibitory avoidance memory. Learn Mem 15:238-243.
Finnegan TF, Chen SR, Pan HL (2006) Mu opioid receptor activation inhibits GABAergic inputs to basolateral amygdala neurons through Kv1.1/1.2 channels. Journal of neurophysiology 95:2032-2041.
Freedman JE, Aghajanian GK (1985) Opiate and alpha 2-adrenoceptor responses of rat amygdaloid neurons: co-localization and interactions during withdrawal. The Journal of neuroscience : the official journal of the Society for Neuroscience 5:3016-3024.
Fulwiler CE, Saper CB (1984) Subnuclear organization of the efferent connections of the parabrachial nucleus in the rat. Brain Res 319:229-259.
Galvez R, Mesches MH, McGaugh JL (1996) Norepinephrine release in the amygdala in response to footshock stimulation. Neurobiology of learning and memory 66:253-257.
Gastard M, Jensen SL, Martin JR, 3rd, Williams EA, Zahm DS (2002) The caudal sublenticular region/anterior amygdaloid area is the only part of the rat forebrain and mesopontine tegmentum occupied by magnocellular cholinergic neurons that

receives outputs from the central division of extended amygdala. Brain Res 957:207-222.
Gean PW, Huang CC, Lin JH, Tsai JJ (1992) Sustained enhancement of NMDA receptor-mediated synaptic potential by isoproterenol in rat amygdalar slices. Brain Res 594:331-334.
Glass MJ, Kruzich PJ, Colago EE, Kreek MJ, Pickel VM (2005) Increased AMPA GluR1 receptor subunit labeling on the plasma membrane of dendrites in the basolateral amygdala of rats self-administering morphine. Synapse 58:1-12.
Glass MJ, Vanyo L, Quimson L, Pickel VM (2009) Ultrastructural relationship between N-methyl-D-aspartate-NR1 receptor subunit and mu-opioid receptor in the mouse central nucleus of the amygdala. Neuroscience 163:857-867.
Goodman J, Leong KC, Packard MG (2012) Emotional modulation of multiple memory systems: implications for the neurobiology of post-traumatic stress disorder. Reviews in the neurosciences 0:1-17.
Gracy KN, Svingos AL, Pickel VM (1997) Dual ultrastructural localization of mu-opioid receptors and NMDA-type glutamate receptors in the shell of the rat nucleus accumbens. The Journal of neuroscience : the official journal of the Society for Neuroscience 17:4839-4848.
Gray TS, Cassell MD, Kiss JZ (1984) Distribution of pro-opiomelanocortin-derived peptides and enkephalins in the rat central nucleus of the amygdala. Brain Res 306:354-358.
Hancock MB (1986) Two-color immunoperoxidase staining: visualization of anatomic relationships between immunoreactive neural elements. The American journal of anatomy 175:343-352.
Harlan RE, Shivers BD, Romano GJ, Howells RD, Pfaff DW (1987) Localization of preproenkephalin mRNA in the rat brain and spinal cord by in situ hybridization. The Journal of comparative neurology 258:159-184.
Harris JA (1996) Descending antinociceptive mechanisms in the brainstem: their role in the animal's defensive system. Journal of physiology, Paris 90:15-25.
Hatfield T, Spanis C, McGaugh JL (1999) Response of amygdalar norepinephrine to footshock and GABAergic drugs using in vivo microdialysis and HPLC. Brain Res 835:340-345.
Helmstetter FJ, Bellgowan PS, Poore LH (1995) Microinfusion of mu but not delta or kappa opioid agonists into the basolateral amygdala results in inhibition of the tail flick reflex in pentobarbital-anesthetized rats. The Journal of pharmacology and experimental therapeutics 275:381-388.
Helmstetter FJ, Tershner SA, Poore LH, Bellgowan PS (1998) Antinociception following opioid stimulation of the basolateral amygdala is expressed through the periaqueductal gray and rostral ventromedial medulla. Brain Res 779:104-118.
Hipolide DC, Moreira KM, Barlow KB, Wilson AA, Nobrega JN, Tufik S (2005) Distinct effects of sleep deprivation on binding to norepinephrine and serotonin transporters in rat brain. Progress in neuro-psychopharmacology & biological psychiatry 29:297-303.
Holbrook TL, Galarneau MR, Dye JL, Quinn K, Dougherty AL (2010) Morphine use after combat injury in Iraq and post-traumatic stress disorder. The New England journal of medicine 362:110-117.

Hopkins DA, Holstege G (1978) Amygdaloid projections to the mesencephalon, pons and medulla oblongata in the cat. Experimental brain research Experimentelle Hirnforschung Experimentation cerebrale 32:529-547.
Huang CC, Hsu KS, Gean PW (1996) Isoproterenol potentiates synaptic transmission primarily by enhancing presynaptic calcium influx via P- and/or Q-type calcium channels in the rat amygdala. The Journal of neuroscience : the official journal of the Society for Neuroscience 16:1026-1033.
Hughes KC, Shin LM (2011) Functional neuroimaging studies of post-traumatic stress disorder. Expert review of neurotherapeutics 11:275-285.
Introini-Collison IB, Ford L, McGaugh JL (1995) Memory impairment induced by intraamygdala beta-endorphin is mediated by noradrenergic influences. Neurobiology of learning and memory 63:200-205.
Introini-Collison IB, Nagahara AH, McGaugh JL (1989) Memory enhancement with intra-amygdala post-training naloxone is blocked by concurrent administration of propranolol. Brain Res 476:94-101.
Izquierdo I, Graudenz M (1980) Memory facilitation by naloxone is due to release of dopaminergic and beta-adrenergic systems from tonic inhibition. Psychopharmacology 67:265-268.
Javidi H, Yadollahie M (2012) Post-traumatic Stress Disorder. The international journal of occupational and environmental medicine 3:2-9.
Kaneko K, Tamamaki N, Owada H, Kakizaki T, Kume N, Totsuka M, Yamamoto T, Yawo H, Yagi T, Obata K, Yanagawa Y (2008) Noradrenergic excitation of a subpopulation of GABAergic cells in the basolateral amygdala via both activation of nonselective cationic conductance and suppression of resting K+ conductance: a study using glutamate decarboxylase 67-green fluorescent protein knock-in mice. Neuroscience 157:781-797.
Kang W, Wilson SP, Wilson MA (2000) Overexpression of proenkephalin in the amygdala potentiates the anxiolytic effects of benzodiazepines. Neuropsychopharmacology : official publication of the American College of Neuropsychopharmacology 22:77-88.
Kemppainen S, Jolkkonen E, Pitkanen A (2002) Projections from the posterior cortical nucleus of the amygdala to the hippocampal formation and parahippocampal region in rat. Hippocampus 12:735-755.
Kishi T, Tsumori T, Yokota S, Yasui Y (2006) Topographical projection from the hippocampal formation to the amygdala: a combined anterograde and retrograde tracing study in the rat. The Journal of comparative neurology 496:349-368.
Krettek JE, Price JL (1978) A description of the amygdaloid complex in the rat and cat with observations on intra-amygdaloid axonal connections. The Journal of comparative neurology 178:255-280.
Kung JC, Chen TC, Shyu BC, Hsiao S, Huang AC (2010) Anxiety- and depressive-like responses and c-fos activity in preproenkephalin knockout mice: oversensitivity hypothesis of enkephalin deficit-induced posttraumatic stress disorder. Journal of biomedical science 17:29.
LeDoux JE (2000) Emotion circuits in the brain. Annual review of neuroscience 23:155-184.

LeDoux JE, Farb CR, Milner TA (1991) Ultrastructure and synaptic associations of auditory thalamo-amygdala projections in the rat. Experimental brain research Experimentelle Hirnforschung Experimentation cerebrale 85:577-586.
LeDoux JE, Iwata J, Cicchetti P, Reis DJ (1988) Different projections of the central amygdaloid nucleus mediate autonomic and behavioral correlates of conditioned fear. The Journal of neuroscience : the official journal of the Society for Neuroscience 8:2517-2529.
LeDoux JE, Sakaguchi A, Reis DJ (1984) Subcortical efferent projections of the medial geniculate nucleus mediate emotional responses conditioned to acoustic stimuli. The Journal of neuroscience : the official journal of the Society for Neuroscience 4:683-698.
Li R, Nishijo H, Ono T, Ohtani Y, Ohtani O (2002) Synapses on GABAergic neurons in the basolateral nucleus of the rat amygdala: double-labeling immunoelectron microscopy. Synapse 43:42-50.
Li R, Nishijo H, Wang Q, Uwano T, Tamura R, Ohtani O, Ono T (2001) Light and electron microscopic study of cholinergic and noradrenergic elements in the basolateral nucleus of the rat amygdala: evidence for interactions between the two systems. The Journal of comparative neurology 439:411-425.
Liao D, Lin H, Law PY, Loh HH (2005) Mu-opioid receptors modulate the stability of dendritic spines. Proceedings of the National Academy of Sciences of the United States of America 102:1725-1730.
Liberzon I, Taylor SF, Amdur R, Jung TD, Chamberlain KR, Minoshima S, Koeppe RA, Fig LM (1999) Brain activation in PTSD in response to trauma-related stimuli. Biological psychiatry 45:817-826.
Liberzon I, Zubieta JK, Fig LM, Phan KL, Koeppe RA, Taylor SF (2002) mu-Opioid receptors and limbic responses to aversive emotional stimuli. Proceedings of the National Academy of Sciences of the United States of America 99:7084-7089.
Likhtik E, Popa D, Apergis-Schoute J, Fidacaro GA, Pare D (2008) Amygdala intercalated neurons are required for expression of fear extinction. Nature 454:642-645.
Lindgren ME, Fagundes CP, Alfano CM, Povoski SP, Agnese DM, Arnold MW, Farrar WB, Yee LD, Carson WE, Schmidt CR, Kiecolt-Glaser JK (2013) Beta-blockers may reduce intrusive thoughts in newly diagnosed cancer patients. Psycho-oncology 22:1889-1894.
Lupien SJ, McEwen BS (1997) The acute effects of corticosteroids on cognition: integration of animal and human model studies. Brain research Brain research reviews 24:1-27.
Ma S, Morilak DA (2005) Norepinephrine release in medial amygdala facilitates activation of the hypothalamic-pituitary-adrenal axis in response to acute immobilisation stress. Journal of neuroendocrinology 17:22-28.
Majak K, Pikkarainen M, Kemppainen S, Jolkkonen E, Pitkanen A (2002) Projections from the amygdaloid complex to the claustrum and the endopiriform nucleus: a Phaseolus vulgaris leucoagglutinin study in the rat. The Journal of comparative neurology 451:236-249.

Majak K, Pitkanen A (2003) Projections from the periamygdaloid cortex to the amygdaloid complex, the hippocampal formation, and the parahippocampal region: a PHA-L study in the rat. Hippocampus 13:922-942.
Mansour A, Khachaturian H, Lewis ME, Akil H, Watson SJ (1987) Autoradiographic differentiation of mu, delta, and kappa opioid receptors in the rat forebrain and midbrain. The Journal of neuroscience : the official journal of the Society for Neuroscience 7:2445-2464.
Maren S, Fanselow MS (1995) Synaptic plasticity in the basolateral amygdala induced by hippocampal formation stimulation in vivo. The Journal of neuroscience : the official journal of the Society for Neuroscience 15:7548-7564.
Mascagni F, McDonald AJ (2003) Immunohistochemical characterization of cholecystokinin containing neurons in the rat basolateral amygdala. Brain Res 976:171-184.
Mason ST, Fibiger HC (1979) Regional topography within noradrenergic locus coeruleus as revealed by retrograde transport of horseradish peroxidase. The Journal of comparative neurology 187:703-724.
Matthies HJ, Han Q, Shields A, Wright J, Moore JL, Winder DG, Galli A, Blakely RD (2009) Subcellular localization of the antidepressant-sensitive norepinephrine transporter. BMC neuroscience 10:65.
McCollum LA, Roche JK, Roberts RC (2012) Immunohistochemical localization of enkephalin in the human striatum: a postmortem ultrastructural study. Synapse 66:204-219.
McDonald AJ (1982a) Cytoarchitecture of the central amygdaloid nucleus of the rat. The Journal of comparative neurology 208:401-418.
McDonald AJ (1982b) Neurons of the lateral and basolateral amygdaloid nuclei: a Golgi study in the rat. The Journal of comparative neurology 212:293-312.
McDonald AJ (1983) Cytoarchitecture of the nucleus of the lateral olfactory tract: a Golgi study in the rat. Brain research bulletin 10:497-503.
McDonald AJ (1985a) Immunohistochemical identification of gamma-aminobutyric acid-containing neurons in the rat basolateral amygdala. Neuroscience letters 53:203-207.
McDonald AJ (1985b) Morphology of peptide-containing neurons in the rat basolateral amygdaloid nucleus. Brain Res 338:186-191.
McDonald AJ (1991) Topographical organization of amygdaloid projections to the caudatoputamen, nucleus accumbens, and related striatal-like areas of the rat brain. Neuroscience 44:15-33.
McDonald AJ (1992) Projection neurons of the basolateral amygdala: a correlative Golgi and retrograde tract tracing study. Brain research bulletin 28:179-185.
McDonald AJ (1994a) Calretinin immunoreactive neurons in the basolateral amygdala of the rat and monkey. Brain Res 667:238-242.
McDonald AJ (1994b) Neuronal localization of glutamate receptor subunits in the basolateral amygdala. Neuroreport 6:13-16.
McDonald AJ (1997) Calbindin-D28k immunoreactivity in the rat amygdala. The Journal of comparative neurology 383:231-244.
McDonald AJ (1998) Cortical pathways to the mammalian amygdala. Progress in neurobiology 55:257-332.

McDonald AJ (2003) Is there an amygdala and how far does it extend? An anatomical perspective. Annals of the New York Academy of Sciences 985:1-21.
McDonald AJ, Augustine JR (1993) Localization of GABA-like immunoreactivity in the monkey amygdala. Neuroscience 52:281-294.
McDonald AJ, Betette RL (2001) Parvalbumin-containing neurons in the rat basolateral amygdala: morphology and co-localization of Calbindin-D(28k). Neuroscience 102:413-425.
McDonald AJ, Mascagni F (1997) Projections of the lateral entorhinal cortex to the amygdala: a Phaseolus vulgaris leucoagglutinin study in the rat. Neuroscience 77:445-459.
McDonald AJ, Mascagni F (2001) Colocalization of calcium-binding proteins and GABA in neurons of the rat basolateral amygdala. Neuroscience 105:681-693.
McDonald AJ, Mascagni F (2002) Immunohistochemical characterization of somatostatin containing interneurons in the rat basolateral amygdala. Brain Res 943:237-244.
McDonald AJ, Mascagni F, Guo L (1996) Projections of the medial and lateral prefrontal cortices to the amygdala: a Phaseolus vulgaris leucoagglutinin study in the rat. Neuroscience 71:55-75.
McDonald AJ, Muller JF, Mascagni F (2002) GABAergic innervation of alpha type II calcium/calmodulin-dependent protein kinase immunoreactive pyramidal neurons in the rat basolateral amygdala. The Journal of comparative neurology 446:199-218.
McDonald AJ, Pearson JC (1989) Coexistence of GABA and peptide immunoreactivity in non-pyramidal neurons of the basolateral amygdala. Neuroscience letters 100:53-58.
McDonald AJ, Shammah-Lagnado SJ, Shi C, Davis M (1999) Cortical afferents to the extended amygdala. Annals of the New York Academy of Sciences 877:309-338.
McGaugh JL (2004) The amygdala modulates the consolidation of memories of emotionally arousing experiences. Annual review of neuroscience 27:1-28.
McGaugh JL, Introini-Collison IB, Nagahara AH (1988) Memory-enhancing effects of posttraining naloxone: involvement of beta-noradrenergic influences in the amygdaloid complex. Brain Res 446:37-49.
McGaugh JL, Izquierdo I (2000) The contribution of pharmacology to research on the mechanisms of memory formation. Trends in pharmacological sciences 21:208-210.
McIntyre CK, Hatfield T, McGaugh JL (2002) Amygdala norepinephrine levels after training predict inhibitory avoidance retention performance in rats. The European journal of neuroscience 16:1223-1226.
Meloni EG, Jackson A, Gerety LP, Cohen BM, Carlezon WA, Jr. (2006) Role of the bed nucleus of the stria terminalis (BST) in the expression of conditioned fear. Annals of the New York Academy of Sciences 1071:538-541.
Millan MJ (2003) The neurobiology and control of anxious states. Progress in neurobiology 70:83-244.
Miner LH, Schroeter S, Blakely RD, Sesack SR (2003) Ultrastructural localization of the norepinephrine transporter in superficial and deep layers of the rat prelimbic prefrontal cortex and its spatial relationship to probable dopamine terminals. The Journal of comparative neurology 466:478-494.

Muller JF, Mascagni F, McDonald AJ (2006) Pyramidal cells of the rat basolateral amygdala: synaptology and innervation by parvalbumin-immunoreactive interneurons. The Journal of comparative neurology 494:635-650.
Muller JF, Mascagni F, McDonald AJ (2007) Serotonin-immunoreactive axon terminals innervate pyramidal cells and interneurons in the rat basolateral amygdala. The Journal of comparative neurology 505:314-335.
Muller JF, Mascagni F, McDonald AJ (2009) Dopaminergic innervation of pyramidal cells in the rat basolateral amygdala. Brain structure & function 213:275-288.
Muller JF, Mascagni F, McDonald AJ (2011) Cholinergic innervation of pyramidal cells and parvalbumin-immunoreactive interneurons in the rat basolateral amygdala. The Journal of comparative neurology 519:790-805.
Muller JF, Mascagni F, Zaric V, McDonald AJ (2013) Muscarinic cholinergic receptor M1 in the rat basolateral amygdala: ultrastructural localization and synaptic relationships to cholinergic axons. The Journal of comparative neurology 521:1743-1759.
Muller M, Fendt M (2006) Temporary inactivation of the medial and basolateral amygdala differentially affects TMT-induced fear behavior in rats. Behavioural brain research 167:57-62.
Nestler EJ HS, Malenka RC (2001) Molecular Neuropharmacology - A Foundation for Clinical Neuroscience.
Nitecka L, Amerski L, Narkiewicz O (1981) The organization of intraamygdaloid connections; an HRP study. Journal fur Hirnforschung 22:3-7.
Olschowka JA, Molliver ME, Grzanna R, Rice FL, Coyle JT (1981) Ultrastructural demonstration of noradrenergic synapses in the rat central nervous system by dopamine-beta-hydroxylase immunocytochemistry. The journal of histochemistry and cytochemistry : official journal of the Histochemistry Society 29:271-280.
Onur OA, Walter H, Schlaepfer TE, Rehme AK, Schmidt C, Keysers C, Maier W, Hurlemann R (2009) Noradrenergic enhancement of amygdala responses to fear. Social cognitive and affective neuroscience 4:119-126.
Osuch EA, Willis MW, Bluhm R, Group CNS, Ursano RJ, Drevets WC (2008) Neurophysiological responses to traumatic reminders in the acute aftermath of serious motor vehicle collisions using [15O]-H2O positron emission tomography. Biological psychiatry 64:327-335.
Ottersen OP (1981) Afferent connections to the amygdaloid complex of the rat with some observations in the cat. III. Afferents from the lower brain stem. The Journal of comparative neurology 202:335-356.
Ottersen OP (1982) Connections of the amygdala of the rat. IV: Corticoamygdaloid and intraamygdaloid connections as studied with axonal transport of horseradish peroxidase. The Journal of comparative neurology 205:30-48.
Packard MG, Cahill L, McGaugh JL (1994) Amygdala modulation of hippocampal-dependent and caudate nucleus-dependent memory processes. Proceedings of the National Academy of Sciences of the United States of America 91:8477-8481.
Packard MG, Gabriele A (2009) Peripheral anxiogenic drug injections differentially affect cognitive and habit memory: role of basolateral amygdala. Neuroscience 164:457-462.

Packard MG, Teather LA (1998) Amygdala modulation of multiple memory systems: hippocampus and caudate-putamen. Neurobiology of learning and memory 69:163-203.
Packard MG, Wingard JC (2004) Amygdala and "emotional" modulation of the relative use of multiple memory systems. Neurobiology of learning and memory 82:243-252.
Paden CM, Krall S, Lynch WC (1987) Heterogeneous distribution and upregulation of mu, delta and kappa opioid receptors in the amygdala. Brain Res 418:349-355.
Papadopoulos GC, Parnavelas JG, Buijs RM (1989) Light and electron microscopic immunocytochemical analysis of the dopamine innervation of the rat visual cortex. Journal of neurocytology 18:303-310.
Pare D, Smith Y (1993) The intercalated cell masses project to the central and medial nuclei of the amygdala in cats. Neuroscience 57:1077-1090.
Pare D, Smith Y, Pare JF (1995) Intra-amygdaloid projections of the basolateral and basomedial nuclei in the cat: Phaseolus vulgaris-leucoagglutinin anterograde tracing at the light and electron microscopic level. Neuroscience 69:567-583.
Parent MB, McGaugh JL (1994) Posttraining infusion of lidocaine into the amygdala basolateral complex impairs retention of inhibitory avoidance training. Brain Res 661:97-103.
Parsons RG, Ressler KJ (2013) Implications of memory modulation for post-traumatic stress and fear disorders. Nature neuroscience 16:146-153.
Paxinos G, Watson C (1986) The rat brain in stereotaxic coordinates. New York: Academic Press.
Pego JM, Morgado P, Pinto LG, Cerqueira JJ, Almeida OF, Sousa N (2008) Dissociation of the morphological correlates of stress-induced anxiety and fear. The European journal of neuroscience 27:1503-1516.
Peters A PS, Webster HD (1991) The fine structure of the nervous system. New York Oxford University Press.
Pikkarainen M, Pitkanen A (2001) Projections from the lateral, basal and accessory basal nuclei of the amygdala to the perirhinal and postrhinal cortices in rat. Cerebral cortex 11:1064-1082.
Pissiota A, Frans O, Fernandez M, von Knorring L, Fischer H, Fredrikson M (2002) Neurofunctional correlates of posttraumatic stress disorder: a PET symptom provocation study. European archives of psychiatry and clinical neuroscience 252:68-75.
Pitkanen A, Amaral DG (1991) Demonstration of projections from the lateral nucleus to the basal nucleus of the amygdala: a PHA-L study in the monkey. Experimental brain research Experimentelle Hirnforschung Experimentation cerebrale 83:465-470.
Pitkanen A, Pikkarainen M, Nurminen N, Ylinen A (2000) Reciprocal connections between the amygdala and the hippocampal formation, perirhinal cortex, and postrhinal cortex in rat. A review. Annals of the New York Academy of Sciences 911:369-391.
Pitman RK, Rasmusson AM, Koenen KC, Shin LM, Orr SP, Gilbertson MW, Milad MR, Liberzon I (2012) Biological studies of post-traumatic stress disorder. Nature reviews Neuroscience 13:769-787.

Poulin JF, Castonguay-Lebel Z, Laforest S, Drolet G (2008) Enkephalin co-expression with classic neurotransmitters in the amygdaloid complex of the rat. The Journal of comparative neurology 506:943-959.
Poulin JF, Chevalier B, Laforest S, Drolet G (2006) Enkephalinergic afferents of the centromedial amygdala in the rat. The Journal of comparative neurology 496:859-876.
Power AE, McGaugh JL (2002) Cholinergic activation of the basolateral amygdala regulates unlearned freezing behavior in rats. Behavioural brain research 134:307-315.
Protopopescu X, Pan H, Tuescher O, Cloitre M, Goldstein M, Engelien W, Epstein J, Yang Y, Gorman J, LeDoux J, Silbersweig D, Stern E (2005) Differential time courses and specificity of amygdala activity in posttraumatic stress disorder subjects and normal control subjects. Biological psychiatry 57:464-473.
Quirarte GL, Galvez R, Roozendaal B, McGaugh JL (1998) Norepinephrine release in the amygdala in response to footshock and opioid peptidergic drugs. Brain Res 808:134-140.
Radley JJ, Farb CR, He Y, Janssen WG, Rodrigues SM, Johnson LR, Hof PR, LeDoux JE, Morrison JH (2007) Distribution of NMDA and AMPA receptor subunits at thalamo-amygdaloid dendritic spines. Brain Res 1134:87-94.
Rauch SL, Whalen PJ, Shin LM, McInerney SC, Macklin ML, Lasko NB, Orr SP, Pitman RK (2000) Exaggerated amygdala response to masked facial stimuli in posttraumatic stress disorder: a functional MRI study. Biological psychiatry 47:769-776.
Ricardo JA, Koh ET (1978) Anatomical evidence of direct projections from the nucleus of the solitary tract to the hypothalamus, amygdala, and other forebrain structures in the rat. Brain Res 153:1-26.
Rizvi TA, Ennis M, Behbehani MM, Shipley MT (1991) Connections between the central nucleus of the amygdala and the midbrain periaqueductal gray: topography and reciprocity. The Journal of comparative neurology 303:121-131.
Romanski LM, Clugnet MC, Bordi F, LeDoux JE (1993) Somatosensory and auditory convergence in the lateral nucleus of the amygdala. Behavioral neuroscience 107:444-450.
Romanski LM, LeDoux JE (1993) Information cascade from primary auditory cortex to the amygdala: corticocortical and corticoamygdaloid projections of temporal cortex in the rat. Cerebral cortex 3:515-532.
Roozendaal B, McEwen BS, Chattarji S (2009) Stress, memory and the amygdala. Nature reviews Neuroscience 10:423-433.
Royer S, Martina M, Pare D (1999) An inhibitory interface gates impulse traffic between the input and output stations of the amygdala. The Journal of neuroscience : the official journal of the Society for Neuroscience 19:10575-10583.
Russchen FT (1982) Amygdalopetal projections in the cat. II. Subcortical afferent connections. A study with retrograde tracing techniques. The Journal of comparative neurology 207:157-176.
Sah P (2006) Canonical organization of opioid modulation of nociceptive circuits. Focus on "mu opioid receptor activation inhibits GABAergic inputs to basolateral

amygdala neurons through Kv1.1/Kv1.2 channels". Journal of neurophysiology 95:2029-2030.
Sah P, Faber ES, Lopez De Armentia M, Power J (2003) The amygdaloid complex: anatomy and physiology. Physiological reviews 83:803-834.
Samson RD, Pare D (2005) Activity-dependent synaptic plasticity in the central nucleus of the amygdala. The Journal of neuroscience : the official journal of the Society for Neuroscience 25:1847-1855.
Santiago AC, Shammah-Lagnado SJ (2004) Efferent connections of the nucleus of the lateral olfactory tract in the rat. The Journal of comparative neurology 471:314-332.
Saper CB (1984) Organization of cerebral cortical afferent systems in the rat. II. Magnocellular basal nucleus. The Journal of comparative neurology 222:313-342.
Saper CB, Loewy AD (1980) Efferent connections of the parabrachial nucleus in the rat. Brain Res 197:291-317.
Savander V, Miettinen R, Ledoux JE, Pitkanen A (1997) Lateral nucleus of the rat amygdala is reciprocally connected with basal and accessory basal nuclei: a light and electron microscopic study. Neuroscience 77:767-781.
Scavone JL, Asan E, Van Bockstaele EJ (2011) Unraveling glutamate-opioid receptor interactions using high-resolution electron microscopy: implications for addiction-related processes. Experimental neurology 229:207-213.
Schroeter S, Apparsundaram S, Wiley RG, Miner LH, Sesack SR, Blakely RD (2000) Immunolocalization of the cocaine- and antidepressant-sensitive l-norepinephrine transporter. The Journal of comparative neurology 420:211-232.
Schwob JE, Price JL (1984) The development of lamination of afferent fibers to the olfactory cortex in rats, with additional observations in the adult. The Journal of comparative neurology 223:203-222.
Seguela P, Watkins KC, Geffard M, Descarries L (1990) Noradrenaline axon terminals in adult rat neocortex: an immunocytochemical analysis in serial thin sections. Neuroscience 35:249-264.
Sevelinges Y, Gervais R, Messaoudi B, Granjon L, Mouly AM (2004) Olfactory fear conditioning induces field potential potentiation in rat olfactory cortex and amygdala. Learn Mem 11:761-769.
Shin MS, Helmstetter FJ (2005) Antinociception following application of DAMGO to the basolateral amygdala results from a direct interaction of DAMGO with Mu opioid receptors in the amygdala. Brain Res 1064:56-65.
Sigurdsson T, Doyere V, Cain CK, LeDoux JE (2007) Long-term potentiation in the amygdala: a cellular mechanism of fear learning and memory. Neuropharmacology 52:215-227.
Smith HR, Porrino LJ (2008) The comparative distributions of the monoamine transporters in the rodent, monkey, and human amygdala. Brain structure & function 213:73-91.
Smith Y, Pare D (1994) Intra-amygdaloid projections of the lateral nucleus in the cat: PHA-L anterograde labeling combined with postembedding GABA and glutamate immunocytochemistry. The Journal of comparative neurology 342:232-248.
Stefanacci L, Farb CR, Pitkanen A, Go G, LeDoux JE, Amaral DG (1992) Projections from the lateral nucleus to the basal nucleus of the amygdala: a light and electron

microscopic PHA-L study in the rat. The Journal of comparative neurology 323:586-601.
Stefano GB, Goumon Y, Casares F, Cadet P, Fricchione GL, Rialas C, Peter D, Sonetti D, Guarna M, Welters ID, Bianchi E (2000) Endogenous morphine. Trends in neurosciences 23:436-442.
Sugita S, North RA (1993) Opioid actions on neurons of rat lateral amygdala in vitro. Brain Res 612:151-155.
Sved AF, Cano G, Passerin AM, Rabin BS (2002) The locus coeruleus, Barrington's nucleus, and neural circuits of stress. Physiology & behavior 77:737-742.
Tomaz C, Dickinson-Anson H, McGaugh JL (1992) Basolateral amygdala lesions block diazepam-induced anterograde amnesia in an inhibitory avoidance task. Proceedings of the National Academy of Sciences of the United States of America 89:3615-3619.
Ubeda-Banon I, Novejarque A, Mohedano-Moriano A, Pro-Sistiaga P, de la Rosa-Prieto C, Insausti R, Martinez-Garcia F, Lanuza E, Martinez-Marcos A (2007) Projections from the posterolateral olfactory amygdala to the ventral striatum: neural basis for reinforcing properties of chemical stimuli. BMC neuroscience 8:103.
Umbriaco D, Garcia S, Beaulieu C, Descarries L (1995) Relational features of acetylcholine, noradrenaline, serotonin and GABA axon terminals in the stratum radiatum of adult rat hippocampus (CA1). Hippocampus 5:605-620.
Van Bockstaele EJ, Chan J, Biswas A (1996) Ultrastructural evidence for convergence of enkephalin and adrenaline-containing axon terminals on common targets and their presynaptic associations in the rat nucleus locus coeruleus. Brain Res 718:61-75.
Veening JG, Swanson LW, Sawchenko PE (1984) The organization of projections from the central nucleus of the amygdala to brainstem sites involved in central autonomic regulation: a combined retrograde transport-immunohistochemical study. Brain Res 303:337-357.
Vermetten E, Schmahl C, Southwick SM, Bremner JD (2007) Positron tomographic emission study of olfactory induced emotional recall in veterans with and without combat-related posttraumatic stress disorder. Psychopharmacology bulletin 40:8-30.
Vizi ES, Fekete A, Karoly R, Mike A (2010) Non-synaptic receptors and transporters involved in brain functions and targets of drug treatment. British journal of pharmacology 160:785-809.
Walker DL, Paschall GY, Davis M (2005) Glutamate receptor antagonist infusions into the basolateral and medial amygdala reveal differential contributions to olfactory vs. context fear conditioning and expression. Learn Mem 12:120-129.
Wang H, Moriwaki A, Wang JB, Uhl GR, Pickel VM (1996) Ultrastructural immunocytochemical localization of mu opioid receptors and Leu5-enkephalin in the patch compartment of the rat caudate-putamen nucleus. The Journal of comparative neurology 375:659-674.
Wang H, Pickel VM (2001) Preferential cytoplasmic localization of delta-opioid receptors in rat striatal patches: comparison with plasmalemmal mu-opioid receptors. The Journal of neuroscience : the official journal of the Society for Neuroscience 21:3242-3250.

Wang J, Swann JM (2006) The magnocellular medial preoptic nucleus I. Sources of afferent input. Neuroscience 141:1437-1456.
Wilensky AE, Schafe GE, Kristensen MP, LeDoux JE (2006) Rethinking the fear circuit: the central nucleus of the amygdala is required for the acquisition, consolidation, and expression of Pavlovian fear conditioning. The Journal of neuroscience : the official journal of the Society for Neuroscience 26:12387-12396.
Wilson MA, Mascagni F, McDonald AJ (2002) Sex differences in delta opioid receptor immunoreactivity in rat medial amygdala. Neuroscience letters 328:160-164.
Wingard JC, Packard MG (2008) The amygdala and emotional modulation of competition between cognitive and habit memory. Behavioural brain research 193:126-131.
Wouterlood FG, Van Denderen JC, Blijleven N, Van Minnen J, Hartig W (1998) Two-laser dual-immunofluorescence confocal laser scanning microscopy using Cy2- and Cy5-conjugated secondary antibodies: unequivocal detection of co-localization of neuronal markers. Brain research Brain research protocols 2:149-159.
Zhang J, Muller JF, McDonald AJ (2013) Noradrenergic innervation of pyramidal cells in the rat basolateral amygdala. Neuroscience 228:395-408.
Zimmerman JM, Rabinak CA, McLachlan IG, Maren S (2007) The central nucleus of the amygdala is essential for acquiring and expressing conditional fear after overtraining. Learn Mem 14:634-644.